ISSN 0956-8549

Macro Strikes Back: Term Structure of Risk Premia

By

Svetlana Bryzgalov

Jiantao Huang

Christian Julliard

FINANCIAL MARKETS GROUP DISCUSSION PAPER NO. 962

July 2026

Macro Strikes Back: Term Structure of Risk Premia*

Svetlana Bryzgalova† Jiantao Huang‡ Christian Julliard§

June 2026

Abstract

We provide a novel *priced* Wold representation that, using the pricing restrictions of a large cross-section of asset returns, sharply identifies shocks common to financial markets and the macroeconomy, and their propagation. These shocks slowly propagate through major macro aggregates, account for $20-47\%$ of their variation and most of their predictability, and trace their business cycle, disciplining all equilibrium models. This propagation, not the overall persistence of macro quantities, yields short-run macro risk premia that are negligible, yet match the equity premium at business cycle horizons. Validating the method, the model-implied prices of dividend strips match observed out-of-sample forward equity yields and their term structure, both conditionally and unconditionally. By identification through elimination, we rule out productivity, investment-specific technology, and pure preference shocks as likely origins of the business cycle. The data point to demand/belief shocks and cost-push shocks propagating through real, nominal, and informational rigidities.

Keywords: Macro-finance, business cycle, identification, asset pricing, Bayesian inference, term structures. *JEL Classification Codes:* C11, C58, E27, E44, G12, G17.

*Any errors or omissions are the responsibility of the authors. For helpful comments, discussions and suggestions, we thank Hengjie Ai, Ravi Bansal, Nina Boyarchenko, Anna Cieslak, Mikhail Chernov, Max Croce, Richard Crump, Magnus Dahlquist, Marco Del Negro, Ian Dew-Becker, Jason Donaldson, Greg Duffee, Martin Eichenbaum, Xiang Fang, Marcelo Fernandes, Can Gao, Domenico Giannone, Bernardo Guimaraes, Valentin Haddad, Kristy Jansen, Ken Judd, Serhiy Kozak, Gabriele La Spada, Lars Lochstoer, Erik Loualiche, Ian Martin, Anna Mikusheva, Tyler Muir, Jun Pan, Lasse Pedersen, Elisabeth Proehl, Walt Pohl, Vincenzo Quadrini, Ricardo, Reis, Mirela Sandulescu, Lukas Schmid, Elizaveta Sizova, Dongho Song, Avanidhar (Subra) Subrahmanyam, Andrea Tamoni, Ivo Welch, Chenjie Xu, Kathy Yuan, Paolo Zaffaroni, and seminar and conference participants at Bocconi University, CEMFI, Copenhagen Business School, CUHK, CUHK Shenzen, DAFI Shanghai, Dartmouth Tuck, FGV São Paulo, FinEML, London Business School, London School of Economics, Maastricht University, Northwestern Kellogg, NY Fed, Pompeu Fabra, Renmin University of China, UCLA Anderson, USC Marshall, UT Sydney, UNSW, University of Lausanne, University of Sydney, Duke/UNC 2024 Asset Pricing conference, SoFiE 2024, CICF 2024, NBER Summer Institute 2024, EEA-ESEM 2024, ESSFM Gerzensee 2024, 11th SAFE Asset Pricing Workshop, Finance Down Under 2025, FIRS 2025, SAIF annual conference 2025, WFA 2025, SITE 2025, EFA 2025, AFA 2026, 5th Frontiers of Factor Investing Conference, TBEAR workshop, SGF, and SoFiE Conference on DSGE Modelling 2026.

†Department of Finance, London Business School, and CEPR; sbryzgalova@london.edu.

‡Faculty of Business and Economics, The University of Hong Kong, huangjt@hku.hk.

§Department of Finance, FMG, and SRC, London School of Economics, and CEPR; c.julliard@lse.ac.uk.

"The general hypothesis [...] is that information about the production of a given period is spread across preceding periods and so affects the stock returns of preceding periods."

— E. F. Fama (1990, p. 1096)

Equilibrium asset prices are jump variables. They incorporate news about current and future states of the economy as soon as it arrives, while real quantities adjust gradually as plans are revised and resources reallocated. This forward-looking character of asset prices has long been recognised as a window onto macroeconomic dynamics. And yet, its systematic use to identify priced macroeconomic shocks has remained elusive. The empirical macro-finance link has been fragile at best: weakly identified, horizon-dependent, and difficult to map cleanly to the predictions of equilibrium models.

We develop a framework that turns this disconnect on its head: a new, theoretically grounded identification scheme that uses the wealth of information in asset returns to recover the priced shocks common to financial markets and the macroeconomy, their propagation through macro time series, and the term structure of risk premia for any covariance-stationary economic factor. The identification rests on a new result, a *priced* Wold decomposition, combined with the pricing restrictions delivered by a large cross-section of equity returns. In the data, it reveals a very large degree of commonality between financial markets and the macroeconomy. And it delivers sharp evidence on which equilibrium mechanisms are, and are not, consistent with the term structure and propagation of priced macroeconomic risk, on the origin of the priced shocks, and on the frictions through which they propagate.

Our analysis reveals that financial markets and macroeconomic aggregates are linked far more tightly than commonly thought. The dynamics of GDP, industrial production, investment, hours worked, unemployment rate, and durable and non-durable consumption are all driven by (almost) identical priced shocks, which account for 20% to 47% of their time-series variance and the great majority of their predictability. The *priced* moving-average components we identify visibly trace the US business cycle, with troughs aligned with every NBER recession and pairwise correlations between 0.60 and 0.97 across these macro aggregates. The risk compensation this shock commands is large: annualised Sharpe ratios of 0.43 to 0.68, on par with the market portfolio, and the shock alone explains 20% to 53% of the variance of the (latent) stochastic discount factor (SDF) spanned by equity returns. In a nutshell, financial markets are of first-order importance for understanding macroeconomic dynamics, and macroeconomic risk is a first-order driver of asset prices.

We focus on the term structure of risk premia of an economic factor: minus the per-period covariance between its multiperiod growth and the SDF. The priced Wold representation can speak to other dynamic asset-pricing objects too,[1] but this metric is the natural one for the task at hand, and it disciplines equilibrium models in three ways. It has a clean marginal-utility interpretation. At each horizon, it pins down how strongly and in which direction a candidate model must covary the factor with marginal utility. It is benchmarked against observable returns. For any tradable claim, the term structure of risk premia can be read directly from data. So our nontraded-factor estimates, and the term structures implied by competing models, are comparable horizon by horizon with what financial markets pay. It is itself a tradable object. The macro risk premia we recover coincide with the per-period payoffs of horizon-specific mimicking portfolios. The existing equity cross-section thus implicitly spans, and could make tradable, the macro hedging instruments that Shiller (1993) called for.

The term structure of risk premia we uncover is unconditionally upward-sloping (in absolute value) for the major real aggregates and strongly countercyclical conditionally: small in expansions and sharply elevated in recessions. Macro risk premia are unconditionally small at quarterly horizons but match the equity premium at two- to three-year horizons. As an out-of-sample test of the conditional accuracy of the method, the implied dividend term structure, estimated *without* strip data, closely tracks the forward equity yields of Bansal et al. (2021).

Our Wold representation, combined with the discipline imposed by a large cross-section of returns, makes the common priced shock a sharply identified object. Hence, we can ask what kinds of disturbances drive it and which frictions propagate it. The findings deliver a sharp empirical target for equilibrium business-cycle models. The fingerprint of the priced common shock matches that of a demand or belief disturbance, propagated through real, nominal, and informational rigidities. The upward-sloping term structures of the core real aggregates reflect the slow propagation of the priced shock through these rigidities. Their strong countercyclicality points to either countercyclical risk aversion or risk-bearing capacity, or a time-varying quantity of risk (perceived or objective) over the cycle. The inflation risk premia we recover are negative, the signature of cost-push pressure dominating in priced inflation.

A natural candidate for the commonality we uncover is total factor productivity, the workhorse driver of business cycles in many equilibrium models. Yet, we find that TFP is *not* significantly priced at any horizon, whether measured by the utilisation-adjusted or the raw Fernald (2014)

[1]For instance, it could be used in estimating the shock elasticities of Borovička et al. (2014).

series. This is not an artefact of TFP mismeasurement or low power of the method. First, using only the directly estimated risk premia of output, hours, and investment, we construct an *implied* risk premium for the Solow residual, an internal consistency check that requires no TFP data, and obtain values close to zero at every horizon. The same priced shock therefore moves output, hours, and investment together, but leaves no priced footprint on measured productivity. Second, as we show, our method detects priced TFP components, if present, even when they account for a very small fraction of TFP variation, as in production-based long-run risk models (e.g., 7–8% in Croce, 2014). This is therefore a challenge for macro-finance models in which the pricing kernel is driven by productivity (e.g., Kydland and Prescott, 1982; Kung and Schmid, 2015), and it aligns with the evidence of Angeletos et al. (2020) that a single "main business-cycle shock" is largely unrelated to TFP.

The picture diverges sharply for inflation, however. Angeletos et al. (2020) report that the main business-cycle shock identified from real activity has near-zero correlation with inflation; we find substantial comovement instead, together with negative inflation risk premia that point to cost-push pressure dominating unconditionally in priced inflation. This difference comes from our ability to separate priced and unpriced components of inflation: most predictability within inflation measures, as we show, is driven by *unpriced* shocks. As a result, the standard VAR approach fails to detect the presence of common priced shocks and their risk premia.

We show, with extensive simulations, that our approach has much higher power to detect priced variables and their risk premia than conventional methods. It precisely pins down priced shocks and their propagation within any variable, yet it does not label them. However, different models of business-cycle fluctuations have sharp predictions about which state variables are priced, and what their term structures should look like. Therefore, this allows us to document which shock origins and economic frictions are supported by the data, and which are not. That is, our method allows us to conduct an exercise of "identification by elimination" of the origins and propagation mechanisms of priced business cycle fluctuations.

We find no empirical support for investment-specific technology and pure-preference shocks being the drivers of the priced macro commonality: the relative price of investment, equipment and structures investment growth, the personal savings rate, and the consumption-to-income ratio all have statistically insignificant term structures of risk premia. Credit-supply variables (Jermann and Quadrini, 2012), in particular the excess bond premium of Gilchrist and Zakrajšek (2012) and the senior loan officer net-tightening survey, display the right qualitative pattern,

but their credible intervals span zero, possibly due to shorter samples.

Which mechanisms are the data most consistent with? A non-technology shock, most plausibly a demand or belief disturbance, that propagates gradually through real, nominal, and informational rigidities. Consumer confidence and the Michigan Consumer Sentiment Index are significantly priced at all horizons, with *flat* term structures of risk premia, high contemporaneous R^2 from the priced shock, and limited additional predictive content: they behave as fast-moving barometers of the common shock rather than slow-diffusing drivers, consistent with the demand- and belief-driven view of business cycles in Angeletos and La'O (2013); Angeletos et al. (2020) and Huo and Takayama (2023). Priced shocks in confidence and sentiment are virtually identical and "almost the same" as those in GDP, hours, investment, and non-durable consumption, with correlations well above 0.9, against raw-variable correlations of 0.08 at best. Cross-forecaster dispersion and the macro-uncertainty index of Jurado et al. (2015) load on the same shock and carry term structures consistent with information frictions as modeled by Lorenzoni (2009) and Angeletos and Huo (2021), with their bite plausibly stronger in bad times.

Our framework also provides a clear view of the propagation mechanism. The textbook q-theory of investment (Hayashi, 1982; Cochrane, 1991) predicts that Δq, as a forward-looking asset price, is approximately unpredictable and therefore carries a *flat* term structure of risk premia. Real quantities such as capacity utilisation, by contrast, respond gradually through capital-adjustment costs. The data display exactly this pattern. The growth rate of aggregate Tobin's q is significantly priced at every horizon, with an essentially flat term structure and an annualised Sharpe ratio of about 0.4. Moreover, 83% of its variation is accounted for by the priced shock: q is overwhelmingly driven by the same systematic risk that prices the equity cross-section. Capacity utilisation, by contrast, exhibits a sharply upward-sloping term structure of risk premia, and its priced shock has a correlation of 0.99 with that of GDP. The contrast, flat for the asset price and upward-sloping for the slow-moving real quantity, is the canonical signature of q-channel transmission: the priced shock is immediately reflected in the shadow value of capital and propagates to real activity only gradually, via real frictions.

The footprint of the identified priced shock on inflation further disciplines the interpretation. Consumer-price inflation, the cyclical inflation measure of Bianchi et al. (2023), and producer-price inflation are all significantly *negatively* priced, with term structures that increase (in absolute value) with horizon. A negative inflation risk premium is the signature of cost-push pressure: inflation that loads on high-marginal-utility states, the "bad inflation" of

Cieslak and Pflueger (2023); Campbell et al. (2020). The slow build-up of the inflation premium across horizons mirrors the gradual response of inflation to the priced shock. This is a typical signature of nominal rigidities (Christiano et al., 2005) and information frictions in price setting (Mankiw and Reis, 2002; Woodford, 2003). Consistent with the latter, the cross-forecaster disagreement about the GDP deflator is negatively priced, sharing nearly the same priced shock (0.97 correlation) as disagreement about real GDP growth: a single informational friction seems to generate disagreement about both nominal and real outcomes. Yet, since standard inflation indices aggregate both demand- and supply-driven pressures, the negative unconditional inflation risk premia we estimate need not imply the absence of a demand-driven premium, which would carry the opposite sign under the Phillips curve. Extending the demand- and supply-driven inflation decomposition of Shapiro (2022) to the producer side confirms exactly: demand-driven PPI carries a *positive* term structure, whereas supply-driven PPI carries a (significantly) negative one, with the latter dominating unconditionally in aggregate PPI.

Our identification rests on three building blocks. First, a Priced Wold Decomposition Theorem expresses the priced part of any covariance-stationary economic factor as a moving average (MA) of current and past SDF innovations, in the spirit of local projections (Jordà, 2005; Olea et al., 2024) and reminiscent of max-share identification in the SVAR literature (Faust, 1998; Uhlig, 2003; Barsky and Sims, 2011; Francis et al., 2014; Angeletos et al., 2020), but with shocks identified through cross-sectional pricing rather than through variance-share or sign restrictions. Second, an approximate factor structure for asset returns (Chamberlain and Rothschild, 1983) ensures that priced shocks are spanned by a small number of latent factors recovered from the cross-section, with both macroeconomic risk premia and the propagation of priced shocks point-identified by a rotation-invariance argument similar to Giglio and Xiu (2021), extended here to the dynamic MA setting. Third, hierarchical Bayesian inference (Bryzgalova et al., 2023, 2024) jointly recovers the time-series and cross-sectional layers of the framework, with all conditional posteriors in closed form and valid credible intervals for the entire term structure.

(Additional) Closely Related Literature

Methodologically, our paper is close to the Bayesian VAR literature (Sims, 1992; Cogley and Sargent, 2005; Primiceri, 2005; Giannone et al., 2015; Del Negro and Primiceri, 2015; Crump et al., 2021), borrowing its hierarchical Gibbs encoding and use of high-dimensional panels. Unlike that tradition, we work directly in IRF space via the priced Wold representation, with shock identification based on cross-sectional pricing restrictions rather than on exclusion or sign

restrictions, providing the macro-finance counterpart to a literature primarily used to forecast and trace monetary or fiscal shocks (Del Negro and Schorfheide, 2004; Sims and Zha, 2006; Bańbura et al., 2010). Our TFP findings also speak to the long-running SVAR debate on the effects of technology shocks (Galí, 1999; Uhlig, 2004; Basu et al., 2006).

Our evaluation of candidate origins of the common priced shock engages with several additional strands of business-cycle theory not already discussed in the introduction. The demand-and-belief strand with which our findings most closely align includes coordination and animal-spirits models (Benhabib et al., 2015), information-friction theories of business-cycle propagation (Blanchard et al., 2013; Chahrour and Jurado, 2018), and demand-driven asset-pricing models (Albuquerque et al., 2016). We also evaluate, and find unsupported by the data as drivers of the common priced shock, investment-specific technology shocks (Greenwood et al., 1997; Fisher, 2006; Justiniano et al., 2010, 2011), pure preference shocks, and labor-market wedges and matching-efficiency shocks (Shimer, 2005; Hagedorn and Manovskii, 2008; Gertler and Trigari, 2009; Hall, 2017; Kehoe et al., 2019). Macro uncertainty measures (Jurado et al., 2015; Bloom, 2009; Bloom et al., 2018; Ludvigson et al., 2021; Baker et al., 2016) comove with the common priced shock to varying degrees and, where significantly priced, behave as fast-moving barometers of it rather than as its slow-propagation source. On the inflation side, our cost-push finding is consistent with the New Keynesian DSGE tradition but does not strictly require nominal rigidities, as cost-push pricing of inflation can arise with fully flexible prices (Finn, 2000). Yet, its slow propagation within inflation measures is suggestive of nominal (or informational) rigidities affecting price adjustments.

We also connect to the literature on inference of risk premia in linear factor models (Black et al., 1972; Fama and French, 1992; Shanken, 1992; Kan et al., 2013) and to recent work using systematic factors from large cross-sections to address omitted-variable and weak-identification problems (Connor and Korajczyk, 1988; Kozak et al., 2020; Kleibergen and Zhan, 2020; Anatolyev and Mikusheva, 2022; Bryzgalova et al., 2023). The priced Wold representation extends cross-sectional pricing to the dynamics of factors and returns, delivering the term structure of risk premia in one consistent framework. This helps reconcile the long-standing disagreement over macro risk premia at different frequencies (Mehra and Prescott, 1985; Parker and Julliard, 2005; Lettau and Ludvigson, 2001; Jagannathan and Wang, 2007; Ortu et al., 2013; Bandi and Tamoni, 2023), accounts for the term-structure patterns of the VIX (Eraker and Wu, 2017; Dew-Becker et al., 2017; Johnson, 2017), and rationalises the failure of standard mimicking

portfolios to price returns across horizons (Chernov et al., 2021): contrary to narratives based on horizon-specific risk attitudes (Andries et al., 2024), the term structure is generated by the *same* priced shocks slowly propagating through macro variables.

Finally, our use of financial markets to identify shocks and trace their macro responses relates to the literature on high-frequency identification of financial and policy shocks (Kuttner, 2001; Bernanke and Kuttner, 2005; Nakamura and Steinsson, 2018; Bianchi et al., 2022) and to work on tradable forward-looking factors (Liew and Vassalou, 2000; Lamont, 2001). Bryzgalova et al. (2026) also model a macro variable via a flexible MA, but with a different question and a different identification method. They study the consumption process embedded in asset prices to resolve the weak identification of consumption risk; we ask instead, crucially, which macro fluctuations are priced, how priced shocks propagate, and what the resulting term structure of risk premia implies for equilibrium models. The shocks are correspondingly identified differently: time-series filtering with asset returns there, cross-sectional pricing restrictions from the latent SDF of a large equity panel here.

The remainder of the paper outlines our method and simulation evidence (Section 1), presents the empirical findings (Section 2), and concludes (Section 3). The Online Appendix collects proofs, additional results, and details.

1 Theory and Method

We aim to test whether a covariance-stationary factor g_t, tradable or nontradable, is priced in a large cross-section of test assets. We work in logs throughout: g_t is the log growth rate of G_t between $t-1$ and t, where G_t can be, for example, portfolio value, investment, or production.

Let $\boldsymbol{r_t} = (r_{1t}, \ldots, r_{Nt})^\top$ denote log returns on N assets in excess of the log risk-free rate r_f. Define the cumulative variables $g_{t-1\to t+S} = \log(G_{t+S}) - \log(G_{t-1})$ and $\boldsymbol{r}_{t-1\to t+S}$, the multiperiod growth rate of G_t and the cumulative log excess returns between $t-1$ and $t+S$.

We assume a linear latent factor model for $\boldsymbol{r}_t$ with K systematic factors:

$$\boldsymbol{r}_t = \boldsymbol{\mu}_r + \boldsymbol{\beta}_{\tilde{v}}\tilde{\boldsymbol{v}}_t + \boldsymbol{w}_{rt}, \quad \tilde{\boldsymbol{v}}_t \overset{\text{iid}}{\sim} \mathcal{N}(\boldsymbol{0}_K, \boldsymbol{I}_K), \quad \boldsymbol{w}_{rt} \overset{\text{iid}}{\sim} \mathcal{N}(\boldsymbol{0}_N, \boldsymbol{\Sigma}_{wr}), \quad \tilde{\boldsymbol{v}}_t \perp \boldsymbol{w}_{rt}, \tag{1}$$

where $\tilde{\boldsymbol{v}}_t$ are K uncorrelated latent factors with loadings $\boldsymbol{\beta}_{\tilde{v}}$, $\boldsymbol{w}_{rt}$ are unpriced idiosyncratic errors, and $\boldsymbol{\mu}_r$ are expected log excess returns. We relax the serial uncorrelation of $\tilde{\boldsymbol{v}}_t$ in Section 1.1. The (log) normality assumption can also be relaxed but, unlike the alternatives, guarantees consistency even if the shocks are not Gaussian (Bollerslev and Wooldridge, 1992).

Asset returns follow an approximate factor structure (Chamberlain and Rothschild, 1983): the largest K eigenvalues of $\boldsymbol{r}_t$'s covariance matrix explode as the number of assets goes to infinity (equivalently, those of $\boldsymbol{\beta}_{\tilde{v}}\boldsymbol{\beta}_{\tilde{v}}^\top$), while those of $\boldsymbol{\Sigma}_{wr}$ remain bounded. We allow for some cross-sectional dependence of $\boldsymbol{w}_{rt}$, as discussed below. The number of latent factors, K, is taken as known in this section.

Factor loadings $\boldsymbol{\beta}_{\tilde{v}}$ partially explain expected returns (Ross, 1976),

$$\tilde{\boldsymbol{\mu}}_r = \boldsymbol{\mu}_r + \frac{1}{2}\boldsymbol{\Upsilon}_r = \boldsymbol{\beta}_{\tilde{v}}\boldsymbol{\lambda}_{\tilde{v}} + \boldsymbol{\alpha}, \tag{2}$$

where $\boldsymbol{\Upsilon}_r = \big(\mathrm{var}(r_{1t}), \ldots, \mathrm{var}(r_{Nt})\big)^\top$, $\boldsymbol{\lambda}_{\tilde{v}}$ are the risk premia of $\tilde{\boldsymbol{v}}_t$, and $\boldsymbol{\alpha}$ is a vector of pricing errors. The Jensen's inequality term $\frac{1}{2}\boldsymbol{\Upsilon}_r$ adjusts mean log excess returns.[2] Each pricing error α_i is iid with zero mean and finite standard deviation, and cross-sectionally independent of factor loadings. This form of misspecification has been commonly used (e.g., Kan et al., 2013; Gospodinov et al., 2014) and has a clear economic interpretation. Equation (2) is equivalent to a log SDF linear in the factors $\tilde{\boldsymbol{v}}_t$ (Cochrane, 2009):[3]

$$m_t - \kappa_m = -\boldsymbol{\lambda}_{\tilde{v}}^\top \tilde{\boldsymbol{v}}_t =: \varepsilon_t^m \tag{3}$$

Since $\tilde{\boldsymbol{v}}_t$ have an identity covariance matrix, their risk prices coincide with their risk premia.

To model each covariance-stationary factor g_t as the sum of a priced and an unpriced component, we apply the Wold representation theorem to the projection of g_t onto the priced subspace. The intuition is direct: if we decompose g_t into a purely priced component (containing no idiosyncratic information orthogonal to systematic risk) and an unpriced one, the former must lie in the linear span of the SDF (Hansen and Richard, 1987); the Wold theorem then expresses the priced part of g_t as a moving average of current and lagged SDF innovations. Appendix A.1 formalizes this as the Priced Wold Decomposition Theorem (Theorem A1) and establishes the existence and uniqueness of the representation. Based on this result and the SDF in (3), we model g_t as the sum of a moving average of asset-return shocks and additional shocks (e.g., measurement error) not spanned by financial markets:

$$g_t = \mu_g + \sum_{s=0}^{\bar{S}} \tilde{\rho}_s \underbrace{\tilde{\boldsymbol{\eta}}_g^\top \tilde{\boldsymbol{v}}_{t-s}}_{f_{t-s}} + w_{gt}, \quad \tilde{\boldsymbol{\eta}}_g^\top \tilde{\boldsymbol{\eta}}_g = 1, \tag{4}$$

[2]The approximation in equation (2) is exact under the lognormality assumption of asset returns.

[3]Our paper does not model the risk-free rate and hence the dynamics of conditional mean of the SDF. For convenience, we normalize the mean of m_t to be an unknown constant κ_m.

where μ_g is the unconditional mean, $\tilde{\boldsymbol{\eta}}_g \propto \boldsymbol{\lambda}_{\tilde{v}}$ (a restriction explored in Sections 2.1.1 and 2.1.3), f_t is the spanned component that may drive both g_t and asset returns, $\{\tilde{\rho}_s\}_{s=0}^{\bar{S}}$ is square-summable, and w_{gt} is a potentially autocorrelated shock unrelated to $\tilde{\boldsymbol{v}}_t$ and $\boldsymbol{w}_{rt}$. Theorem A1 ensures existence of this representation (possibly with $\bar{S} = \infty$); square-summability of the MA coefficients implies that finite $\bar{S}$ introduces only a finite approximation error.

Since f_t is a white-noise innovation, $\{\tilde{\rho}_s\}_{s=0}^{\bar{S}}$ are g_t's impulse responses to the asset-return shock f_t: $\tilde{\rho}_s = \mathbb{E}\left[g_{t+s} \mid f_t = 1; \{f_{t-j}\}_{j=1}^{\bar{S}}\right] - \mathbb{E}\left[g_{t+s} \mid f_t = 0; \{f_{t-j}\}_{j=1}^{\bar{S}}\right]$, analogous to the local projection (LP) coefficient of g_{t+s} on f_t (Jordà, 2005), with f_t identified from a large cross-section of asset returns. Like LPs, our framework recovers the impulse response of g to financial shocks without the fragility of selecting a stringent autoregressive structure (Olea et al., 2024). The single-equation MA also extracts information from all leads and lags of g_t jointly, rather than from $\bar{S}$ separate regressions with correlated residuals, simplifying and sharpening inference.

Several features of equation (4) are noteworthy. First, the representation projects g_t onto the history of asset-return shocks $\{\tilde{\boldsymbol{v}}_{t-s}\}_{s\geq 0}$ rather than onto g_t's own Wold innovations: since asset returns are what the SDF must price, conditioning on the information set spanned by tradable shocks is the natural basis for testing risk premia. The loading on both current and lagged shocks reflects that asset prices are jump variables, immediately incorporating news about current and future economic states, whereas nontradable factors may respond with delay, consistent with most equilibrium models and with the documented ability of returns to forecast macroeconomic variables (e.g., Liew and Vassalou (2000), Lamont (2001)). Second, when g_t comoves only with the contemporaneous asset-return shock ($\tilde{\rho}_s = 0$ for $s > 0$), the formulation nests Giglio and Xiu (2021) as a special case and attains comparable power.[4] For persistent factors, by contrast, allowing for MA propagation greatly increases the power of the test for risk premia, as we show below. Third, we adopt a general long-MA representation rather than a low-order ARMA. As Online Appendix OA.1 shows, model selection over the low-dimensional ARMA processes typically postulated for consumption, TFP, and profitability is fragile and rarely recovers the true process; the long-MA representation is therefore robust to ARMA-order misspecification. Where canonical selection fails, our representation succeeds: under the challenging calibration of Croce (2014), in which the priced conditional-mean component accounts for less than 8% of TFP variance, our MA-based method accurately recovers the cumulative impulse responses of TFP growth to the priced shock (Online Appendix OA.1).

[4]Since they use simple (not log) returns, the nesting is exact up to the log-linearization approximation error.

Our representation is very general and covers all macro-finance models with a covariance-stationary SDF.[5] We illustrate with examples how the framework in Equations (1)–(4) maps into canonical models under particular parametric restrictions.[6]

Example 1. *Adrian et al. (2014) measure a financial intermediary SDF, i.e.,* $m_t = \kappa_m - \lambda \cdot LevFac_t$*, where* $LevFac_t$ *is the shock to the leverage of security broker-dealers. Our framework maps into theirs with:* $\tilde{v}_t = f_t = LevFac_t$*,* $\bar{S} = 0$*,* $\tilde{\rho}_0 = 1$*, and* g_t *is a noisy proxy for* $LevFac_t$*.*

Example 2. *In the canonical long-run risk model of Bansal and Yaron (2004), the log consumption growth is modeled as* $g_t = \Delta c_t = x_{t-1} + \sigma_{t-1}\eta_t$*, where* σ_{t-1} *is the stochastic volatility process,* x_{t-1} *is the conditional consumption mean following an AR(1) process,* $x_t = \rho_x x_{t-1} + \varphi_e \sigma_{t-1} e_t = \sum_{s=0}^{\infty} \varphi_e \rho_x^s \sigma_{t-s-1} e_{t-s}$*, and* $\sigma_{t-1}\eta_t$ *is the short-run consumption shock. Within this framework, the log SDF is linear in three independent shocks, i.e.,* $\varepsilon_t^m := m_t - \mathbb{E}_{t-1}(m_t) = \lambda_{m,\eta}\sigma_{t-1}\eta_t - \lambda_{m,e}\sigma_{t-1}e_t - \lambda_{m,\omega}\sigma_\omega\omega_t$ *($\sigma_\omega\omega_t$ is the shock to σ_t^2). The SDF in equation (3) maps into the Bansal and Yaron model with i)* $\tilde{\boldsymbol{v}}_t = (\sigma_{t-1}\eta_t, \sigma_{t-1}e_t, \sigma_\omega\omega_t)^\top$ *and ii)* $\boldsymbol{\lambda}_{\tilde{v}} = (\lambda_{m,\eta}, -\lambda_{m,e}, -\lambda_{m,\omega})^\top$*. The fundamental priced Wold representation in equation (A1) yields the coefficient restrictions:*[7] $\bar{S} = \infty$*,* $\tilde{\rho}_0 = \frac{\lambda_{m,\eta}\,\mathbb{E}[\sigma_{t-1}^2]}{\sigma_\varepsilon^2}$*,* $\tilde{\rho}_{j\geq 1} = \frac{-\rho_x^{j-1}\varphi_e\,\lambda_{m,e}\,\mathbb{E}[\sigma_{t-1}^2]}{\sigma_\varepsilon^2}$ *and* $\sigma_\varepsilon^2 = \left(\lambda_{m,\eta}^2 + \lambda_{m,e}^2\right)\mathbb{E}[\sigma_{t-1}^2] + \lambda_{m,\omega}^2\sigma_\omega^2$*.*

We apply the risk premium definition of Cochrane (2009, Chapter 6) to g_t: $\lambda_g = -\text{cov}(g_t, m_t)$. When g_t is a traded log excess return, $\mathbb{E}\big[\exp(m_t + g_t + r_f)\big] = 1$ implies $\mathbb{E}[g_t] + \frac{1}{2}\text{var}(g_t) = -\text{cov}(g_t, m_t)$ under joint lognormality. For a nontradable factor, $-\text{cov}(g_t, m_t)$ is the pseudo expected excess return of g_t if it were tradable: the risk premium on an asset whose payoff grows at rate g_t. More broadly, it measures (the negative of) the covariance of g_t with marginal utility. We extend this to a term structure: the average per-period risk premium of g from $t-1$ to $t+S$ ($0 \leq S \leq \bar{S}$) is the multiperiod covariance between the factor and the SDF, divided by the number of holding periods:

$$\lambda_g^S = -\frac{\text{cov}(m_{t-1\to t+S}, g_{t-1\to t+S})}{1+S} = \frac{\sum_{\tau=0}^{S}\sum_{s=0}^{\tau}\tilde{\rho}_s}{1+S} \cdot \underbrace{\tilde{\boldsymbol{\eta}}_g^\top \boldsymbol{\lambda}_{\tilde{\boldsymbol{v}}}}_{\lambda_f}. \tag{5}$$

Equation (5) admits two interpretations. First, λ_g^S is the per-period risk premium on the mimicking portfolio for g at horizon S: the portfolio of returns whose multi-period payoff

[5] Our formulation allows shocks to be driven by a jump process. In the empirical applications, however, we model shocks as continuous since at the quarterly and monthly frequencies we focus on, the implied jumps would be small and well approximated by, and hard to distinguish from, continuous processes (Aït-Sahalia (2004)).

[6] Additional examples, e.g., Croce (2014) and Belo and Li (2023), are discussed in Online Appendix OA.1.

[7] The Wold representation is identical to the original variable in the Hilbert space sense: it preserves all first and second moments and therefore yields the same pricing implications and impulse responses.

best tracks $g_{t-1\to t+S}$. In a large cross-section, this per-period risk premium converges to λ_g^S as $N \to \infty$ (Proposition OA.1 of Online Appendix OA.2.1). The direct construction of this portfolio is, however, challenging in exactly the large-N regime that would extract the most cross-sectional information from financial markets.[8] By contrast, our priced moving-average approach delivers λ_g^S from a K-dimensional projection and gains precision as N grows.

Second, λ_g^S decomposes into a loading and a risk price, where the loading is the cumulative impulse response of g to f averaged over the $S+1$ horizons of the holding window, and λ_f is the risk premium of the spanned shock $f_t = \tilde{\boldsymbol{\eta}}_g^\top \tilde{\boldsymbol{v}}_t$ that drives both returns and g_t. In our approach, f_t is itself a tradable portfolio of returns and λ_f is its risk premium, recoverable from the cross-section without the high-dimensional projection that the first interpretation requires.

The risk-price component λ_f admits a transparent interpretation in terms of the SDF. Specifically, the SDF in equation (3) admits the orthogonal decomposition $m_t = \kappa_m - \lambda_f f_t - \boldsymbol{\lambda}_u^\top \boldsymbol{\Sigma}_u^{-1} \boldsymbol{u}_t$, where $\boldsymbol{u}_t$ is the component of the latent factors orthogonal to f_t (see Online Appendix OA.2.2). Hence λ_f is the risk price of f_t after controlling for the omitted sources of priced risk captured by $\boldsymbol{u}_t$, and equals the per-period Sharpe ratio of the f_t shock; $\lambda_f^2/\mathrm{var}(m_t)$ quantifies the relative importance of f_t in the SDF.

Example 3. *Suppose that the CAPM holds: $f_t = \tilde{v}_t = r_t^{mkt}$, with r_t^{mkt} independent over time and normalized to have unit variance. The SDF is then $m_t \propto -\lambda_{mkt} r_t^{mkt}$. For any factor g_t the term structure of its risk premia is:*

$$\lambda_g^S = -\frac{\mathrm{cov}(m_{t-1\to t+S}, g_{t-1\to t+S})}{1+S} = \left[\beta_0^g + \frac{1}{1+S}\overbrace{\sum_{\tau=1}^{S}\sum_{s=1}^{\tau}}^{\text{“forward”-}\beta s}\beta_s^g\right]\lambda_{mkt},$$

where the forward betas, $\beta_S^g \equiv \frac{\mathrm{cov}(g_{t-1+s\to t+s}, r_t^{mkt})}{\sigma_{mkt}^2}$, capture the predictability of g. The term structure of risk premia is determined by how the same priced shock propagates through the factor. The mimicking portfolio based on the single-period market beta (β_0^g) is uninformative about the multi-period risk premia, since it ignores the information in forward betas.

The example illustrates a sharp connection between predictability and the slope of the term structure. The forward betas β_s^g for $s \geq 1$ capture how strongly the factor responds to lagged market shocks: if g is unpredictable from past returns ($\beta_s^g = 0$ for $s \geq 1$), the forward-beta sum drops out and the term structure is flat at $\beta_0^g \lambda_{mkt}$, regardless of horizon. Predictability is

[8] The projection weights require inverting an $N \times N$ return covariance matrix that becomes poorly conditioned once the cross-section is comparable to or larger than the sample length, and the difficulty is compounded at long horizons, where the use of $(S+1)$-period cumulative quantities shrinks the effective sample size.

therefore a precondition for any non-trivial term structure, and its shape determines the term structure's slope. When g responds slowly to the priced shock, with forward betas of the same sign as β_0^g, the sum accumulates with S and the term structure is upward-sloping in absolute value. When g mean-reverts, with forward betas of opposite sign, the sum partially cancels and the term structure is downward-sloping.

Frequentist inference on λ_g^S is challenging: it is a function of $\{\tilde{\rho}_s\}_{s=0}^{\bar{S}}$, $\tilde{\boldsymbol{\eta}}_g$, and $\boldsymbol{\lambda}_{\tilde{v}}$, with the first two mutually dependent, so the asymptotic covariance matrix is complex despite being closed-form. We therefore adopt a Bayesian framework. As shown in Proposition A1 of Appendix A.2, under canonical diffuse priors the hierarchical structure of the time series and cross-sectional layers of our representation in (1)–(5) yields well-defined and well-understood conditional posterior distributions for all parameters. Consequently, we characterize the joint posterior of all quantities of interest via a Gibbs sampler. A potential concern is that, in the data, the asset-return shocks $\tilde{\boldsymbol{v}}_t$ are not directly observable: only a linear rotation of them is. As shown in Online Appendix OA.2.3, however, g_t's risk premium is point-identified: both the impulse-response coefficients $\{\tilde{\rho}_s\}$ and the term structure λ_g^S are invariant to the rotation.

1.1 Time-Varying Risk Premia and Their Term Structures

A salient feature of many macro-finance equilibrium models is time variation in risk premia. We now extend our Bayesian framework to estimate time-varying term structures. We require the SDF to price assets *conditionally*. Following Hansen and Jagannathan (1991), we focus on the conditional SDF projection on the space of returns:

$$m_{t+1} - \kappa_m = -\boldsymbol{b}_t^\top \big(\boldsymbol{r}_{t+1} - \mathbb{E}_t[\boldsymbol{r}_{t+1}]\big), \quad \text{where} \quad \boldsymbol{b}_t = \mathrm{cov}_t(\boldsymbol{r}_{t+1})^{-1}\tilde{\boldsymbol{\mu}}_{rt}. \tag{6}$$

The return process again follows an approximate factor structure as in equation (1) but, importantly, the priced systematic factors $\tilde{\boldsymbol{v}}_t$ are no more iid and are instead potentially predictable: $\tilde{\boldsymbol{v}}_t = \boldsymbol{\mu}_{\tilde{v},t-1} + \boldsymbol{\epsilon}_{\tilde{v}t}$, with $\boldsymbol{\mu}_{\tilde{v},t-1} \equiv \mathbb{E}_{t-1}[\tilde{\boldsymbol{v}}_t]$, $\boldsymbol{\mu}_{\tilde{v},t-1} \perp \boldsymbol{\epsilon}_{\tilde{v}t}$, and innovations are normalized so that $\mathrm{cov}(\boldsymbol{\epsilon}_{\tilde{v}t}) = \boldsymbol{I}_K$. As before, unconditional mean returns are partially explained by $\boldsymbol{\beta}_{\tilde{v}}$ in (2). Under the assumption that the eigenvalues of $\mathrm{cov}(\boldsymbol{\mu}_{\tilde{v},t-1})$ are bounded, the SDF becomes:[9]

$$m_{t+1} = \kappa_m - \boldsymbol{\lambda}_{\tilde{v}}^\top \boldsymbol{\epsilon}_{\tilde{v},t+1} - \boldsymbol{\mu}_{\tilde{v}t}^\top \boldsymbol{\epsilon}_{\tilde{v},t+1}, \tag{7}$$

where $\boldsymbol{\mu}_{\tilde{v}t}^\top \boldsymbol{\epsilon}_{\tilde{v},t+1}$ captures the time-varying risk premia of return shocks. Hence, since the Wold

[9]This result follows from derivations similar to those in Appendix OA.2.1, as $N \to \infty$.

representation requires the MA to depend only on innovations, the process for g becomes:[10]

$$g_t = \mu_g + \sum_{s=0}^{\bar{S}} \tilde{\rho}_s \underbrace{\tilde{\boldsymbol{\eta}}_g^\top \boldsymbol{\epsilon}_{\tilde{v},t-s}}_{f_{t-s}} + w_{gt}, \quad \tilde{\boldsymbol{\eta}}_g^\top \tilde{\boldsymbol{\eta}}_g = 1. \tag{8}$$

The time-varying term structure is then:

$$\lambda_{g,t-1}^S = -\frac{\operatorname{cov}_{t-1}(m_{t-1\to t+S}, g_{t-1\to t+S})}{1+S} = \sum_{\tau=0}^{S}\sum_{s=0}^{\tau} \frac{\tilde{\rho}_s \tilde{\boldsymbol{\eta}}_g^\top (\boldsymbol{\lambda}_{\tilde{v}} + \mathbb{E}_{t-1}[\boldsymbol{\mu}_{\tilde{v},t+\tau-s-1}])}{1+S}. \tag{9}$$

Four observations are in order. First, the dynamics of $\boldsymbol{\mu}_{\tilde{v},t-1}$ drive the time variation of the term structure. Second, since $\mathbb{E}[\boldsymbol{\mu}_{\tilde{v},t-1}] = 0$ by construction, the implied unconditional term structure coincides with (5); hence, the unconditional estimator remains consistent under time-varying risk premia. Third, the risk premia of g remain point-identified by rotation invariance (Online Appendix OA.2.5). Fourth, eliciting the time variation requires a model for the conditional mean of $\tilde{\boldsymbol{v}}$. We let $\tilde{\boldsymbol{v}}_t$ depend on its own lags and on external predictors $\boldsymbol{z}_t$. Defining $\boldsymbol{x}_t = (\tilde{\boldsymbol{v}}_t^\top, \boldsymbol{z}_t^\top)^\top$, we assume $\boldsymbol{x}_t$ follows a VAR of order q. This requires only a minimal change to the Gibbs sampler: $\boldsymbol{v}_t$ now follows a VAR rather than an iid normal. Under the canonical diffuse prior the conditional posterior is normal-inverse-Wishart and can be sampled directly. The full sampler is in Proposition OA.3 of Online Appendix OA.2.5.

Our time-varying framework connects to the literature on affine term structure models. In Cochrane and Piazzesi (2008), $\boldsymbol{x}_t$ contains three latent yield factors (level, slope, curvature) plus the bond-return forecasting factor of Cochrane and Piazzesi (2005), with risk prices linear in the lagged forecasting factor. Unlike them, we focus on risk premia and do not model the risk-free-rate dynamics. We share several modelling choices with Giglio et al. (2023), but differ on two first-order dimensions: we estimate the term structure of risk premia for all (traded and nontraded) factors of equilibrium models, where they focus on dividend yields; and they specify asset-price dynamics and reverse-engineer dividend-growth dynamics, where instead we specify a general MA representation for g_t that always exists.

1.2 Finite-sample Properties

We study the finite-sample properties of our method via Monte Carlo simulations, calibrated to the cross-section of Fama-French 275 portfolios (FF275) and to two sample sizes, $T \in$

[10] This MA representation is exact only in the continuous-time limit. We focus on it for expositional simplicity and because the discrete-time omitted term, $\boldsymbol{\mu}_{\tilde{v}t}^\top \boldsymbol{\epsilon}_{\tilde{v},t+1}$, is quantitatively irrelevant: it captures less than 1% of macro variation, and the CIRFs of g to a one-standard-deviation innovation in it are not significantly different from zero for 18 of 21 economic variables (Section OA.5 of the Online Appendix).

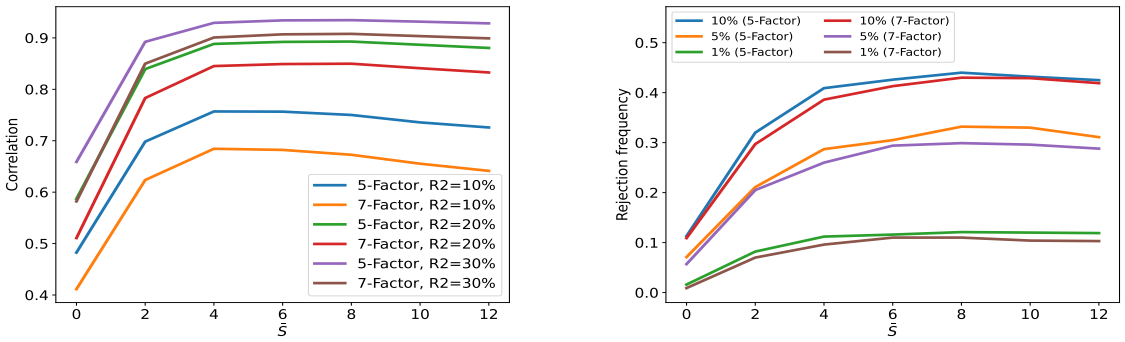

(a) $\text{corr}(\hat{f}_t, f_t)$, $T = 200$ **(b)** Power, $R_g^2 = 30\%$, $T = 200$

Figure 1: Identification and power gains from the MA representation

Left panel: average correlation between true and estimated priced shock, $\text{corr}(\hat{f}_t, f_t)$ with $\hat{f}_t = \hat{\boldsymbol{\eta}}_g^\top \hat{\boldsymbol{v}}_t$, across 1,000 simulations, for strong factors with $R_g^2 \in \{10\%, 20\%, 30\%\}$. Right panel: frequency, in 1,000 simulations, of rejecting $H_0 : \lambda_g^{\bar{S}} = 0$ based on the 90%, 95%, and 99% Bayesian credible intervals from Proposition A1, for strong factors with $R_g^2 = 30\%$. $\lambda_g^{\bar{S}}$ is defined in equation (5). Both panels use $T = 200$; the corresponding $T = 600$ figures and additional configurations (different K and $\bar{S}$) are reported in Online Appendix OA.3.

$\{200, 600\}$, matching the quarterly and monthly frequencies, respectively. Online Appendix OA.3 reports the full design and results. Here we summarize the main takeaways.

First, the estimator delivers correctly-sized credible intervals for the term structure of g_t's risk premia as long as we include all priced latent factors in the estimation, even when the signal-to-noise ratio is low and the sample size is small. Including *more* factors than in the pseudo-true model has no sizable detrimental effect on coverage, so the procedure is conservative in this dimension. Omitting a priced factor instead generates bias.

Second, the inclusion of lagged asset return shocks in g_t's equation is essential for both identification and power. Figure 1 shows, on the left, that the average correlation between the true priced shock f_t and its estimate $\hat{f}_t = \hat{\boldsymbol{\eta}}_g^\top \hat{\boldsymbol{v}}_t$ is modest when $\bar{S} = 0$ (between 0.4 and 0.65) and rises sharply with $\bar{S}$. The right panel reports the corresponding power of the test of zero risk premia: at $\bar{S} = 0$ power is low, and rises substantially as more lagged latent factors enter g_t's equation. Hence the MA representation of g_t is the key ingredient for detecting significant risk premia in persistent factors.

Third, our estimator does not generate the spurious significance that canonical frequentist procedures display for useless factors (see, e.g., Kan and Zhang 1999): credible intervals for the risk premia of useless persistent factors are conservative. Including many lags of multiple latent factors does not generate overfitting of g_t. In the special case of factors that correlate only with contemporaneous asset return shocks, the size and power of our test are almost identical to

those of the frequentist procedure of Giglio and Xiu (2021). Finally, the time-varying extension of Section 1.1 delivers similar size and power, with only a minimal degree of attenuation bias and increased posterior uncertainty, despite the significant added generality.

2 Empirical Analysis

In this section, we apply our Bayesian framework to investigate whether macroeconomic factors are priced, their unconditional and time-varying term structures, how these premia connect to the business cycle, and the structural origins of the commonality between financial markets and the macroeconomy.

2.1 Unconditional Risk Premia

We begin with unconditional risk premia. Our analysis relies on a large cross-section of FF275, covering 1963:Q3–2019:Q4. Throughout, we standardize tested factors to unit variance per period. Definitions, sample periods, and data sources are in Online Appendix OA.4.

To conduct the Bayesian estimation of Section 1, we need the number of latent factors, K. We estimate $K = 5$ in FF275 at both monthly and quarterly frequencies.[11] The first few latent factors explain most of the time-series and cross-sectional variation. The first five PCs account for over 93% of time-series variation at both frequencies; the sixth and seventh add little. Cross-sectionally, the five-, six-, and seven-factor models explain 55.0%, 58.6%, and 58.7% (59.0%, 59.3%, and 72.9%) of variation in average returns at quarterly (monthly) frequency. The statistical test in the footnote, together with the time-series and cross-sectional fits, points to the five-factor model as a reasonable benchmark, which we adopt in baseline estimations (with $K = 6$ or 7 as robustness). As a sanity check, Figure OA.5 of the Online Appendix plots the term structure of risk premia for the Fama and French (1993) three factors, estimated using Proposition A1 ($\bar{S} = 24$, $K = 5$): the Bayesian point estimates closely track the time-series Sharpe ratios, which in turn lie within the 68% credible intervals, confirming that our method recovers the term structure of excess returns of tradable factors.

2.1.1 Term Structure of Risk Premia

We start with the term structure of risk premia for the core macroeconomic variables featured in typical macro-finance models, reported in Table 1. Variables tied to specific theoretical

[11] We follow Online Appendix I.1 of Giglio and Xiu (2021), setting $K_{\max} = 15$. Alternatively, the spike-and-slab prior of Bryzgalova et al. (2023) can select or aggregate factors in the SDF. We re-estimated the key results with six- and seven-factor specifications and obtained virtually identical point estimates.

Table 1: Factors' risk premia

Panel A. Quarterly variables, $\bar{S} = 12$ quarters										
S = (quarters)	0	2	4	6	8	10	12	R^2_g	$R^2_{g,pred}$	$R^2_{err,pred}$
GDP growth	0.026*	0.084***	0.133***	0.164***	0.180***	0.195***	0.204***	25.7%	23.9%	9.9%
IP growth	0.008	0.087***	0.145***	0.177***	0.194***	0.204***	0.205***	39.0%	38.8%	9.7%
Durable consumption growth	-0.014	0.079**	0.122***	0.140***	0.147***	0.153***	0.158***	20.8%	20.0%	8.1%
Nondurable consumption growth	0.042***	0.103***	0.141***	0.179***	0.206***	0.226***	0.244***	25.1%	22.3%	7.1%
Unemployment rate change	-0.024	-0.117***	-0.203***	-0.269***	-0.322***	-0.366***	-0.403***	47.1%	46.0%	9.0%
Hours worked growth	0.024	0.095***	0.169***	0.223***	0.261***	0.295***	0.319***	35.9%	34.7%	9.0%
Investment growth	0.010	0.091***	0.158***	0.201***	0.223***	0.240***	0.248***	36.1%	35.9%	5.4%
Dividend growth	0.009	0.045*	0.109***	0.175***	0.245***	0.306***	0.357***	41.8%	41.5%	17.6%
Nondurable + service	0.028*	0.067*	0.099*	0.127**	0.148*	0.163**	0.181**	19.8%	17.4%	23.4%
Service consumption growth	0.006	0.013	0.020	0.027	0.035	0.041	0.045	11.0%	9.7%	26.5%
TFP growth	0.023	0.052	0.066	0.070	0.065	0.060	0.054	18.7%	15.4%	12.4%
TFP growth (util)	0.000	0.000	0.000	-0.001	-0.002	-0.001	0.000	12.2%	12.0%	8.1%
AEM intermediary	0.082***	0.077**	0.078**	0.063	0.046	0.026	0.019	16.7%	11.3%	5.8%
Labor income growth	0.000	0.002	0.003	0.004	0.005	0.005	0.009	7.5%	7.2%	8.3%
Panel B. Monthly variables, $\bar{S} = 24$ months										
S = (months)	0	4	8	12	16	20	24	$R^2_{g,total}$	$R^2_{g,pred}$	$R^2_{err,pred}$
Nontraded HKM intermediary	0.098***	0.101***	0.097***	0.093***	0.091***	0.089***	0.088***	62.1%	2.7%	1.1%
Traded HKM intermediary	0.114***	0.115***	0.110***	0.104***	0.100***	0.098***	0.096***	71.8%	2.7%	1.1%
PS liquidity	0.050***	0.074***	0.086***	0.097***	0.108***	0.118***	0.126***	17.2%	5.7%	4.4%
$\Delta \log(\text{VIX})$	-0.131***	-0.079***	-0.062***	-0.049***	-0.042***	-0.037***	-0.032***	53.6%	8.6%	5.5%

Bayesian estimates of factors' risk premia from Proposition A1; λ_g^S defined in eq. (5). Base assets: 275 Fama-French characteristic-sorted portfolios; five-factor model. Panel A: quarterly, $\bar{S} = 12$. Panel B: monthly, $\bar{S} = 24$. *, **, ***: 90%, 95%, 99% Bayesian CI excludes zero. R^2_g: total from priced shocks; $R^2_{g,pred}$: predictive, excluding contemporaneous shock; $R^2_{err,pred}$: from error w_{gt} via AR(12). Data sources: Online Appendix OA.4.

channels are analyzed in Section 2.1.4, and inflation-related risk premia in Section 2.1.5. For quarterly (monthly) variables, we use Proposition A1 with 12-quarter (24-month) lags in g_t's equations. Several findings stand out.

First, priced shocks explain a large share of the time series variance (R^2_g) of priced macro variables and capture most of their predictability ($R^2_{g,pred}$ vs $R^2_{err,pred}$). This commonality between macro and financial quantities is much larger and more sharply identified than under traditional approaches (e.g., the consumption–returns link is weakly identified at best in Kleibergen and Zhan (2020)). Our identification strategy recovers the priced innovations from a large cross-section of asset returns rather than from standalone macro variables or their AR(1) residuals. The last three columns of Table 1 reveal why the standard approach fails: priced and unpriced components of macro time series have quite different persistence. For GDP growth, priced shocks explain over a quarter of the time series variation with a predictive R^2 of about 24%, while unpriced shocks are predictable to a much lower extent (predictive R^2 of about 10%). Conflating the two via AR(1) residuals yields inconsistent estimates with attenuation bias.

Second, our identification reveals a rich set of priced macro factors. Many macro factors carry significant risk premia: industrial production, GDP, durable and nondurable consumption,

dividends,[12] unemployment, hours worked, and investment. Strikingly, most have *increasing* (in absolute value) term structures. At quarterly frequency ($S = 0$) most are weakly identified at best, but at business cycle frequencies (two to three years) their risk premia are as large as the market's. Macro aggregates are thus riskier from the perspective of long-term than short-term investors. Yet TFP is not significantly priced at any horizon. As we show in Section 2.1.3, the commonality is driven by macro factors loading on essentially the same priced shock, which is not a TFP shock. This presents a novel challenge for general equilibrium macro-finance models, taken up in Section 2.1.4.

Third, the findings are not a byproduct of factor persistence. Durable consumption growth, the AEM intermediary factor, and labour income growth have similar autocorrelation structures, but very different term structures of risk premia: upward-sloping for durable consumption, slightly downward-sloping for AEM, and flat for labour income. The term structure is driven by how the economic factor responds to the f_t shock over time, not by its persistence.

The term structure of VIX risk premia (in absolute value) is downward-sloping. The mimicking portfolio hedging monthly VIX changes earns a sizable risk premium of -0.13, while the two-year risk premium falls to -0.03 (still significant). This is consistent with previous work using derivative contracts of different expirations (Eraker and Wu, 2017; Dew-Becker et al., 2017; Johnson, 2017).

We further verify the baseline estimates by directly projecting g onto the SDF shocks, i.e., imposing the theoretical restriction $\boldsymbol{\eta_g} \propto \boldsymbol{\lambda_v}$. Under this restricted model, macro factors identified as priced in the unrestricted version display very similar risk-premia magnitudes and term-structure shapes: the restriction barely affects the point estimates, and the reduced time-series fit only widens the credible intervals. TFP growth, especially the utilization-adjusted measure, remains unpriced.[13]

Moreover, the estimates reveal that, as predicted by our priced moving-average representation, canonical mimicking portfolios based on single-period exposures fail to capture the term structure of persistent variables. Figure 2 plots estimates for the traded and nontraded He et al. (2017) (HKM) intermediary factors (Panel (a)) and the Pástor and Stambaugh (2003) (PS) liquidity factors (Panel (b)). The HKM traded and nontraded factors command nearly

[12]Dividend growth is the quarterly growth of smoothed aggregate S&P 500 dividends over the previous 12 months, smoothed to remove the mechanical seasonality in payments.

[13]We also confirm that the term-structure estimates can be interpreted as horizon-specific mimicking portfolios that display increasing term structures of risk premia similar to those in Table 1.

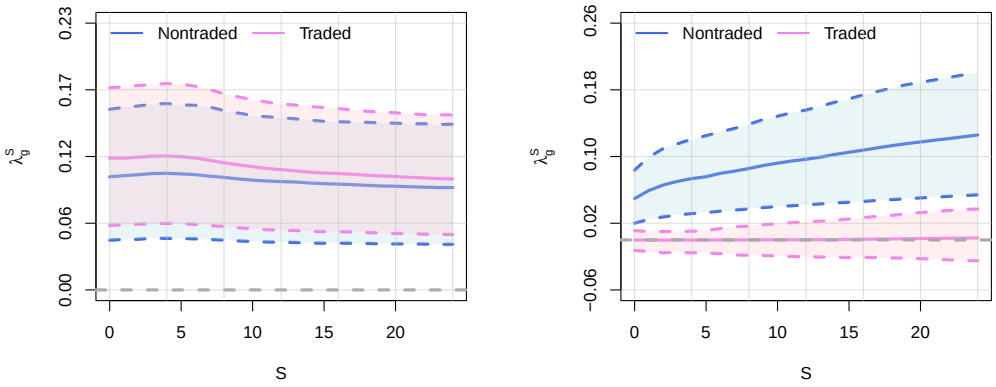

(a) HKM intermediary factors **(b)** PS liquidity factors

Figure 2: Term structure of factor's risk premia: Traded vs. Nontraded versions

Term structure of monthly risk premia for traded and nontraded He et al. (2017) intermediary and Pástor and Stambaugh (2003) liquidity factors. Base assets: 275 Fama-French characteristic-sorted portfolios. Five-factor model for returns. Point estimates shown with shaded 90% Bayesian CIs. Data sources: Online Appendix OA.4.

identical risk premia across horizons; their term structures are flat, so the nontraded HKM factor has near-zero forward betas (Example 3). Conversely, the tradable PS liquidity factor, which ignores the positive forward betas, fails to capture the upward-sloping term structure.

The contrast in Table 1 is striking: financial markets, which appear weakly related to macro aggregates contemporaneously, in fact strongly predict their future values. At $S = 0$ most macro factors have small and statistically insignificant premia, but at business-cycle horizons ($S = 8$ to 12 quarters) the same factors carry premia comparable to the market's. The mechanism lives in the cumulative impulse responses: macro variables respond strongly to priced asset-return shocks over the following two to three years, so financial markets encode information about future macroeconomic states that the contemporaneous covariance entirely misses.

This pattern is not an artifact of the lag structure: as shown in Online Appendix OA.6, it survives re-estimation with $\bar{S} = 0$ and with the frequentist estimator of Giglio and Xiu (2021). AR(1)-residual estimates are likewise small and largely insignificant because priced and unpriced components have different persistence (the gap between $R^2_{g,pred}$ and $R^2_{err,pred}$), so the AR(1) filter conflates them and induces attenuation. Our MA representation instead takes no stance on the data-generating process and recovers priced innovations directly from a large cross-section, connecting to but going beyond the literature on weak factors with small or vanishing correlations with returns.[14] Many factors that look weak at short horizons are strongly identified

[14]See, e.g., Kan et al. (2013), Gospodinov et al. (2014), Kleibergen and Zhan (2020), Anatolyev and Mikusheva (2022), and Bryzgalova et al. (2023).

once their multi-period propagation is properly accounted for. This perspective also reconciles the long-standing conflicting evidence on priced consumption risk: insignificant and weakly identified at quarterly horizons, strongly priced at business cycle horizons.[15] These apparently conflicting estimates are not in contradiction: they all reflect the multi-period response of macro variables to priced financial shocks. Our approach identifies the entire term structure of risk premia together with the propagation mechanism that generates it.

Our results are also robust to the base assets used to recover the SDF. The Elkamhi et al. (2023) cross-section of *corporate bonds* yields term structure estimates virtually identical to those in Table 1, albeit with wider credible intervals reflecting a sample that is 18 years shorter.

2.1.2 Implied TFP Risk Premia via the Solow Residual

A natural consistency check on the finding that TFP growth is unpriced at all horizons is to compute the *implied* TFP risk premium from the Solow residual decomposition, using the directly estimated risk premia of GDP, hours worked, and investment. This exercise is internally consistent with our use in Table 1 of the Fernald (2014) TFP series, constructed as the Cobb–Douglas Solow residual $\Delta \text{tfp}_t = \Delta y_t - a_t\, \Delta \log K_t - (1-a_t)\, \Delta \log L_t$, where Δy_t, $\Delta \log K_t$, $\Delta \log L_t$ denote real GDP, capital stock, and hours worked growth, and a_t is the time-varying capital income share. Since risk premia are linear operators and we estimate unconditional premia, only the sample mean $\bar{a} \approx 1/3$ (close to the US average of 0.33–0.34 over 1963:Q3–2019:Q4) matters: interaction terms between the slow drift in a_t and priced shocks are negligible.

Since the λ_g^S in Table 1 are Sharpe ratios of the standardized factor g_t (hence the corresponding level risk premium is $\text{RP}_g^S = \lambda_g^S\, \sigma_g$), the Solow decomposition implies

$$\text{RP}_{\text{tfp}}^S \;\approx\; \lambda_{\Delta y}^S\, \sigma_{\Delta y} \;-\; \bar{a}\, \frac{I/K}{1+I/K}\, \lambda_{\Delta \log I}^S\, \sigma_{\Delta \log I} \;-\; (1-\bar{a})\, \lambda_{\Delta \log L}^S\, \sigma_{\Delta \log L}, \tag{10}$$

using $\Delta \log K_t \approx \frac{I/K}{1+I/K}\, \Delta \log I_t$ from the first-order linearization of the capital accumulation equation around its balanced growth path.

With quarterly $I/K = 0.055$ and standard deviations $\sigma_{\Delta y} = 0.80\%$, $\sigma_{\Delta \log I} = 2.91\%$, $\sigma_{\Delta \log L} = 0.69\%$, we report the implied TFP risk premia in Table 2.[16] The implied premia are

[15] See, e.g., the disagreement among consumption risk premia estimates in Lettau and Ludvigson (2001), Jagannathan and Wang (2007), Hansen et al. (2008), Ortu et al. (2013), Kleibergen and Zhan (2020), and Bandi and Tamoni (2023).

[16] The capital term enters with coefficient $\bar{a} \cdot I/K/(1+I/K) \approx 0.017$, so the result is insensitive to investment volatility or I/K. Including labor quality (whose risk premia are near zero at all horizons) leaves the implied TFP premia unchanged; we omit it because pre-1979 quarterly values are extrapolated (Fernald, 2014).

Table 2: Implied TFP risk premia via the Solow Residual

S = (quarters)	0	2	4	6	8	10	12
GDP contribution: $\lambda^S_{\Delta y}\,\sigma_{\Delta y}$	+0.021	+0.068	+0.106	+0.131	+0.145	+0.157	+0.163
Capital contribution: $-\bar{a}\,\frac{I/K}{1+I/K}\,\lambda^S_{\Delta\log I}\,\sigma_{\Delta\log I}$	−0.001	−0.005	−0.008	−0.010	−0.011	−0.012	−0.013
Hours contribution: $-(1-\bar{a})\,\lambda^S_{\Delta\log L}\,\sigma_{\Delta\log L}$	−0.011	−0.043	−0.078	−0.102	−0.120	−0.135	−0.146
Implied $\mathrm{RP}^S_{\mathrm{tfp}}$	+0.009	+0.020	+0.021	+0.019	+0.013	+0.009	+0.004

Implied TFP risk premium (level, % per quarter) from equation (10), using $\bar{a} = 1/3$ (sample average of Fernald's time-varying capital shares) and $I/K = 0.055$ (quarterly). Sharpe ratios for GDP, investment, and hours worked from Table 1, Panel A.

small and near zero at all horizons. Since both implied and direct premia measure the same Cobb–Douglas residual, the agreement is a genuine internal consistency check: production accounting and direct Bayesian estimation independently agree that TFP is unpriced. The priced common shock therefore moves output, labor, and capital together without affecting measured productivity in a priced form, posing a direct challenge to models in which the pricing kernel is driven by productivity (Kydland and Prescott, 1982; Kung and Schmid, 2015).

One possible response to this challenge is that total TFP growth conflates a small but persistent long-run component with a dominant short-run noise term, and that only the former is priced (Croce, 2014; Ai et al., 2018). This objection does not apply to our method: Online Appendix OA.1 shows that, under the Croce (2014) calibration, our method recovers the priced shock with an average correlation of 0.90 with the true shock in simulated samples of the same length as our data, despite the low signal-to-noise ratio. Ai et al. (2018) identify the long-run TFP component as a linear combination of the price-dividend ratio, Treasury yield measures, and integrated equity volatility; using the series kindly provided by the authors, we find that its AR(1) innovation is marginally priced, but the implied risk premium remains an order of magnitude smaller than those of GDP, hours worked, or investment. Moreover, a Bayesian analysis of the same quarterly TFP series using only its time-series properties yields a posterior probability of 57.3% that the data are compatible with the assumed AR(1)+noise decomposition; conditional on compatibility, the posterior mean long-run variance share is 57.9% (95% credible interval: 19.5%–96.3%), and the 7.5% figure obtained by projecting TFP onto financial instruments carries a Bayesian p-value below 1%, suggesting it reflects co-movement between TFP and financial markets rather than the intrinsic persistence of productivity. Long-run TFP risk is therefore unlikely to be the main driver of the macroeconomic risk premia that we uncover.

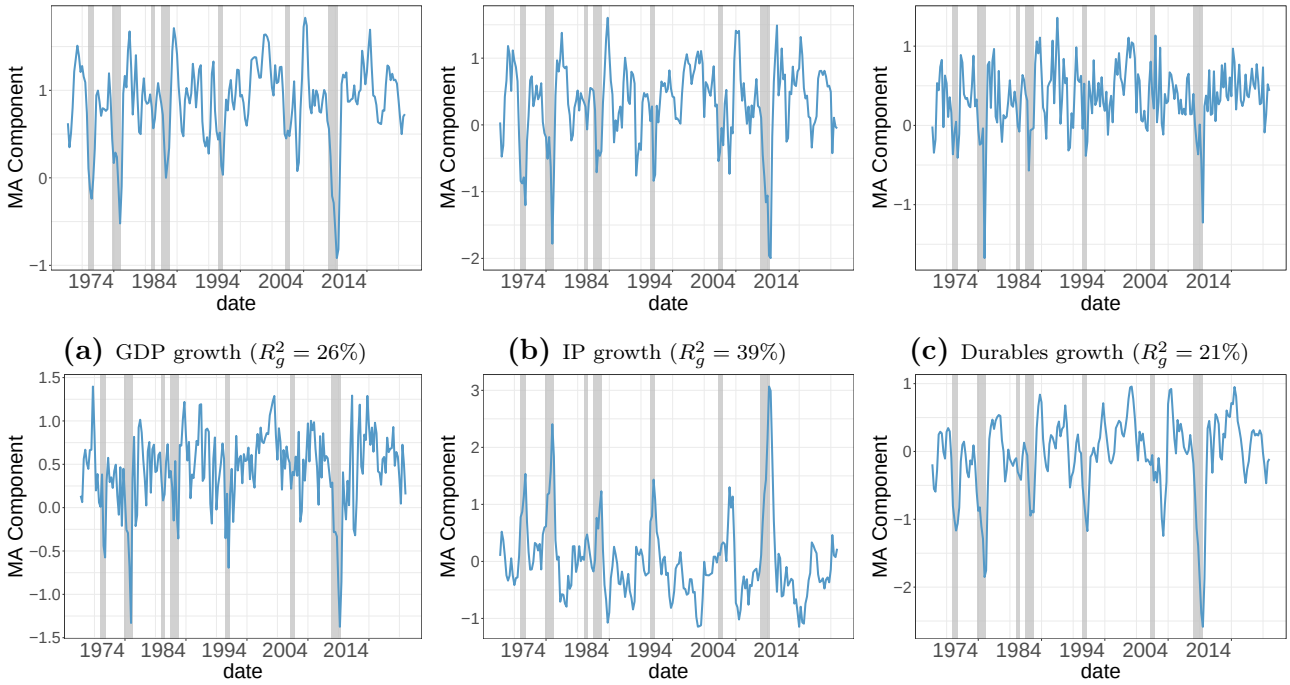

(a) GDP growth ($R^2_g = 26\%$) **(b)** IP growth ($R^2_g = 39\%$) **(c)** Durables growth ($R^2_g = 21\%$)

(d) Nondurables growth ($R^2_g = 25\%$) **(e)** Δ Unemployment rate ($R^2_g = 47\%$) **(f)** Hours worked growth ($R^2_g = 36\%$)

Figure 3: Moving average components of some macro factors

Time series of moving average components (posterior means) spanned by latent factors: $\sum_{s=0}^{\bar{S}} \rho_s \boldsymbol{\eta}_g^\top \boldsymbol{v}_{t-s}$, with $\bar{S} = 12$ quarters. Base assets: 275 Fama-French characteristic-sorted portfolios. Five-factor model for returns. Data sources in Online Appendix OA.4. Sample: 1963Q3–2019Q4.

2.1.3 Commonality of Macro Factors and Their Pricing

Perhaps the most surprising finding is that macro variables carry much larger risk premia at long horizons ($S = 8$ to 12 quarters) than at quarterly frequency ($S = 0$). What is the economic intuition? Is the commonality among macro variables caused by their exposure to the same priced shocks, as implied by Theorem A1? We now verify this hypothesis.

Figure 3 plots the posterior means of the MA components of six priced macro variables. These priced components account for a substantial share of the time-series variation of each variable ($R^2_g = 21\%$–47% in Table 1, very close to the 22%–57% business-cycle variance shares estimated with the Baxter and King (1999) band-pass filter for the same variables) and all display clear business-cycle patterns. As shown in Table 3, GDP, IP, unemployment, hours worked, and investment have highly correlated MA components, often around 90%.

What drives the commonality? Several macro variables load on almost identical priced shocks, as Theorem A1 implies. To illustrate, suppose that $\hat{f}_t$ is the financial shock identified as the driver of the (priced) conditional mean of g_t. We can elicit the responses of *other* macro

Table 3: Are the priced MA components of macro factors similar?

	GDP growth	IP growth	Durable	Nondurable	Unemployment	Hours worked	Investment
IP growth	0.90						
Durable	0.69	0.72					
Nondurable	0.70	0.70	0.64				
Unemployment	-0.86	-0.83	-0.66	-0.76			
Hours worked	0.90	0.82	0.63	0.64	-0.97		
Investment	0.95	0.90	0.70	0.60	-0.86	0.90	
Dividend growth	0.39	0.35	0.32	0.48	-0.72	0.65	0.39

Correlation among moving average components spanned by latent factors, $\sum_{s=0}^{\bar{S}} \rho_s \boldsymbol{\eta}_g^\top \boldsymbol{v}_{t-s}$, with $\bar{S} = 12$ quarters. Base assets: 275 Fama-French characteristic-sorted portfolios. Five-factor model for returns. Data sources in Online Appendix OA.4.

variables (GDP, consumption, unemployment, etc.) to the same shock. If these shocks are interchangeable, the impulse responses should be roughly the same. Figure 4 reports six macro variables: GDP, IP, durable and nondurable consumption, unemployment, and hours worked. For each, we estimate impulse responses to six different f_t shocks identified by targeting the individual factors. Shaded areas show 90% confidence bands for each variable's CIRF to its own f_t shock. The financial shocks are almost interchangeable, with the possible exception of durable consumption. The commonality in priced conditional means comes from a common response pattern to priced financial shocks. In most models, such commonality would arise from total factor productivity (Angeletos et al., 2020); yet, as Table 1 and Section 2.1.2 show, TFP shocks are not significantly priced at any horizon considered, presenting a new challenge for equilibrium macro-finance models.

Are these (almost interchangeable) priced shocks, which drive most of the business-cycle dynamics and predictability of macroeconomic factors, also important for financial markets? We address this question using the SDF decomposition introduced in Section 1: $m_t = \kappa_m - \lambda_f f_t - \boldsymbol{\lambda}_u^\top \boldsymbol{\Sigma}_u^{-1} \boldsymbol{u}_t$, where $\boldsymbol{u}_t$ is orthogonal to f_t and controls for omitted sources of priced risk. Table 4 reports the risk-price estimates of f_t for several priced nontraded factors from Table 1. These f_t shocks are significantly priced in the cross-section with extremely similar risk prices, as Theorem A1 implies, again pointing to a common origin for the risk compensation demanded by these macro quantities. The annualized Sharpe ratios implied by these f_t shocks are economically large yet not excessive, 0.43 to 0.68, on par with the market index. Importantly, the linear combinations f_t are themselves observable, tradable portfolios: existing equity markets thus implicitly span, and in principle make tradable, the aggregate macroeconomic risks for which Shiller (1993) called for the creation of dedicated hedging instruments. The column

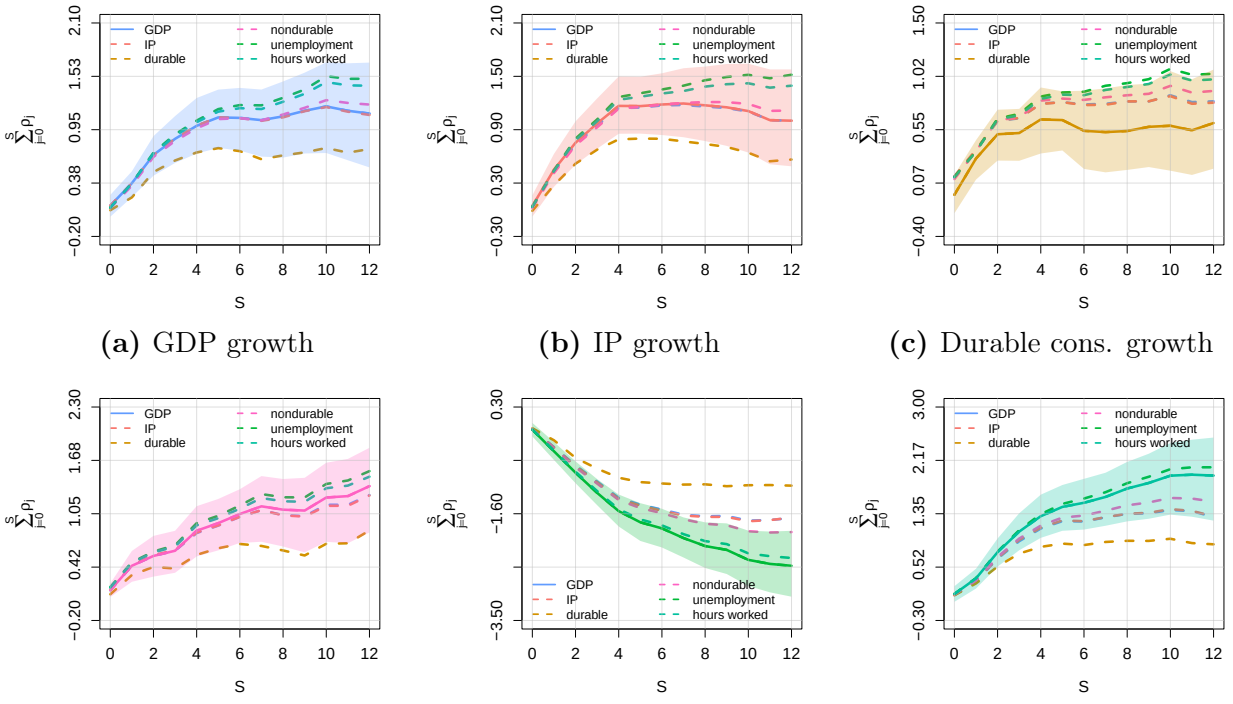

(a) GDP growth **(b)** IP growth **(c)** Durable cons. growth

(d) Nondurable cons. growth **(e)** Δunemployment rate **(f)** Δ log(hours worked)

Figure 4: Cumulative IRFs to Different Financial Shocks

Impulse-response functions of macro time series to priced shocks driving their priced conditional means. Panel (a): GDP priced shock; panel (b): IP priced shock, etc. Shaded areas show posterior 90% confidence regions for each variable's response to its own shock. Base assets: 275 Fama-French characteristic-sorted portfolios. Data sources: Online Appendix OA.4.

$\mathbb{E}\left[SR_f^2/SR_m^2 \mid \text{data}\right]$ quantifies the importance of f_t in the latent SDF: these macro sources of risk individually explain about 20 to 53% of the latent SDF's variance.

Macroeconomic risk is therefore of first-order importance in financial markets. Yet, as the last column of Table 4 highlights, about half or more of the maximal squared Sharpe ratio in the economy is *not* captured by these economic factors. Hence, using standalone macro variables, or their AR(1) innovations, in canonical asset pricing exercises (e.g., Fama-MacBeth regressions) is problematic without controlling for omitted variables (Bryzgalova et al., 2024).

What equilibrium picture is consistent with these findings? Persistent shocks like the ones we have identified, which propagate slowly through the state variables of the business cycle, solve the equity premium and risk-free rate puzzles in endowment economies under Epstein-Zin preferences (Bryzgalova et al., 2026). In a production economy, however, the mechanism requires *frictions* that generate persistence: without them, agents absorb the shock instantaneously, the marginal value of capital stays essentially constant, and equity carries no exposure to the shock (Croce, 2014). Real, nominal, or informational rigidities can all play this role.

Table 4: Risk price of the f_t shock to macroeconomic factors

	λ_f	$\mathbb{E}[SR_f \mid \text{data}]$	$\mathbb{E}\left[\frac{SR_f^2}{SR_m^2} \mid \text{data}\right]$
GDP growth	0.226 [0.098, 0.353]	0.452 [0.196, 0.706]	0.231 [0.047, 0.513]
IP growth	0.223 [0.096, 0.341]	0.447 [0.192, 0.682]	0.221 [0.046, 0.479]
Durable consumption growth	0.340 [0.190, 0.472]	0.681 [0.393, 0.944]	0.528 [0.201, 0.826]
Nondurable consumption growth	0.283 [0.157, 0.411]	0.567 [0.314, 0.822]	0.358 [0.122, 0.660]
Nondurable + service	0.212 [0.046, 0.369]	0.425 [0.114, 0.740]	0.204 [0.015, 0.558]
Dividend growth	0.245 [0.120, 0.375]	0.491 [0.240, 0.750]	0.270 [0.072, 0.558]
Unemployment rate change	-0.241 [-0.361, -0.123]	0.483 [0.246, 0.722]	0.262 [0.076, 0.511]
Hours worked growth	0.243 [0.119, 0.363]	0.487 [0.238, 0.726]	0.264 [0.073, 0.527]
Investment growth	0.253 [0.126, 0.371]	0.507 [0.253, 0.742]	0.280 [0.083, 0.546]

Risk price of f_t shock to nontraded factors (λ_f); annualized Sharpe ratio of $\lambda_f f_t$ ($\mathbb{E}[SR_f \mid \text{data}]$); share of SDF variance explained by f_t ($\mathbb{E}[SR_f^2/SR_m^2 \mid \text{data}]$). SDF decomposition in Online Appendix OA.2.2; setup as in Table 1. Posterior median and 90% credible intervals.

What remains open is the *origin* of the shock. Since TFP seems unpriced, we turn next to alternative disturbances (e.g., demand or sentiment and credit supply) and to the real, nominal, and informational frictions consistent with our findings.

2.1.4 The Macroeconomic Origins of Priced Shocks

Having established that the priced shocks have a common footprint, we turn to their origins. Intermediary-based state variables are significantly priced, but with flat (He et al., 2017) or weakly decreasing (Adrian et al., 2014) term structures; rationalising the sharply increasing term structures of the macro aggregates requires more. For each class of potential mechanisms, we focus on the state variables that should span the shocks driving the business cycle and analyze the term structure of their risk premia, checking whether the sign and shape, and the correlation of their priced shocks with the other macro variables, are consistent with each theory. Inflation and nominal frictions warrant a separate analysis and are discussed in Section 2.1.5.

Expenditure-switching/Tobin's q channel (Hayashi, 1982; Cochrane, 1991). In this class of models, a shock to expected returns on capital moves equity prices immediately, shifting Tobin's q, and propagates gradually (via real frictions) to investment, hiring, and consumption. Since q is essentially a forward-looking asset price, Δq should be approximately unpredictable, implying a flat term structure. Capacity utilization (Greenwood et al., 1988; Basu et al., 2006), by contrast, adjusts gradually and should display an upward-sloping term structure. If this channel is at play, the investment R_g^2 should exceed the consumption one in Table 1.

Panel A of Table 5 reports the term structures for Δq and capacity utilization. The results strongly support this propagation channel. Δq is strongly priced (annualized Sharpe ratio of about 0.4), highly significant at 99% across all horizons, with the flat term structure expected

Table 5: Footprint of priced shocks in the macroeconomy

S = (quarters)	0	2	4	6	8	10	12	R^2_g	$R^2_{g,pred}$	$R^2_{err,pred}$
Panel A. Tobin's Q channel										
ΔTobin's Q (1963Q3-2019Q4)	0.195***	0.200***	0.202***	0.202***	0.201***	0.202***	0.200***	83.0%	0.3%	2.1%
Capacity utilization growth (1967Q2-2019Q4)	0.007	0.077**	0.124**	0.147**	0.155**	0.152**	0.145**	37.4%	37.2%	10.9%
Panel B. Consumer sentiment/confidence										
ΔConsumer confidence (1963Q3-2019Q4)	0.106***	0.104***	0.102***	0.101***	0.095***	0.088***	0.084***	30.2%	6.0%	8.7%
ΔMichigan consumer sentiment (1963Q3-2019Q4)	0.091***	0.101***	0.101***	0.101***	0.098***	0.092***	0.088***	24.3%	5.7%	11.7%
SPF GDP forecast error (1969Q1-2019Q4)	0.014	0.038	0.050	0.055	0.055	0.057	0.058	19.1%	16.1%	12.3%
Panel C. Noise/dispersed-information shocks										
SPF c.f. dispersion (GDP growth, 1968Q4-2019Q4)	-0.023	-0.041	-0.069	-0.098*	-0.122*	-0.142*	-0.161*	18.3%	16.8%	50.8%
Macro uncertainty (3-month, 1963Q3-2019Q4)	-0.047**	-0.075**	-0.073**	-0.067**	-0.050	-0.037	-0.023	26.8%	20.6%	13.4%
Macro uncertainty (12-month, 1963Q3-2019Q4)	-0.055***	-0.085***	-0.081***	-0.071**	-0.050	-0.032	-0.016	26.7%	19.2%	22.2%
GDP revision magnitudes (1965Q3-2019Q4)	0.007	0.003	0.001	0.000	-0.002	-0.001	0.000	8.1%	7.8%	10.1%
Panel D. Real and policy uncertainty										
Real uncertainty (3-month, 1963Q3-2019Q4)	-0.029*	-0.046*	-0.047*	-0.052*	-0.044*	-0.040	-0.032	17.8%	15.1%	15.9%
Real uncertainty (12-month, 1963Q3-2019Q4)	0.000	0.002	0.002	0.003	0.004	0.004	0.004	7.1%	7.0%	16.3%
Economic Policy Uncertainty, EPU (1963Q3-2019Q4)	-0.007	-0.006	-0.005	-0.005	-0.005	-0.005	-0.005	29.2%	4.7%	19.9%
Panel E. Preference shocks with slow real adjustment										
ΔPersonal savings rate (1963Q3-2019Q4)	-0.006	-0.007	-0.008	-0.009	-0.012	-0.013	-0.015	12.4%	9.0%	18.4%
ΔConsumption-to-income ratio (1963Q3-2019Q4)	0.003	0.008	0.010	0.012	0.014	0.015	0.014	8.1%	7.2%	14.7%
Panel F. Credit supply shocks										
Excess bond premium (1973Q1-2019Q4)	-0.028	-0.054	-0.076	-0.094	-0.108	-0.119	-0.128	67.8%	47.6%	14.0%
Bank credit growth (1963Q3-2019Q4)	-0.025*	-0.024	-0.006	0.015	0.043	0.072	0.098	35.1%	31.5%	34.0%
Senior Loan Officer net tightening (1990Q2-2019Q4)	-0.021	-0.065	-0.111	-0.156	-0.192	-0.227	-0.255	72.5%	67.3%	9.1%
Panel G. Investment-specific technology shocks										
Growth of relative price of investment (1963Q3–2019Q4)	-0.004	-0.011	-0.039	-0.062	-0.078	-0.082	-0.086	15.6%	15.4%	36.7%
Equipment investment growth (1963Q3–2019Q4)	0.002	0.023	0.045	0.059	0.068	0.072	0.073	27.9%	27.6%	12.3%
Structures investment growth (1963Q3–2019Q4)	-0.006	0.000	0.015	0.036	0.053	0.068	0.080	28.8%	27.9%	16.2%
Panel H. Matching efficiency shocks										
ΔJob finding rate (1967Q3–2007Q2)	0.003	0.032	0.066	0.102	0.128	0.154	0.179	17.2%	17.1%	22.4%
ΔSeparation rate (1967Q3–2007Q2)	-0.002	-0.030	-0.044	-0.047	-0.046	-0.046	-0.043	13.5%	13.2%	20.1%

Bayesian estimates of factors' risk premia from Proposition A1; λ_g^S defined in eq. (5). Base assets: 275 Fama-French characteristic-sorted portfolios; five-factor model. All data are at the quarterly frequency. We estimate factor risk premia using 12-quarter lags in g_t's equations. *, **, ***: 90%, 95%, 99% Bayesian CI excludes zero. R^2_g: total from priced shocks; $R^2_{g,pred}$: predictive, excluding contemporaneous shock; $R^2_{err,pred}$: from error w_{gt} via AR(12). Data sources: Online Appendix OA.4.

of an efficient asset price ($\lambda_g^S \approx 0.20$ at all horizons, $R^2_{g,pred} = 0.3\%$). Striking is the explanatory power: priced shocks account for 83% of the total time series variation in Δq, confirming that q is overwhelmingly driven by the same systematic risk that prices equities.

Capacity utilization has a significantly upward-sloping term structure (from 0.007 to 0.145 quarterly Sharpe ratios), confirming the slow propagation of priced shocks into real quantities. The correlation between this variable's priced shock and GDP's is almost perfect at 99.2% (versus a raw-variable correlation of about 61%). The contrast between the flat term structure of Δq and the upward-sloping ones of real quantities is consistent with q acting as a transmission channel: the priced shock is immediately reflected in the shadow value of capital, propagating only gradually (via real frictions) to the real economy. This does not imply that priced shocks originate from q; it confirms our method's ability to recover priced shocks (any priced shock should be reflected in q) and points to real frictions as the slow-propagation mechanism.

Demand/sentiment/confidence shocks (Angeletos et al., 2020; Angeletos and La'O, 2013; Huo and Takayama, 2023; Benhabib et al., 2015). A non-technology demand or belief shock could drive coordinated booms and busts: asset prices jump while real quantities adjust slowly as beliefs propagate. Panel B of Table 5 reports the term structure for three potential state variables: consumer confidence, the Michigan Consumer Sentiment Index, and the SPF GDP forecast error (mean forecast minus realized). If this channel is operative, the priced shocks in the first two should be highly correlated with those driving GDP risk premia, and the forecast error should be unpriced or at most have a flat term structure (a pure belief shock generates no systematic ex-post forecast errors). Consumer confidence and Michigan sentiment are both significantly priced at all horizons, with flat term structures and essentially identical risk premia. The SPF GDP forecast error is unpriced, as expected for a pure belief shock that generates no systematic ex-post forecast errors. The priced shocks in confidence and sentiment are virtually identical (correlation 99.5%) and "almost the same" as those in GDP, hours, investment, and non-durable consumption: correlations with f above 90%, against raw-variable contemporaneous correlations of 8% at best. Both series behave like jump variables: high contemporaneous R^2_g (24%–30%) but low predictive $R^2_{g,pred}$ (about 6%). They reflect the priced shock in real time without the gradual adjustment of GDP and similar aggregates: fast-moving barometers of the common shock, not slowly-diffusing drivers.

Noise/dispersed-information shocks (Lorenzoni, 2009; Blanchard et al., 2013; Chahrour and Jurado, 2018; Angeletos and Huo, 2021). If agents receive noisy signals, asset prices aggregate information quickly while real quantities respond with delay as signals diffuse across heterogeneous agents. Panel C of Table 5 reports term structures for GDP revision magnitudes (final minus advance release), SPF cross-forecaster dispersion, and the Jurado et al. (2015) (JLN) macro uncertainty indices at 3- and 12-month horizons. GDP revisions are unpriced, as expected (they are akin to measurement noise). Cross-forecaster dispersion is negatively priced and significantly so at longer horizons, with a term structure that increases in absolute value. The JLN macro uncertainty measures display hump-shaped term structures peaking around $S = 2$–4, and their priced shocks are highly correlated with those of real quantities and consumer confidence. The upward-sloping term structure of SPF dispersion may seem unexpected, as most models would predict flat or downward-sloping estimates. But in Lorenzoni (2009) and Angeletos and Huo (2021), disagreement is high precisely when the informational friction binds, i.e., when agents receive heterogeneous signals about the common shock. If dispersion proxies

for the degree of informational friction (which is itself persistent and cyclical), the upward-sloping shape is consistent with SPF dispersion measuring the intensity of the coordination problem. That said, priced shocks contribute relatively little to this proxy ($R^2_g = 18\%$), which exhibits substantial *unpriced* persistence ($R^2_{err,pred} = 51\%$). The evidence is partially supportive and, as we discuss below, the information channel is reinforced by the inflation evidence, where cross-forecaster dispersion of the GDP deflator expectations appears to be significantly priced.

Real and policy uncertainty (Bloom, 2009; Bloom et al., 2018; Ludvigson et al., 2021). Macro uncertainty operating through real options on irreversible investment and hiring could propagate slowly and generate the upward-sloping term structure of macro variables. Panel D of Table 5 reports the term structure for three uncertainty measures. Only the three-month uncertainty measure of Ludvigson et al. (2021) is marginally priced (negative, significant at 90% at short-to-medium horizons), with small risk premia and a modest contribution of priced shocks to its dynamics ($R^2_g = 17.8\%$); but its priced shocks are highly correlated with those of GDP, consumption, etc. The Baker et al. (2016) economic policy uncertainty index is unpriced.

Discount rate/preference shocks with slow real adjustment (Basu and Bundick, 2017). A shock to household patience or willingness to spend could hit asset prices via discount rates and propagate slowly through adjustment costs and nominal rigidities. We find no support for this mechanism: both the savings rate and the consumption-to-income ratio are unpriced, with tiny R^2_g (12.4% and 8.1%) and flat term structures. These findings rule out only pure preference shocks over consumption (Basu and Bundick, 2017), not discount rate shocks operating through the labor market: for instance, Hall (2017) models a discount rate shock that affects firm hiring decisions, whereby firms discount future profits from filled vacancies more heavily and reduce job creation. Given that unemployment has the highest R^2_g (47%), this channel remains viable, and we analyze labor wedge and matching efficiency shocks below.

Credit supply shocks (Jermann and Quadrini, 2012; Gilchrist and Zakrajšek, 2012). In these models, tightening credit conditions propagate to investment and hiring, with asset prices responding first. Panel F of Table 5 reports our findings for the standard state variables. The excess bond premium (EBP) has a negative, monotonically increasing (in absolute value) term structure from -0.028 to -0.128, exactly the shape predicted by the theory, but the credible intervals include zero throughout. This is plausibly a power issue: the EBP has $R^2_g = 67.8\%$ and $R^2_{g,pred} = 47.6\%$, so priced shocks explain the bulk of its dynamics, mostly via lagged

propagation. Bank credit growth flips sign from negative (short horizon) to positive (long horizon), with $R^2_g = 35.1\%$ and similar magnitudes for its priced and unpriced predictive components. The Senior Loan Officer net tightening survey has the right shape (negative, steeply increasing in absolute value, reaching -0.255) with $R^2_g = 72.5\%$ and $R^2_{g,pred} = 67.3\%$, but also fails significance, likely due to the short sample starting in 1990. The credit-channel variables all have the right fingerprint (high R^2_g, slow propagation, right signs) but lack power to reach significance individually. The findings are qualitatively consistent with this theory, though statistical support is weak.

Investment-specific technology (IST) shocks (Greenwood et al., 1997; Fisher, 2006; Justiniano et al., 2010). The evidence in Sections 2.1.1 and 2.1.2 does not support the view that the priced shocks in macro quantities are factor-neutral productivity shocks. An alternative is heterogeneous technology shocks, in particular to the efficiency of producing capital goods. In Panel G of Table 5 we turn to the term structure of the growth rate of the relative price of investment goods (the standard IST proxy), equipment, and structures investment. These models imply that the relative price of investment should have a significantly priced, upward-sloping term structure, with equipment investment having a steeper one (since IST shocks hit equipment directly more than structures). The relative price of equipment has a negative but insignificant risk premium at all horizons. Equipment and structures investment both show upward-sloping term structures, but neither is significant, and equipment does not dominate structures as IST predicts. The relative price variable also has a low R^2_g (15.6%) and a very high $R^2_{err,pred}$ (36.7%), so most of its predictability comes from unpriced shocks. IST is unlikely to be the common priced shock.[17]

Labor wedge/matching efficiency shocks (Shimer, 2005; Hall, 2017; Kehoe et al., 2019; Hagedorn and Manovskii, 2008; Gertler and Trigari, 2009). Hours worked and unemployment have the highest R^2_g from priced shocks in Table 1 (35% and 47%), and their priced shocks are nearly perfectly correlated (-0.97). A labor search model with a matching efficiency shock would generate this pattern: such shocks would be reflected in prices immediately but propagate to real quantities with delay as employment and production adjust gradually. Panel H of Table 5 reports the term structure for job-finding and separation rates. Consistent with the theory,

[17] Justiniano et al. (2010) also find that marginal efficiency of investment (MEI) shocks account for the largest share of business-cycle variance in output, hours, and investment. These latentshocks correlate strongly with credit spreads (Justiniano et al., 2011) and financial conditions indices like those in Panel F of Table 5.

the separation rate is unpriced (separation shocks are typically modeled as idiosyncratic), while the job-finding rate displays an upward-sloping term structure. Nevertheless, these risk premia are not statistically significant, so empirical support for this origin is limited.[18]

Other: fiscal, monetary, and financial. Empirical proxies of fiscal shocks (government spending growth and Ramey (2011) defence news shocks), monetary shocks (Nakamura and Steinsson (2018) shocks and federal funds rate changes), financial risk perceptions (Pflueger et al., 2020), and household financial obligations are all unpriced in the cross-section of equity returns[19] with low R_g^2.

2.1.5 Inflation and Nominal Frictions

In New Keynesian models with sticky prices (Christiano et al., 2005; Smets and Wouters, 2007), an aggregate demand shock moves inflation and real activity in the same direction through the Phillips curve.[20] Demand-driven inflation should therefore carry a *positive* risk premium (higher inflation coincides with low-marginal-utility states), and its priced shock should comove with the one driving real quantities (Cieslak and Pflueger, 2023; Campbell et al., 2020).

Cost-push shocks, by contrast, move inflation and real activity in opposite directions: cost-driven inflation should carry a *negative* risk premium (higher inflation coincides with high-marginal-utility states, so that a payoff growing at the rate of inflation hedges bad times). Nominal rigidities are not required for this "bad inflation" premium to arise, since stagflation dynamics can emerge with fully flexible prices (Finn, 2000); nominal rigidities nonetheless amplify the effect and generate inflation persistence. Similarly, models with information frictions in price setting (Mankiw and Reis, 2002; Woodford, 2003) generate endogenously time-varying cross-forecaster disagreement about both inflation and real activity, both of which we measure using SPF cross-forecaster dispersions. As disagreement is elevated in bad times, it should carry a negative risk premium; if a common informational friction drives disagreement about both, the priced shocks in the two dispersions should comove.

[18] Similarly, in unreported results with even shorter time series, we find sharply increasing yet insignificant term structures of risk premia for JOLTS vacancy rates and labor market tightness.

[19] These unconditional findings do not preclude conditional risk premia under policy regime shifts (Sims and Zha, 2006; Campbell et al., 2020).

[20] All inflation risk premia reported in this section are estimated from the equity cross-section. Under fully integrated markets, equity-implied premia coincide with those from any other priced claim on inflation; under segmentation they need not. Bahaj et al. (2025) document substantial segmentation in the UK inflation swap market across horizons and trader types, with short-horizon prices primarily reflecting liquidity shocks rather than expected inflation.

Table 6: Inflation Risk Premia

Panel A. Quarterly variables, $\bar{S} = 12$ quarters										
S = (quarters)	0	2	4	6	8	10	12	R^2_g	$R^2_{g,pred}$	$R^2_{err,pred}$
CPI growth (1963Q3–2019Q4)	-0.040	-0.076*	-0.093*	-0.113*	-0.130*	-0.146*	-0.164*	14.9%	12.1%	39.8%
BNS cyclical inflation (1963Q3–2019Q4)	-0.048	-0.088*	-0.133*	-0.181**	-0.221**	-0.256**	-0.285**	24.1%	21.0%	51.5%
SPF c.f. dispersion (GDP deflator, 1968Q4–2019Q4)	-0.023	-0.049*	-0.082*	-0.106*	-0.127**	-0.148**	-0.170**	24.3%	22.9%	29.9%
Inflation volatility (1967Q3–2019Q4)	0.000	0.001	0.002	0.003	0.003	0.003	0.004	7.3%	7.2%	15.8%
Unit labor cost growth (nominal, 1963Q3–2019Q4)	-0.015	-0.018	-0.025	-0.031	-0.035	-0.038	-0.042	9.3%	7.2%	22.2%
Unit labor cost growth (real, 1963Q3–2019Q4)	0.005	0.005	0.004	0.002	0.001	0.001	0.001	10.4%	9.5%	15.1%
Labor share growth (1963Q3–2019Q4)	-0.001	-0.002	-0.001	0.000	0.001	0.002	0.003	10.7%	10.0%	12.2%
Panel B. Monthly variables, $\bar{S} = 24$ months										
S = (months)	0	4	8	12	16	20	24	R^2_g	$R^2_{g,pred}$	$R^2_{err,pred}$
PPI growth, all commodities (July 1963 to Dec 2019)	-0.018	-0.029	-0.046	-0.060*	-0.075*	-0.085*	-0.091**	7.8%	6.9%	16.5%
PPI growth, industrial commodities (July 1963 to Dec 2019)	-0.024*	-0.034	-0.057	-0.076*	-0.094*	-0.108*	-0.117**	9.8%	8.6%	23.2%
PPI growth, metals (July 1963 to Dec 2019)	-0.016	-0.044	-0.074*	-0.100*	-0.124*	-0.142*	-0.157*	10.5%	9.6%	43.7%

Bayesian estimates of factors' risk premia from Proposition A1; λ_g^S defined in eq. (5). Base assets: 275 Fama-French characteristic-sorted portfolios; five-factor model. Panel A: quarterly, $\bar{S} = 12$. Panel B: monthly, $\bar{S} = 24$. *, **, ***: 90%, 95%, 99% Bayesian CI excludes zero. R^2_g: total from priced shocks; $R^2_{g,pred}$: predictive, excluding contemporaneous shock; $R^2_{err,pred}$: from w_{gt} via AR(12). Data: Online Appendixes OA.4 and OA.7.

Panel A of Table 6 reports results for four inflation-related variables. CPI growth is significantly *negatively* priced from $S = 2$ onward, with a sharply increasing (in absolute value) term structure. Priced shocks explain a much lower share of CPI variation and predictability than for the core macro quantities in Table 1, and most of CPI's predictability is unpriced. The Bianchi, Nicolò, and Song (2023) cyclical inflation measure, which strips out low-frequency trend movements such as the Volcker disinflation, is significantly negatively priced also from $S = 2$ onward, with a steeply upward-sloping (in absolute value) term structure and larger risk premia than CPI growth.[21] The negative sign of the term structure directly identifies the priced part of cyclical inflation as loading on high-marginal-utility states: a cost-push signature. The increasing magnitude, in turn, implies that the response of cyclical inflation to the priced shock builds up gradually rather than being absorbed instantaneously, a slow-propagation pattern characteristic of nominal or informational rigidities.[22]

Cross-forecaster dispersion of the GDP deflator tells a complementary story: significantly negatively priced, with priced shock highly correlated with the GDP (0.78) and unemployment-rate (0.76) priced shocks, and almost perfectly correlated (0.97) with that of real GDP growth dispersion. A single informational friction appears to generate disagreement about both nominal

[21] GDP deflator and CPI core inflation, untabulated, show similar patterns but with wider confidence bounds.

[22] In contrast to the near-zero correlation between business-cycle drivers of inflation and labor markets in Angeletos et al. (2020), our identification recovers correlations of 0.32 and 0.50 between cyclical inflation's priced shock and the priced shocks in GDP and unemployment. The disparity reflects different identifications: Angeletos et al. (2020) maximize the variance contribution in a fixed-coefficient VAR, while we use cross-sectional pricing restrictions on equity returns, isolating the parts of macro series that load on the SDF.

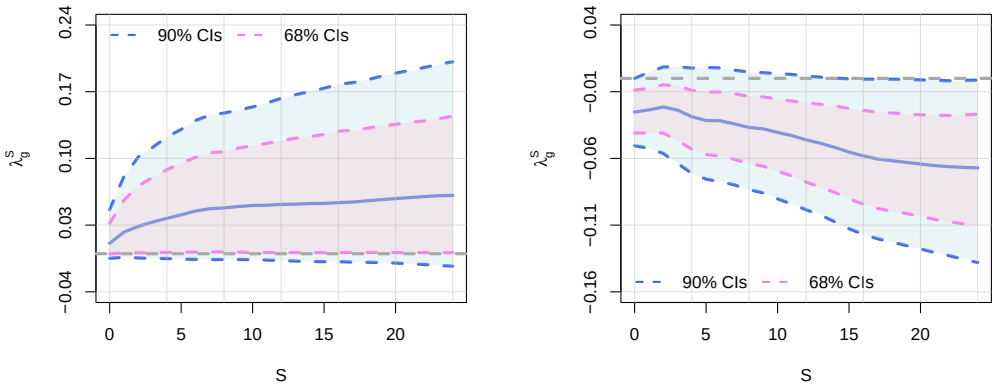

(a) Demand-driven PPI inflation, π_t^D **(b)** Supply-driven PPI inflation, π_t^S

Figure 5: Term structure of risk premia: demand- and supply-driven PPI inflation

Term structure of monthly risk premia (Sharpe ratio units) from Proposition A1; λ_g^S defined in eq. (5). The two macro factors are the demand- (π_t^D) and supply-driven (π_t^S) components of monthly producer-price inflation (construction in Online Appendix OA.7.2). Base assets: 275 Fama-French characteristic-sorted portfolios; five-factor model; $\bar{S} = 24$. Shaded areas: 68% (pink) and 90% (blue) Bayesian CI. Data sources: Online Appendix OA.4. Sample: February 1978–December 2019 (start dictated by PPI decomposition availability).

and real outcomes. Inflation volatility, by contrast, is unpriced at all horizons ($R_g^2 = 7.3\%$): the relevant nominal channel operates through the level and dispersion of inflation expectations, not through inflation uncertainty.

We investigate the cost-push hypothesis further through two sets of empirical proxies: three PPI measures of input costs (Panel B) and three labor-cost measures (bottom rows of Panel A). All PPI growth measures display negative and increasing (in absolute value) term structures of risk premia, statistically significant from at least twelve months onward. The labor-cost proxies yield small and insignificant risk premia, suggesting that non-labor costs are the primary drivers of cost-push shocks in our sample. Across both panels, R_g^2 for the cost-push proxies is small relative to Table 1, and most predictability is driven by unpriced shocks.

Since all inflation measures in Table 6, including the PPI ones, implicitly aggregate both demand- and supply-driven price pressures, our results do not imply the absence of a demand-driven inflation risk premium: only that, unconditionally, the "bad inflation" (negative) premia dominate the "good inflation" (positive) ones. We address this compositional issue by extending the demand/supply-driven inflation decomposition of Shapiro (2022) to the producer side, constructing a demand- (π_t^D) and supply-driven (π_t^S) series as equal-weighted averages across twelve disaggregated PPI/NAICS-3 industrial-production pairs.[23] Figure 5 reports the two

[23]The aggregate supply-driven series spikes at each major cost-push episode, while the demand-driven series

components and confirms the predicted decomposition: demand-driven PPI inflation carries a positive term structure of risk premia, whereas supply-driven PPI inflation a negative one. Credible intervals are wide, plausibly reflecting the shorter sample (February 1978 onward, dictated by the availability of the NAICS-3 IP series), and exclude zero only for the supply-driven component, and only at short and long horizons. The cleanly opposite signs reinforce the cost-push reading of the aggregate negative inflation premia in Table 6: within the priced inflation shocks, a positive demand-driven premium seems present but is unconditionally dominated by the negative supply-driven one.

2.2 Time-Varying Macro Risk Premia: Estimation and Validation

Many macro-finance equilibrium models feature time-varying risk premia. This section applies our framework to two complementary tasks. First, Section 2.2.1 estimates the time-varying term structures of risk premia for the macro factors of Section 2.1. Since macroeconomic risk premia have no observable counterpart, a direct validation of the conditional properties of our method is infeasible; Section 2.2.2 addresses this through an indirect but stringent test. We apply the same priced moving-average machinery to dividend growth, itself one of the macro factors of Section 2.1, and generate model-implied forward equity yields. These yields are observable for the post-2004 period (Bansal et al., 2021) but are *not used* in our estimation, providing out-of-sample evidence on the conditional properties of our priced-Wold representation. The comparison is also of independent interest, connecting our framework to the literature on dividend strips and forward equity yields (van Binsbergen et al., 2012; Bansal et al., 2021; Giglio et al., 2023).

2.2.1 Time-Varying Term Structure of Macroeconomic Risk Premia

We estimate the time variation in the term structure of macro factors' risk premia, applying the method of Section 1.1. Following past literature (e.g., Campbell and Vuolteenaho (2004), Campbell et al. (2013), Gagliardini et al. (2016)), we use as external predictors the price-earnings ratio and the term, default, and value spreads. With this formulation, we re-estimate the term structures of unconditional risk premia for the same set of variables as in Table 1, as a check on the unconditional estimates of Section 2.1. The conditional-model estimates are almost identical to those reported earlier, with occasional minor attenuation and wider intervals due to the additional VAR parameters: our unconditional estimates remain consistent even if

contracts in NBER recessions. See Online Appendix OA.7.2 for details.

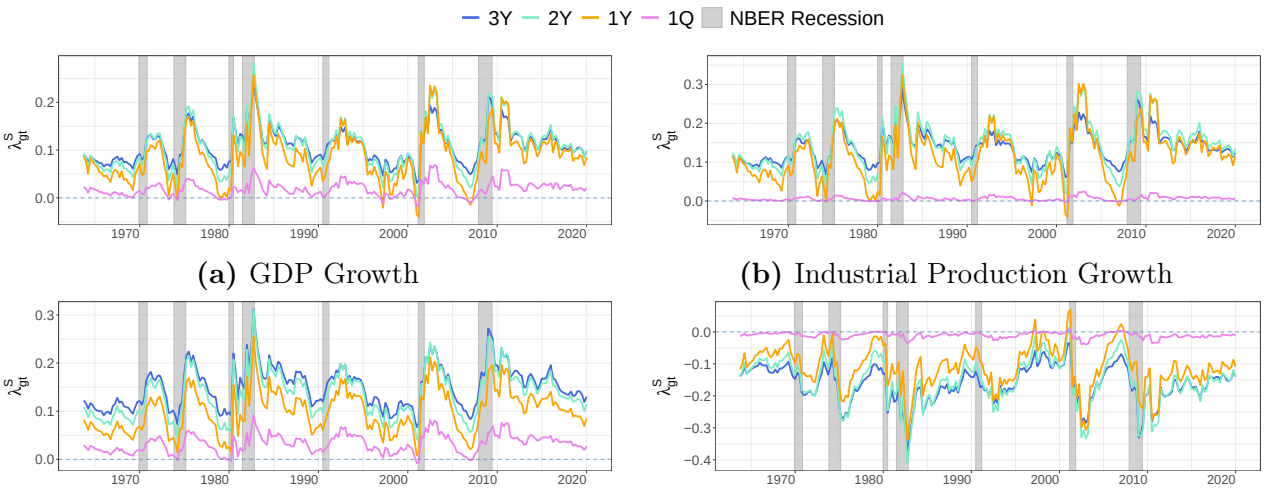

(a) GDP Growth

(b) Industrial Production Growth

(c) Nondurable Consumption Growth

(d) Unemployment Rate Change

Figure 6: Time-varying term structure of macroeconomic factor's risk premia

Time-varying term structure of quarterly risk premia following Section 1.1; latent risk prices linear in four external predictors: S&P 500 PE ratio, term spread, default spread, and value spread. Base assets: 275 Fama-French characteristic-sorted portfolios. Data sources: Online Appendix OA.4.

the true model is time-varying.

Figure 6 reports the posterior means of the time-varying risk premia at one-quarter to three-year horizons for nondurable consumption, GDP, industrial-production growth, and unemployment rate change (Panels (a)–(d)).[24] Two observations are in order. First, the average level is strongly countercyclical: small premia in expansions, sharply increasing premia in recessions. Second, short-maturity (e.g., one-quarter) macro risk premia exhibit minimal time variation, confirming that macro variables are weak factors at best at short horizons, even conditionally. The clear commonality in the business-cycle behavior of the term structures of macro risk premia across factors further reinforces the unconditional-finding of Section 2.1: a single priced shock drives the conditional means of macro factors at business-cycle frequencies.

These findings impose a sharp discipline on equilibrium macro-finance models: a satisfactory model should generate countercyclical risk premia for the core macroeconomic factors, with comparable business-cycle sensitivity across them and relatively muted at short horizons. The two canonical channels for generating such time variation are a time-varying price of risk, through countercyclical risk aversion or risk-bearing capacity (e.g., Campbell and Cochrane, 1999; He et al., 2017), and a time-varying quantity of risk, through countercyclical conditional volatility or perceived uncertainty (e.g., Bansal and Yaron, 2004; Bloom, 2009). Our conditional

[24] We obtain similar results for durable consumption, dividends, and hours worked.

evidence is consistent with both being at play.

2.2.2 Term Structure of (Dividend) Risk Premia vs. Strips

We connect the term structure of dividend risk premia defined in equation (9) to forward equity yields, which provide an observable counterpart against which to validate the conditional properties of our priced moving-average representation. In Online Appendix OA.8, we show that under joint log-normality of the SDF and dividend growth, the forward equity yield (e^f) and dividend risk premia satisfy

$$e^f_{s,t} = \lambda^s_{dt} - \mathbb{E}_t[g_{d,t,t+s}] - \frac{1}{2s}\text{var}_t(\Delta d_{t,t+s}) \approx \lambda^s_{dt} - \mathbb{E}_t[g_{d,t,t+s}], \tag{11}$$

where $g_{d,t,t+s} = \frac{1}{s}\log\left(\frac{D_{t+s}}{D_t}\right)$ is the per-period log dividend growth rate, $\Delta d_{t,t+s} = \log\left(\frac{D_{t+s}}{D_t}\right)$ is multiperiod dividend growth, and $\lambda^s_{dt} = -\frac{1}{s}\text{cov}_t(m_{t,t+s}, \Delta d_{t,t+s})$ is the s-period dividend risk premium defined in equation (9). Since $\text{var}_t(\Delta d_{t,t+s})$ is empirically negligible, the forward equity yield is well approximated by $\lambda^s_{dt} - \mathbb{E}_t[g_{d,t,t+s}]$.

Equation (11) makes clear the distinction between the term structure of dividend risk premia and that of strips: the forward equity yields are driven by *both* dividend risk premia and expected dividend growth. As shown in Online Appendix OA.8, dividend risk premia can be interpreted as the per-period risk premium on hold-to-maturity dividend strips. We estimate the term structure of unconditional dividend risk premia using our MA formulation, and Figure OA.6 of the Online Appendix shows that our estimated one- to five-year premia are very close to those reported in Bansal et al. (2021), despite an entirely different data, sample, and method.

To obtain the term structure of dividend strips, we estimate the conditional mean of dividend growth using equation (4):

$$\mathbb{E}_t[g_{d,t,t+s}] = \frac{1}{s}\sum_{\tau=1}^{s}\mathbb{E}_t[\Delta d_{t+\tau}], \quad \mathbb{E}_t[\Delta d_{t+\tau}] = \mu_g + \sum_{s=\tau}^{\bar{S}}\tilde{\rho}_s f_{t+\tau-s}. \tag{12}$$

Equation (12) projects the conditional mean of dividend growth onto the priced part of our representation only: the unspanned component w_{gt} in equation (4) is allowed to be persistent but its dynamics are left unmodelled. This unpriced predictability is non-trivial in the data: $R^2_{err,pred} = 17.6\%$ in Table 1 for dividend growth. Consequently, the forward equity yields implied by our priced MA representation are not guaranteed to match the empirically observed ones exactly, with the gap attributable to the omitted unpriced predictability of dividends.

We estimate forward equity yields for one-, two-, and five-year holding horizons using equa-

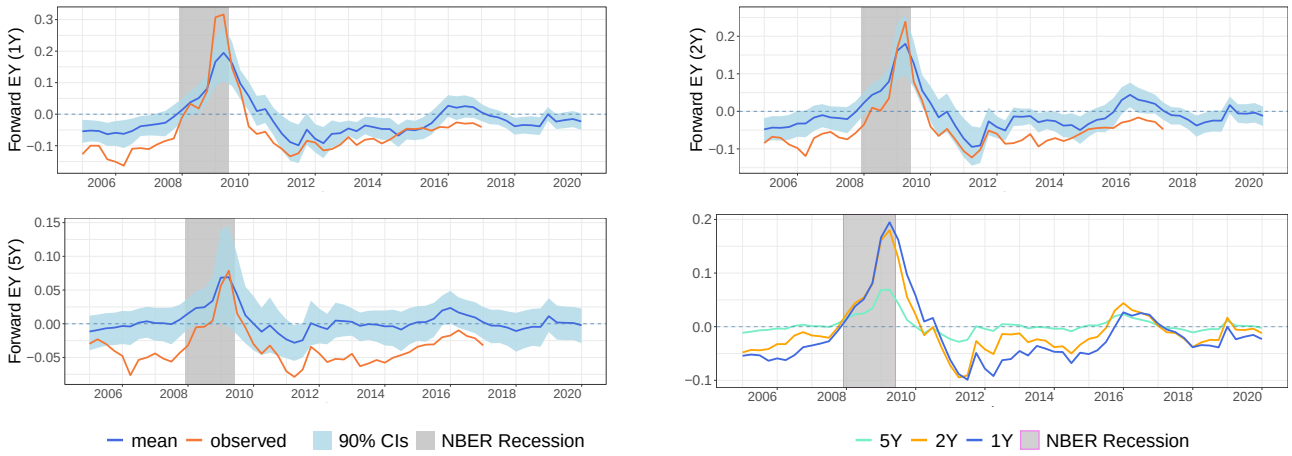

Figure 7: Time series of estimated forward equity yields

Estimated time-varying forward equity yields from our MA model with 20 lags. Five-factor model on FF275, 1963Q3–2019Q4; plot restricted to 2004Q4–2019Q4 (observed-data period, not used in estimation). Bottom-right panel: posterior means at all horizons. Observed yields from Bansal et al. (2021).

tion (11). The estimation uses the full sample (1963Q3–2019Q4), but Figure 7 displays only 2004Q4–2019Q4, the period with observed forward equity yield data, which are *not used* in our estimation.[25] The figure shows that our model generates a downward-sloping term structure of equity yields in bad economic states and an upward-sloping one during expansions, consistent with the observed data. The bottom right panel reports our estimates for all horizons; the remaining panels show observed yields alongside our estimates and 90% credible intervals. Our estimates are also strongly countercyclical and closely track the observed data. As noted around equation (12), our MA formulation allows for unmodelled sources of *unpriced* dividend predictability, likely driving the minor differences between our estimates and the observed yields. Overall, our priced moving-average representation, estimated without using any forward equity yield data, reproduces the level, dynamics, and term-structure shape of the observed yields, providing out-of-sample evidence on the conditional properties of our method.

3 Conclusion

We develop a new identification scheme, rooted in a priced Wold decomposition, that uses the cross-section of asset returns to recover the shocks common to financial markets and the macroeconomy, their propagation through macroeconomic time series, and the term structure of risk premia for any covariance-stationary economic factor. Hierarchical Bayesian inference

[25]The data on realized one-, two-, and five-year forward equity yields are from Bansal et al. (2021). We thank the authors for sharing the data with us.

delivers valid credible intervals for the entire term structure, both unconditional and time-varying, with all conditional posteriors available in closed form.

Using a large cross-section of equity portfolios, the framework reveals a striking commonality between financial markets and the macroeconomy. The business-cycle dynamics of GDP, industrial production, investment, hours worked, the unemployment rate, and durable and nondurable consumption are pervaded by an almost identical priced shock, which accounts for 20–47% of their variances and the great majority of their predictability. Macro risk premia are small at quarterly horizons but match the equity premium at two- to three-year holding horizons. At those horizons, they are strongly countercyclical: small in expansions and sharply elevated in recessions. Macro risk strikes back at business-cycle frequencies. As an out-of-sample test of the conditional properties of our representation, the implied dividend term structure closely tracks observed forward equity yields *without* using strip data.

The common priced shock is unlikely to be a TFP shock, a finding corroborated by a novel internal-consistency check that reconstructs an implied Solow residual risk premium from the directly estimated GDP, hours, and investment risk premia and yields values close to zero at all horizons. Investment-specific technology and pure-preference shocks are unpriced as well, and standard fiscal and monetary proxies do not carry significant unconditional risk premia.

The picture most consistent with the evidence is that of a non-technology demand or belief disturbance, propagating through real, nominal, and informational rigidities: the textbook Tobin's q channel of investment is sharply identified, inflation carries the cost-push signature of "bad inflation" with a steeply increasing (in absolute value) term structure, and a single informational friction appears to generate disagreement about both nominal and real outcomes. The strongly countercyclical term structures we document also require either countercyclical risk aversion or risk-bearing capacity, or a time-varying quantity of risk (perceived or objective) over the cycle. Overall, our findings deliver a sharp new empirical target for equilibrium models.

References

Adrian, T., E. Etula, and T. Muir (2014). Financial intermediaries and the cross-section of asset returns. *Journal of Finance 69*(6), 2557–2596.

Ai, H., M. M. Croce, A. M. Diercks, and K. Li (2018). News shocks and the production-based term structure of equity returns. *The Review of Financial Studies 31*(7), 2423–2467.

Aït-Sahalia, Y. (2004). Disentangling diffusion from jumps. *Journal of Financial Economics 74*(3), 487–528.

Albuquerque, R., M. Eichenbaum, V. X. Luo, and S. Rebelo (2016). Valuation risk and asset pricing. *Journal of Finance 71*(6), 2861–2904.

Anatolyev, S. and A. Mikusheva (2022). Factor models with many assets: strong factors, weak factors, and the two-pass procedure. *Journal of Econometrics 229*(1), 103–126.

Andries, M., T. M. Eisenbach, and M. C. Schmalz (2024). Horizon-dependent risk aversion and the timing and pricing of uncertainty. *The Review of Financial Studies 37*(11), 3272–3334.

Angeletos, G.-M., F. Collard, and H. Dellas (2020). Business-cycle anatomy. *American Economic Review 110*(10), 3030–3070.

Angeletos, G.-M. and Z. Huo (2021, April). Myopia and anchoring. *American Economic Review 111*(4), 1166–1200.

Angeletos, G.-M. and J. La'O (2013). Sentiments. *Econometrica 81*(2), 739–779.

Bahaj, S., R. Czech, S. Ding, and R. Reis (2025). The market for inflation risk. Working paper, London School of Economics.

Bai, J. and S. Ng (2002). Determining the number of factors in approximate factor models. *Econometrica 70*(1), 191–221.

Baker, S. R., N. Bloom, and S. J. Davis (2016). Measuring economic policy uncertainty. *The Quarterly Journal of Economics 131*(4), 1593–1636.

Bańbura, M., D. Giannone, and L. Reichlin (2010). Large Bayesian vector auto regressions. *Journal of Applied Econometrics 25*(1), 71–92.

Bandi, F. M. and A. Tamoni (2023). Business-cycle consumption risk and asset prices. *Journal of Econometrics*.

Bansal, R., D. Kiku, and A. Yaron (2016). Risks for the long run: Estimation with time aggregation. *Journal of Monetary Economics 82*, 52–69.

Bansal, R., S. Miller, D. Song, and A. Yaron (2021). The term structure of equity risk premia. *Journal of Financial Economics 142*(3), 1209–1228.

Bansal, R. and A. Yaron (2004). Risks for the long run: A potential resolution of asset pricing puzzles. *Journal of Finance 59*(4), 1481–1509.

Barsky, R. B. and E. R. Sims (2011). News shocks and business cycles. *Journal of Monetary Economics 58*(3), 273–289.

Basu, S. and B. Bundick (2017). Uncertainty shocks in a model of effective demand. *Econometrica 85*(3), 937–958.

Basu, S., J. G. Fernald, and M. S. Kimball (2006). Are technology improvements contractionary? *American Economic Review 96*(5), 1418–1448.

Baxter, M. and R. G. King (1999). Measuring business cycles: Approximate band-pass filters for economic time series. *Review of Economics and Statistics 81*(4), 575–593.

Belo, F. and X. Li (2023). Production-based stochastic discount factors. *Available at SSRN 4287502*.

Benhabib, J., P. Wang, and Y. Wen (2015, March). Sentiments and aggregate demand fluctuations. *Econometrica 83*(2), 549–585.

Bernanke, B. S. and K. N. Kuttner (2005). What explains the stock market's reaction to federal reserve policy? *The Journal of Finance 60*(3), 1221–1257.

Bianchi, F., S. C. Ludvigson, and S. Ma (2022). A structural approach to high-frequency event studies: The fed and markets as case history. Working Paper 30072, National Bureau of Economic Research.

Bianchi, F., G. Nicolò, and D. Song (2023). Inflation and real activity over the business cycle. NBER Working Paper 31075, National Bureau of Economic Research.

Black, F., M. C. Jensen, and M. Scholes (1972). The capital asset pricing model: Some empirical tests. In M. C. Jensen (Ed.), *Studies in the Theory of Capital Markets*, pp. 79–121. New York: Praeger Publishers.

Blanchard, O. J., J.-P. L'Huillier, and G. Lorenzoni (2013). News, noise, and fluctuations: An empirical exploration. *American Economic Review 103*(7), 3045–3070.

Bloom, N. (2009, May). The impact of uncertainty shocks. *Econometrica 77*(3), 623–685.

Bloom, N., M. Floetotto, N. Jaimovich, I. Saporta-Eksten, and S. J. Terry (2018). Really uncertain business cycles. *Econometrica 86*(3), 1031–1065.

Bollerslev, T. and J. M. Wooldridge (1992). Quasi-maximum likelihood estimation and inference in dynamic models with time-varying covariances. *Econometric Reviews 11*(2), 143–172.

Borovička, J., L. P. Hansen, and J. A. Scheinkman (2014). Shock elasticities and impulse responses. *Mathematics and Financial Economics 8*(4), 333–354.

Braun, R., A. Flaaen, and S. Hacıoğlu Hoke (2024, February). Supply vs demand factors influencing prices of manufactured goods. FEDS notes, Board of Governors of the Federal Reserve System. February 23.

Bryzgalova, S., J. Huang, and C. Julliard (2023). Bayesian solutions for the factor zoo: We just ran two quadrillion models. *Journal of Finance 78*(1), 487–557.

Bryzgalova, S., J. Huang, and C. Julliard (2024). Bayesian Fama-MacBeth regressions. SSRN Working Paper 4989615, SSRN Electronic Journal.

Bryzgalova, S., J. Huang, and C. Julliard (2026). Consumption in asset returns. *Journal of Finance*. Forthcoming.

Campbell, J. Y. and J. H. Cochrane (1999). By force of habit: A consumption-based explanation of aggregate stock market behavior. *Journal of Political Economy 107*(2), 205–251.

Campbell, J. Y., S. Giglio, and C. Polk (2013). Hard times. *Review of Asset Pricing Studies 3*(1), 95–132.

Campbell, J. Y., C. Pflueger, and L. M. Viceira (2020). Macroeconomic drivers of bond and equity risks. *Journal of Political Economy 128*(8), 3148–3185.

Campbell, J. Y. and T. Vuolteenaho (2004). Bad beta, good beta. *American Economic Review 94*(5), 1249–1275.

Chahrour, R. and K. Jurado (2018). News or noise? the missing link. *American Economic Review 108*(7), 1702–1736.

Chamberlain, G. and M. Rothschild (1983). Arbitrage, factor structure, and mean-variance analysis on large asset markets. *Econometrica: Journal of the Econometric Society 51*(5), 1281–1304.

Chernov, M., L. A. Lochstoer, and S. R. H. Lundeby (2021). Conditional dynamics and the multihorizon risk-return trade-off. *Review of Financial Studies 35*(3), 1310–1347.

Christiano, L. J., M. Eichenbaum, and C. L. Evans (2005). Nominal rigidities and the dynamic effects of a shock to monetary policy. *Journal of Political Economy 113*(1), 1–45.

Cieslak, A. and C. Pflueger (2023). Inflation and asset returns. *Annual Review of Financial Economics 15*, 433–448.

Cochrane, J. (2009). *Asset Pricing: Revised Edition*. Princeton University Press.

Cochrane, J. H. (1991). Production-based asset pricing and the link between stock returns and economic fluctuations. *The Journal of Finance 46*(1), 209–237.

Cochrane, J. H. and M. Piazzesi (2005). Bond risk premia. *American Economic Review 95*(1), 138–160.

Cochrane, J. H. and M. Piazzesi (2008). Decomposing the yield curve. *Available at SSRN 1333274*.

Cogley, T. and T. J. Sargent (2005). Drifts and volatilities: monetary policies and outcomes in the post WWII US. *Review of Economic Dynamics 8*(2), 262–302.

Connor, G. and R. A. Korajczyk (1988). Risk and return in an equilibrium APT: Application of a new test methodology. *Journal of Financial Economics 21*(2), 255–289.

Croce, M. M. (2014). Long-run productivity risk: A new hope for production-based asset pricing. *Journal of Monetary Economics 66*, 13–31.

Crump, R. K., S. Eusepi, D. Giannone, E. Qian, and A. M. Sbordone (2021, August). A large bayesian var of the united states economy. Staff Report 976, Federal Reserve Bank of New York.

Del Negro, M. and G. E. Primiceri (2015). Time-varying structural vector autoregressions and monetary policy: A corrigendum. *Review of Economic Studies 82*(4), 1342–1345.

Del Negro, M. and F. Schorfheide (2004). Priors from general equilibrium models for VARs. *International*

Economic Review 45(2), 643–673.

Dew-Becker, I., S. Giglio, A. Le, and M. Rodriguez (2017). The price of variance risk. *Journal of Financial Economics 123*(2), 225–250.

Elkamhi, R., C. Jo, and Y. Nozawa (2023). A one-factor model of corporate bond premia. *Management Science*.

Eraker, B. and Y. Wu (2017). Explaining the negative returns to VIX futures and ETNs: An equilibrium approach. *Journal of Financial Economics 125*(1), 72–98.

Fama, E. F. (1990). Stock returns, expected returns, and real activity. *The Journal of Finance 45*(4), 1089–1108.

Fama, E. F. and K. R. French (1992). The cross-section of expected stock returns. *The Journal of Finance 47*(2), 427–465.

Fama, E. F. and K. R. French (1993). Common risk factors in the returns on stocks and bonds. *Journal of Financial Economics 33*(1), 3–56.

Faust, J. (1998). The robustness of identified var conclusions about money. In *Carnegie-Rochester conference series on public policy*, Volume 49, pp. 207–244. Elsevier.

Fernald, J. (2014). A quarterly, utilization-adjusted series on total factor productivity. *Working paper*.

Finn, M. G. (2000). Perfect competition and the effects of energy price increases on economic activity. *Journal of Money, Credit and Banking 32*(3), 400–416.

Fisher, J. D. (2006). The dynamic effects of neutral and investment-specific technology shocks. *Journal of Political Economy 114*(3), 413–451.

Francis, N., M. T. Owyang, J. E. Roush, and R. DiCecio (2014). A flexible finite-horizon alternative to long-run restrictions with an application to technology shocks. *Review of Economics and Statistics 96*(4), 638–647.

Gagliardini, P., E. Ossola, and O. Scaillet (2016). Time-varying risk premium in large cross-sectional equity data sets. *Econometrica 84*(3), 985–1046.

Galí, J. (1999). Technology, employment, and the business cycle: Do technology shocks explain aggregate fluctuations? *American Economic Review 89*(1), 249–271.

Gertler, M. and A. Trigari (2009). Unemployment fluctuations with staggered nash wage bargaining. *Journal of Political Economy 117*(1), 38–86.

Giannone, D., M. Lenza, and G. E. Primiceri (2015). Prior selection for vector autoregressions. *Review of Economics and Statistics 97*(2), 436–451.

Giglio, S., B. T. Kelly, and S. Kozak (2023). Equity term structures without dividend strips data. *Journal of Finance (forthcoming)*.

Giglio, S. and D. Xiu (2021). Asset pricing with omitted factors. *Journal of Political Economy 129*(7), 1947–1990.

Gilchrist, S. and E. Zakrajšek (2012). Credit spreads and business cycle fluctuations. *American Economic Review 102*(4), 1692–1720.

Gospodinov, N., R. Kan, and C. Robotti (2014). Misspecification-robust inference in linear asset-pricing models with irrelevant risk factors. *Review of Financial Studies 27*(7), 2139–2170.

Greenwood, J., Z. Hercowitz, and G. W. Huffman (1988). Investment, capacity utilization, and the real business cycle. *American Economic Review 78*(3), 402–417.

Greenwood, J., Z. Hercowitz, and P. Krusell (1997). Long-run implications of investment-specific technological change. *American Economic Review 87*(3), 342–362.

Hagedorn, M. and I. Manovskii (2008). The cyclical behavior of equilibrium unemployment and vacancies revisited. *American Economic Review 98*(4), 1692–1706.

Hall, R. E. (2017). High discounts and high unemployment. *American Economic Review 107*(2), 305–330.

Hansen, L. and R. Jagannathan (1991). Implications of security market data for models of dynamic economies. *Journal of Political Economy 99*(2), 225–262.

Hansen, L. P., J. C. Heaton, and N. Li (2008). Consumption strikes back? Measuring long-run risk. *Journal of*

Political Economy 116(2), 260–302.

Hansen, L. P. and S. F. Richard (1987). The role of conditioning information in deducing testable restrictions implied by dynamic asset pricing models. *Econometrica 55*(3), 587–613.

Hayashi, F. (1982). Tobin's marginal q and average q: A neoclassical interpretation. *Econometrica 50*(1), 213–224.

He, Z., B. Kelly, and A. Manela (2017). Intermediary asset pricing: New evidence from many asset classes. *Journal of Financial Economics 126*(1), 1–35.

Huo, Z. and N. Takayama (2023). Higher-order beliefs, confidence, and business cycles. SSRN Working Paper 4173060.

Ingersoll, J. E. (1984). Some results in the theory of arbitrage pricing. *Journal of Finance 39*(4), 1021–1039.

Jagannathan, R. and Y. Wang (2007). Lazy investors, discretionary consumption, and the cross-section of stock returns. *Journal of Finance 62*(4), 1623–1661.

Jermann, U. and V. Quadrini (2012). Macroeconomic effects of financial shocks. *American Economic Review 102*(1), 238–271.

Johnson, T. L. (2017). Risk premia and the VIX term structure. *Journal of Financial and Quantitative Analysis 52*(6), 2461–2490.

Jordà, Ò. (2005). Estimation and inference of impulse responses by local projections. *American Economic Review 95*(1), 161–182.

Jurado, K., S. C. Ludvigson, and S. Ng (2015). Measuring uncertainty. *American Economic Review 105*(3), 1177–1216.

Justiniano, A., G. E. Primiceri, and A. Tambalotti (2010). Investment shocks and business cycles. *Journal of Monetary Economics 57*(2), 132–145.

Justiniano, A., G. E. Primiceri, and A. Tambalotti (2011). Investment shocks and the relative price of investment. *Review of Economic Dynamics 14*(1), 101–121.

Kan, R., C. Robotti, and J. Shanken (2013). Pricing model performance and the two-pass cross-sectional regression methodology. *Journal of Finance 68*(6), 2617–2649.

Kan, R. and C. Zhang (1999). GMM tests of stochastic discount factor models with useless factors. *Journal of Financial Economics 54*(1), 103–127.

Kehoe, P. J., V. Midrigan, and E. Pastorino (2019, August). Debt constraints and employment. *Journal of Political Economy 127*(4), 1926–1991.

Kleibergen, F. and Z. Zhan (2020). Robust inference for consumption-based asset pricing. *Journal of Finance 75*(1), 507–550.

Kozak, S., S. Nagel, and S. Santosh (2020). Shrinking the cross-section. *Journal of Financial Economics 135*(2), 271–292.

Kung, H. and L. Schmid (2015). Innovation, growth, and asset prices. *Journal of Finance 70*(3), 1001–1037.

Kuttner, K. N. (2001). Monetary policy surprises and interest rates: Evidence from the fed funds futures market. *Journal of Monetary Economics 47*(3), 523–544.

Kydland, F. E. and E. C. Prescott (1982). Time to build and aggregate fluctuations. *Econometrica 50*(6), 1345–1370.

Lamont, O. A. (2001). Economic tracking portfolios. *Journal of Econometrics 105*(1), 161–184.

Lettau, M. and S. Ludvigson (2001). Consumption, aggregate wealth, and expected stock returns. *Journal of Finance 56*(3), 815–849.

Liew, J. and M. Vassalou (2000). Can book-to-market, size and momentum be risk factors that predict economic growth? *Journal of Financial Economics 57*(2), 221–245.

Lorenzoni, G. (2009). A theory of demand shocks. *American Economic Review 99*(5), 2050–2084.

Ludvigson, S. C., S. Ma, and S. Ng (2021). Uncertainty and business cycles: Exogenous impulse or endogenous

response? *American Economic Journal: Macroeconomics 13*(4), 369–410.

Mankiw, N. G. and R. Reis (2002). Sticky information versus sticky prices: A proposal to replace the New Keynesian Phillips curve. *Quarterly Journal of Economics 117*(4), 1295–1328.

Mehra, R. and E. C. Prescott (1985). The equity premium: A puzzle. *Journal of Monetary Economics 15*(2), 145–161.

Müller, U. K. (2013). Risk of Bayesian inference in misspecified models, and the sandwich covariance matrix. *Econometrica 81*(5), 1805–1849.

Nakamura, E. and J. Steinsson (2018). High-frequency identification of monetary non-neutrality: The information effect. *Quarterly Journal of Economics 133*(3), 1283–1330.

Newey, W. K. and K. D. West (1987). A simple, positive semi-definite, heteroskedasticity and autocorrelation consistent covariance matrix. *Econometrica 55*(3), 703–708.

Olea, J. L. M., M. Plagborg-Møller, E. Qian, and C. K. Wolf (2024). Double robustness of local projections and some unpleasant varithmetic. Technical report, National Bureau of Economic Research.

Ortu, F., A. Tamoni, and C. Tebaldi (2013). Long-run risk and the persistence of consumption shocks. *Review of Financial Studies 26*(11), 2876–2915.

Parker, J. A. and C. Julliard (2005). Consumption risk and the cross section of expected returns. *Journal of Political Economy 113*(1), 185–222.

Pástor, L. and R. F. Stambaugh (2003). Liquidity risk and expected stock returns. *Journal of Political Economy 111*(3), 642–685.

Pflueger, C., E. Siriwardane, and A. Sunderam (2020). Financial market risk perceptions and the macroeconomy. *Quarterly Journal of Economics 135*(3), 1443–1491.

Primiceri, G. E. (2005). Time varying structural vector autoregressions and monetary policy. *Review of Economic Studies 72*(3), 821–852.

Ramey, V. A. (2011). Identifying government spending shocks: It's all in the timing. *Quarterly Journal of Economics 126*(1), 1–50.

Ross, S. A. (1976). The arbitrage theory of capital asset pricing. *Journal of Economic Theory 13*(3), 341–360.

Shanken, J. (1992). On the estimation of beta-pricing models. *Review of Financial Studies 5*(1), 1–33.

Shapiro, A. H. (2022). Decomposing supply and demand driven inflation. Working Paper 2022-18, Federal Reserve Bank of San Francisco.

Shiller, R. J. (1993). *Macro Markets: Creating Institutions for Managing Society's Largest Economic Risks*. Clarendon Lectures in Economics. Oxford University Press.

Shimer, R. (2005). The cyclical behavior of equilibrium unemployment and vacancies. *American Economic Review 95*(1), 25–49.

Sims, C. A. (1992). Interpreting the macroeconomic time series facts: The effects of monetary policy. *European Economic Review 36*(5), 975–1000.

Sims, C. A. and T. Zha (2006). Were there regime switches in u.s. monetary policy? *American Economic Review 96*(1), 54–81.

Smets, F. and R. Wouters (2007). Shocks and frictions in US business cycles: A Bayesian DSGE approach. *American Economic Review 97*(3), 586–606.

Uhlig, H. (2003). What moves gnp? *Unpublished*.

Uhlig, H. (2004). Do technology shocks lead to a fall in total hours worked? *Journal of the European Economic Association 2*(2–3), 361–371.

van Binsbergen, J. H., M. Brandt, and R. Koijen (2012). On the timing and pricing of dividends. *American Economic Review 102*(4), 1596–1618.

Woodford, M. (2003). Imperfect common knowledge and the effects of monetary policy. In P. Aghion, R. Frydman, J. Stiglitz, and M. Woodford (Eds.), *Knowledge, Information, and Expectations in Modern Macroeconomics: In Honor of Edmund S. Phelps*, pp. 25–58. Princeton University Press.

Appendices

A.1 The Priced Wold Representation

Theorem A1 (Priced Wold Decomposition)**.** *Let the demeaned (log) stochastic discount factor* $\{\tilde{m}_t\}_{t\in\mathbb{Z}}$ *and the scalar process* $\{g_t\}_{t\in\mathbb{Z}}$ *with mean* μ_g *be covariance-stationary with finite second moments on* $(\Omega, \mathcal{F}, P)$*. Define* $\mathcal{M}_t := \overline{\text{span}}\{\tilde{m}_s : s \le t\} \subset L^2(\Omega, \mathcal{F}, P)$ *and* $\varepsilon_t^m := \tilde{m}_t - \Pi_{\mathcal{M}_{t-1}}(\tilde{m}_t)$ *where* $\Pi_{\mathcal{S}}(\cdot)$ *denotes the orthogonal projection onto a closed subspace* $\mathcal{S} \subset L^2(\Omega, \mathcal{F}, P)$*, and let* $\sigma_\varepsilon^2 := \text{Var}(\varepsilon_t^m) > 0$*. Assume that for all* t*, the mean-zero component of* g_t *can be written as* $g_t - \mu_g = \tilde{g}_t + \tilde{w}_t^g$*,* $\tilde{g}_t \in \mathcal{M}_t$*,* $\tilde{w}_t^g \perp \mathcal{M}_t$*. Then there exists a sequence* $\{\theta_j\}_{j=0}^\infty$ *satisfying* $\sum_{j=0}^\infty \theta_j^2 < \infty$*, and a process* w_t^g *orthogonal to* $\tilde{m}_t$*, such that*

$$g_t = \mu_g + \sum_{j=0}^{\infty} \theta_j \, \varepsilon_{t-j}^m + w_t^g, \qquad \theta_j = \frac{\mathbb{E}[(g_t - \mu_g)\, \varepsilon_{t-j}^m]}{\sigma_\varepsilon^2}, \tag{A1}$$

and this representation is unique.

Proof. By the Wold theorem for $\{\tilde{m}_t\}$, $\mathcal{M}_t = \mathcal{H}_t \oplus \mathcal{V}$, $\mathcal{H}_t := \overline{\text{span}}\{\varepsilon_s^m : s \le t\}$, $\mathcal{V} := \bigcap_{n\ge 1} \mathcal{M}_{t-n}$, where $\mathcal{V}$ denotes the deterministic subspace. Decompose the mean-zero part of g_t as $g_t - \mu_g = \tilde{g}_t + \tilde{w}_t^g$, with $\tilde{g}_t \in \mathcal{M}_t$ and $\tilde{w}_t^g \perp \mathcal{M}_t$. Apply the Wold decomposition to the priced component $\tilde{g}_t$: $\tilde{g}_t = \tilde{g}_t^{ND} + \tilde{g}_t^D$, $\tilde{g}_t^{ND} \in \mathcal{H}_t$, $\tilde{g}_t^D \in \mathcal{V}$. Since $\{\varepsilon_{t-j}^m\}_{j\ge 0}$ is an orthogonal basis of $\mathcal{H}_t$, expand $\tilde{g}_t^{ND} = \sum_{j=0}^\infty \theta_j \, \varepsilon_{t-j}^m$, $\theta_j = \frac{\mathbb{E}[\tilde{g}_t^{ND}\, \varepsilon_{t-j}^m]}{\sigma_\varepsilon^2}$. Because both $\tilde{g}_t^D$ and $\tilde{w}_t^g$ are orthogonal to all ε_{t-j}^m, we also have $\theta_j = \frac{\mathbb{E}[(g_t - \mu_g)\, \varepsilon_{t-j}^m]}{\sigma_\varepsilon^2}$. Parseval's identity implies $\mathbb{E}[(\tilde{g}_t^{ND})^2] = \sigma_\varepsilon^2 \sum_{j=0}^\infty \theta_j^2 < \infty$, so $\{\theta_j\} \in \ell^2$. Setting $w_t^g := \tilde{g}_t^D + \tilde{w}_t^g$ (collecting the deterministic and unpriced components) yields the expression in equation (A1). Uniqueness follows from the uniqueness of the innovation process $\varepsilon_t^m = \tilde{m}_t - \Pi_{\mathcal{M}_{t-1}}(\tilde{m}_t)$ and the orthogonality of the innovation basis. □

A.2 Bayesian Estimation of Risk Premia

We describe our hierarchical Bayesian framework, starting from the *time-series* dimension. We make the following distributional assumptions:

$$g_t = \mu_g + \sum_{s=0}^{\bar{S}} \rho_s \boldsymbol{\eta}_g^\top (\boldsymbol{v}_{t-s} - \boldsymbol{\mu}_{\boldsymbol{v}}) + w_{gt}, \quad w_{gt} \overset{\text{iid}}{\sim} \mathcal{N}(0, \sigma_{wg}^2), \quad \boldsymbol{v}_t \overset{\text{iid}}{\sim} \mathcal{N}(\boldsymbol{\mu}_{\boldsymbol{v}}, \boldsymbol{\Sigma}_{\boldsymbol{v}}), \tag{A2}$$

$$\boldsymbol{r}_t = \boldsymbol{\mu}_r + \boldsymbol{\beta}_v(\boldsymbol{v}_t - \boldsymbol{\mu}_v) + \boldsymbol{w}_{rt}, \quad \boldsymbol{w}_{rt} \overset{\text{iid}}{\sim} \mathcal{N}(\mathbf{0}_N, \boldsymbol{\Sigma}_{wr}), \quad \boldsymbol{\Sigma}_{wr} = \text{diag}\{\sigma_{1,wr}^2, \ldots, \sigma_{N,wr}^2\}, \text{ and} \tag{A3}$$

$$\boldsymbol{v}_t \perp w_{gt} \perp \boldsymbol{w}_{rt}, \text{ and let } \boldsymbol{\rho}_g = (\mu_g, \rho_0, \ldots, \rho_{\bar{S}})^\top, \tag{A4}$$

where $\boldsymbol{v}_t$ are nonsingular linear rotations of the true K factors $\tilde{\boldsymbol{v}}_t$. Since these rotations are arbitrary, we estimate their means ($\boldsymbol{\mu}_{\boldsymbol{v}}$) and covariance matrix ($\boldsymbol{\Sigma}_{\boldsymbol{v}}$); direct modeling of $\boldsymbol{\mu}_v$ is

critical for proper posterior coverage of expected returns $\boldsymbol{\mu}_r$.[26] The orthogonality assumption in (A4) implies that parameters of g_t and $\boldsymbol{r}_t$ can be estimated separately.

We assign standard uninformative priors to the time series parameters:

$$\begin{aligned}&\pi(\boldsymbol{\rho}_g, \boldsymbol{\eta}_g, \sigma^2_{wg}) \propto (\sigma^2_{wg})^{-1}, \quad \pi(\boldsymbol{v}) \propto 1, \quad \pi(\boldsymbol{\mu}_v, \boldsymbol{\Sigma}_v) \propto |\boldsymbol{\Sigma}_v|^{-\frac{K+1}{2}}, \text{ and} \\ &\pi(\boldsymbol{\beta}_v) \propto 1, \quad \pi(\boldsymbol{\mu}_r, \boldsymbol{\Sigma}_{wr}) \propto |\boldsymbol{\Sigma}_{wr}|^{-\frac{N+1}{2}}.\end{aligned} \tag{A5}$$

In the *cross-sectional* dimension, conditional on $\boldsymbol{v}_t$, the SDF and risk prices $\boldsymbol{\lambda}_v$ follow the Bayesian-SDF estimator (B-SDF) of Bryzgalova et al. (2023), Definition 1:

$$m_t = \kappa_m - \boldsymbol{\lambda}_v^\top \boldsymbol{\Sigma}_v^{-1} \boldsymbol{v}_t \;\Rightarrow\; \tilde{\boldsymbol{\mu}}_r = \boldsymbol{\beta}_v \boldsymbol{\lambda}_v, \tag{A6}$$

where $\tilde{\boldsymbol{\mu}}_r = \boldsymbol{\mu}_r + \frac{1}{2}\boldsymbol{\Upsilon}_r$ and both $\boldsymbol{\mu}_r$ and $\boldsymbol{\Upsilon}_r$ are estimated in the time series step. Pricing errors are still allowed, as in (2). Section 1.2 confirms via extensive simulations that this approach delivers valid posterior distributions.

The hierarchical structure yields standard conditional posteriors that combine via Gibbs sampling. Proposition A1 formalizes the sampler; derivations are in Online Appendix OA.2.4.

Proposition A1 (Gibbs sampler of the baseline model)**.** *Under the assumptions in equations (A2)–(A6), the posterior distribution of the model parameters can be sampled from the following conditional distributions:*

(1) Conditional on data and latent factors, the g_t process parameters (σ^2_{wg}, $\boldsymbol{\rho}_g$, $\boldsymbol{\eta}_g$) follow the normal-inverse-gamma distribution in equations (OA.3)–(OA.5) of Online Appendix OA.2.4, with draws of $\boldsymbol{\rho}_g$ and $\boldsymbol{\eta}_g$ normalized such that $\boldsymbol{\eta}_g^\top \boldsymbol{\eta}_g = 1$ for point identification.

(2) Conditional on asset returns, $\{\boldsymbol{r}_t\}_{t=1}^T$, and latent factors, the parameters of the $\boldsymbol{r}_t$ process, $\boldsymbol{\Sigma}_{wr}$ and $\boldsymbol{B}_r^\top = (\boldsymbol{\mu}_r, \boldsymbol{\beta}_v)$, follow the normal-inverse-Wishart distribution in equations (OA.6)–(OA.7) of Online Appendix OA.2.4.

(3) Conditional on returns and $(\boldsymbol{\mu}_r, \boldsymbol{\beta}_v, \boldsymbol{\Sigma}_{wr})$, latent factors, $\boldsymbol{v}_t$, and their moments follow:

$$\boldsymbol{v}_t \mid \boldsymbol{r}_t, \boldsymbol{\mu}_r, \boldsymbol{\beta}_v, \boldsymbol{\Sigma}_{wr}, \boldsymbol{\mu}_v, \boldsymbol{\Sigma}_v \sim \mathcal{N}\Big(\big(\boldsymbol{\beta}_{\boldsymbol{v}}^\top \boldsymbol{\Sigma}_{\boldsymbol{wr}}^{-\mathbf{1}} \boldsymbol{\beta}_{\boldsymbol{v}}\big)^{-1} \big[\boldsymbol{\beta}_{\boldsymbol{v}}^\top \boldsymbol{\Sigma}_{\boldsymbol{wr}}^{-\mathbf{1}} (\boldsymbol{r}_t - \boldsymbol{\mu}_r + \boldsymbol{\beta}_{\boldsymbol{v}} \boldsymbol{\mu}_v)\big],\ \big(\boldsymbol{\beta}_{\boldsymbol{v}}^\top \boldsymbol{\Sigma}_{\boldsymbol{wr}}^{-\mathbf{1}} \boldsymbol{\beta}_{\boldsymbol{v}}\big)^{-1} \Big), \tag{A7}$$

$$\boldsymbol{\Sigma}_v \mid \{\boldsymbol{v}_t\}_{t=1}^T \sim \mathcal{W}^{-1}\Big(T-1,\ \sum_{t=1}^T (\boldsymbol{v}_t - \bar{\boldsymbol{v}})(\boldsymbol{v}_t - \bar{\boldsymbol{v}})^\top \Big), \text{ and} \tag{A8}$$

$$\boldsymbol{\mu}_v \mid \boldsymbol{\Sigma}_v, \{\boldsymbol{v}_t\}_{t=1}^T \sim \mathcal{N}\Big(\bar{\boldsymbol{v}},\ \boldsymbol{\Sigma}_v / T \Big), \tag{A9}$$

[26] The sample average of $\boldsymbol{r}_t$ is $\boldsymbol{\mu}_r + \boldsymbol{\beta}_v \frac{1}{T}\sum_{t=1}^T (\boldsymbol{v}_t - \boldsymbol{\mu}_v) + \frac{1}{T}\sum_{t=1}^T \boldsymbol{w}_{rt}$. If we always demean the latent factors to have zero sample averages, the first source of uncertainty about $\boldsymbol{\mu}_r$, originated from $\frac{1}{T}\sum_{t=1}^T (\boldsymbol{v}_t - \boldsymbol{\mu}_v)$, will disappear. Consequently, the credible intervals for $\boldsymbol{\mu}_r$ will be too tight if we do not directly model $\boldsymbol{\mu}_v$.

where $\mathcal{N}(\cdot)$ *and* $\mathcal{W}^{-1}(\cdot)$ *denote, respectively, the normal and inverse-Wishart distributions.*

(4) Conditional on the draws from the time series steps (1)–(3), the posterior distribution of $\boldsymbol{\lambda}_v$ *is a Dirac distribution at* $(\boldsymbol{\beta}_v^\top \boldsymbol{\beta}_v)^{-1}\boldsymbol{\beta}_v^\top \tilde{\boldsymbol{\mu}}_r$*, yielding a Dirac conditional posterior for the term structure of* g_t*'s risk premia at* $\lambda_g^S = \frac{\sum_{\tau=0}^{S}\sum_{s=0}^{\tau}\rho_s}{1+S} \cdot \boldsymbol{\eta}_g^\top \boldsymbol{\lambda}_{\boldsymbol{v}}$*, where* $0 \leq S \leq \bar{S}$*.*

Several features of the sampler are worth highlighting. *First*, the residual w_{gt} may be serially correlated; following Müller (2013), posteriors remain asymptotically normal and centered at the MLE, with the canonical posterior covariance of $\boldsymbol{\rho}_g$ and $\boldsymbol{\eta}_g$ replaced by a Newey and West (1987)-type sandwich estimator.[27] *Second*, the posterior of $\boldsymbol{v}_t$ in Step 3 conditions only on returns and ignores the information in g_t (incorporating it via a Kalman filter is feasible but more demanding, and the omitted information is asymptotically negligible as $N \to \infty$); this also provides a level playing field when comparing risk premia across different g_t. Since our identification recovers $f_t = \boldsymbol{\eta}_g^\top \boldsymbol{v}_t$ as the linear combination maximizing the share of g_t explained by $\{f_{t-s}\}_{s=0}^{\bar{S}}$, the procedure echoes the max-share identification of Faust (1998), Uhlig (2003), Barsky and Sims (2011), Francis et al. (2014), and Angeletos et al. (2020). *Third*, Proposition A1 does *not* require a diagonal $\boldsymbol{\Sigma}_{wr}$. We impose diagonality only when N approaches the sample size to avoid numerical difficulties. Our simulations confirm that this has negligible effects on posterior inference, consistent with the frequentist intuition that such misspecification affects efficiency but not consistency. *Fourth*, through sequential resampling, Step 4 accounts for uncertainty in expected returns, factor loadings, and the latent means $\boldsymbol{\mu}_v$. *Fifth*, beyond risk premia the framework delivers valid posteriors for other quantities of interest, including R_g^2, the cumulative impulse responses $\{\tilde{\rho}_s\}_{s=0}^{\bar{S}}$ of g_t to return shocks, and the cross-sectional fit of average returns. *Sixth*, identifying risk premia from principal components avoids the omitted-variable and attenuation biases of traditional Fama-MacBeth and GMM estimators, which also suffer from weak identification of macro factors (e.g., Kan and Zhang, 1999). By exploiting the cumulative loadings $\{\tilde{\rho}_s\}_{s=0}^{\bar{S}}$, our estimator is robust to weak identification and recovers macro factor risk premia in both simulations and real data.

[27] The number of lags is set to $\bar{S}$ since $w_{gt}\boldsymbol{x}_t$ and $w_{g,t-l}\boldsymbol{x}_{t-l}$ become serially uncorrelated for $l > \bar{S}$, where $\boldsymbol{x}_t$ denotes the regressors in g_t's equation and is the linear transformation of latent factors $\{v_{t-s}\}_{s=0}^{\bar{S}}$.

Online Appendix for:

Macro Strikes Back: Term Structure of Risk Premia

Svetlana Bryzgalova,[a] Jiantao Huang,[b] and Christian Julliard[c*]

[a] *London Business School*

[b] *University of Hong Kong*

[c] *London School of Economics, FMG, SRC, and CEPR*

Abstract

This Online Appendix provides additional propositions, proofs, tables, figures, and empirical results supporting the main text.

[*] *Email addresses*: sbryzgalova@london.edu (S. Bryzgalova), huangjt@hku.hk (J. Huang), and c.julliard@lse.ac.uk (C. Julliard).

OA.1 Macro ARMA Processes: Calibration and Selection

We consider a general simulation setup for g_t as follows:

$$g_t = \mu_g + x_{t-1} + \sigma_{t-1} e_{gt},\ x_t = \rho_x x_{t-1} + \varphi_x \sigma_{t-1} e_{xt},\ \sigma_t^2 = \sigma^2(1-\nu) + \nu\sigma_{t-1}^2 + \sigma_\sigma e_{\sigma t}, \tag{OA.1}$$

where $e_{gt}, e_{xt}, e_{\sigma t} \overset{\text{iid}}{\sim} \mathcal{N}(0,1)$. In particular, x_{t-1} is the slow-moving component in g_t; e_{xt} is the shock to the persistent component; e_{gt} is the contemporaneous shock to g_t; $e_{\sigma t}$ is the shock to the potentially time-varying volatility. Then, g_t can be calibrated to match several model specifications in the literature: (i) Log consumption growth in Bansal and Yaron (2004). We calibrate the quarterly log growth following Table 6, "Quarterly" column, of Bansal, Kiku, and Yaron (2016). (ii) Log productivity/TFP growth in Croce (2014). We adopt the quarterly calibration therein, which studies a constant volatility process in the baseline analysis. (iii) Log aggregate profitability growth in Belo and Li (2023). We calibrate the quarterly log profitability growth using the parameter estimates in Table 1 therein.

BIC and AIC specification selection results for the above specifications are reported in Table OA.I. Overwhelmingly, in samples as long as the historical ones, canonical specification selection fails to recover the pseudo-true calibrated processes with very high probability, and very often, the selected specification implies no predictability in the macro quantities.

While canonical ARIMA selection fails to recover the data-generating process, our priced MA representation succeeds. Consider the Croce (2014) calibration of equation (OA.1), in

Table OA.I: ARIMA model selection (240 quarters)

Bansal et al. (2016): consumption				Croce (2014): TFP				Belo and Li (2023): profitability			
BIC		AIC		BIC		AIC		BIC		AIC	
$p\ d\ q$	freq	$p\ d\ q$	freq	$p\ d\ q$	freq	$p\ d\ q$	freq	$p\ d\ q$	freq	$p\ d\ q$	freq
0 0 0	78.1%	0 0 0	51.0%	0 0 0	60.7%	0 0 0	32.6%	1 0 1	31.6%	1 0 1	30.3%
0 1 1	8.0%	0 0 1	6.3%	0 1 1	16.5%	1 0 1	11.2%	0 1 1	25.6%	0 1 1	12.3%
1 1 1	3.0%	1 0 1	5.7%	1 1 1	6.0%	0 1 1	8.5%	0 0 0	13.3%	1 1 1	6.2%
1 0 0	2.9%	1 0 0	5.2%	1 0 1	4.4%	0 0 1	6.6%	1 0 0	9.7%	2 0 1	6.1%
0 0 1	1.7%	2 0 2	4.4%	1 0 0	3.3%	1 1 1	4.8%	2 0 0	6.5%	1 0 2	4.8%
1 1 2	1.2%	0 1 1	3.4%	2 1 1	2.3%	1 0 0	4.0%	1 1 1	4.8%	2 0 0	3.8%
2 1 1	1.2%	1 1 1	2.9%	0 0 1	1.9%	1 1 2	3.5%	3 0 0	2.3%	2 0 2	3.5%
1 0 1	0.6%	1 1 2	2.1%	1 1 2	1.6%	2 0 2	2.9%	0 0 1	1.6%	0 1 2	3.4%
3 1 1	0.6%	2 0 0	2.1%	3 1 1	0.5%	2 0 0	2.5%	0 1 2	1.0%	1 1 2	3.3%
2 0 0	0.4%	1 0 2	1.3%	2 1 2	0.4%	2 0 1	2.5%	1 1 2	0.9%	0 0 1	3.1%

Frequency of ARIMA(p,d,q) models selected by BIC and AIC in 1,000 simulations of the latent AR(1) model in equation (OA.1). Top 10 most frequently selected models shown.

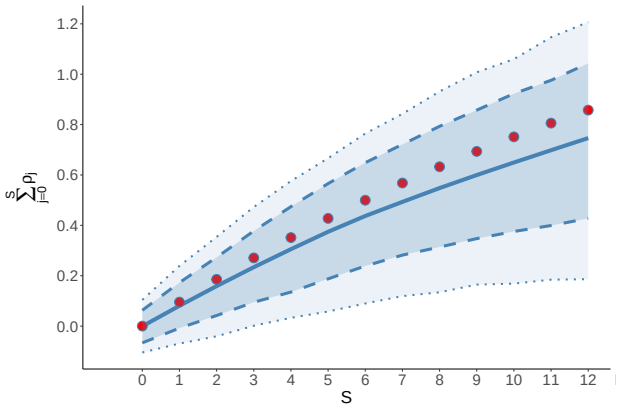

Figure OA.1: Cumulative IRF of TFP growth to a one-standard-deviation shock to its conditional mean under the Croce (2014) calibration.

Mean and 68% and 90% intervals of the cumulative IRF across 1,000 simulations; red dots are pseudo-true values. Sample length: 240 quarters. The MA representation is estimated with $\bar{S} = 12$.

which x_{t-1}, the priced conditional-mean component, accounts for less than 8% of the quarterly variation in TFP growth. We let the shock e_{xt} drive a calibrated panel of equity returns through the first principal component of FF275, with a second uncorrelated factor (PC2 of FF275) acting as an additional source of priced systematic risk, and Gaussian idiosyncratic noise calibrated to the cross-section. In estimation we observe only g_t and the panel of returns, and must infer both the latent shock e_{xt} and the cumulative impulse responses of g_t to it. Across 1,000 simulations of 240 quarters, the identified shock $\hat{f}_t$ has an average correlation of 0.90 with the true e_{xt}, and Figure OA.1 shows that the MA representation with $\bar{S} = 12$ accurately recovers the cumulative IRF of TFP growth despite the extremely low signal-to-noise ratio.

OA.2 Additional Propositions and Proofs

OA.2.1 Mimicking-Portfolio Interpretation of λ_g^S

We first state a technical lemma about the projection of returns onto the factor space.

Lemma OA.1. *As $N \to \infty$, $\tilde{\boldsymbol{\mu}}_r^\top \mathrm{cov}(\boldsymbol{r}_t)^{-1} \boldsymbol{\beta}_{\tilde{v}} \to \boldsymbol{\lambda}_{\tilde{v}}^\top$ under the following assumptions:*

i. The K eigenvalues of $\boldsymbol{\beta}_{\tilde{v}}^\top \boldsymbol{\beta}_{\tilde{v}}$ explode as $N \to \infty$, whereas $\boldsymbol{\Sigma}_{wr}$ has bounded eigenvalues: $\gamma(\boldsymbol{\beta}_{\tilde{v}}^\top \boldsymbol{\beta}_{\tilde{v}}) = O_p(N)$ and $\gamma(\boldsymbol{\Sigma}_{wr}) = O_p(1)$;

ii. $\frac{\boldsymbol{\beta}_{\tilde{v}}^\top \boldsymbol{\beta}_{\tilde{v}}}{N}$ and $\boldsymbol{\Sigma}_{wr}$ converge to positive-definite matrices with bounded entries;

iii. Asset returns and their expectations follow equations (1) and (2). In particular, α_i is IID and cross-sectionally independent of factor loadings, with a zero mean and satisfying that

$\frac{\boldsymbol{\alpha}^\top \boldsymbol{\Sigma}_{wr}^{-1}\boldsymbol{\beta}_{\tilde{v}}}{N} \to \mathbf{0}_K^\top$ *as* $N \to \infty$. *All elements in* $\boldsymbol{\beta}_{\tilde{v}}$ *are bounded.*[2]

Proof. Assumptions in equation (2) imply that

$$\tilde{\boldsymbol{\mu}}_r^\top \mathrm{cov}(\boldsymbol{r}_t)^{-1}\boldsymbol{\beta}_{\tilde{v}} = \underbrace{\boldsymbol{\alpha}^\top \mathrm{cov}(\boldsymbol{r}_t)^{-1}\boldsymbol{\beta}_{\tilde{v}}}_{(I)} + \underbrace{\boldsymbol{\lambda}_{\tilde{v}}^\top \boldsymbol{\beta}_{\tilde{v}}^\top \mathrm{cov}(\boldsymbol{r}_t)^{-1}\boldsymbol{\beta}_{\tilde{v}}}_{(II)}.$$

Assumptions in equation (1) imply that $\mathrm{cov}(\boldsymbol{r}_t) = \boldsymbol{\beta}_{\tilde{v}}\boldsymbol{\beta}_{\tilde{v}}^\top + \boldsymbol{\Sigma}_{wr}$. Using the Woodbury matrix identity, we can rewrite the inverse of $\mathrm{cov}(\boldsymbol{r}_t)$ as follows: $\mathrm{cov}(\boldsymbol{r}_t)^{-1} = \boldsymbol{\Sigma}_{wr}^{-1} - \boldsymbol{\Sigma}_{wr}^{-1}\boldsymbol{\beta}_{\tilde{v}}(\boldsymbol{I}_K + \boldsymbol{\beta}_{\tilde{v}}^\top \boldsymbol{\Sigma}_{wr}^{-1}\boldsymbol{\beta}_{\tilde{v}})^{-1}\boldsymbol{\beta}_{\tilde{v}}^\top \boldsymbol{\Sigma}_{wr}^{-1}$.

We now consider the behaviors of components (I) and (II) as $N \to \infty$.

$$(I) = \boldsymbol{\alpha}^\top \big[\boldsymbol{\Sigma}_{wr}^{-1} - \boldsymbol{\Sigma}_{wr}^{-1}\boldsymbol{\beta}_{\tilde{v}}(\boldsymbol{I}_K + \boldsymbol{\beta}_{\tilde{v}}^\top \boldsymbol{\Sigma}_{wr}^{-1}\boldsymbol{\beta}_{\tilde{v}})^{-1}\boldsymbol{\beta}_{\tilde{v}}^\top \boldsymbol{\Sigma}_{wr}^{-1}\big]\boldsymbol{\beta}_{\tilde{v}} = \frac{\boldsymbol{\alpha}^\top \boldsymbol{\Sigma}_{wr}^{-1}\boldsymbol{\beta}_{\tilde{v}}}{N} \cdot \Big(\frac{\boldsymbol{I}_K + \boldsymbol{\beta}_{\tilde{v}}^\top \boldsymbol{\Sigma}_{wr}^{-1}\boldsymbol{\beta}_{\tilde{v}}}{N}\Big)^{-1}.$$

Assumption (ii) implies that $\frac{\boldsymbol{I}_K + \boldsymbol{\beta}_{\tilde{v}}^\top \boldsymbol{\Sigma}_{wr}^{-1}\boldsymbol{\beta}_{\tilde{v}}}{N}$ converges to a positive-definite matrix with bounded entries. Due to assumption (iii), $\frac{\boldsymbol{\alpha}^\top \boldsymbol{\Sigma}_{wr}^{-1}\boldsymbol{\beta}_{\tilde{v}}}{N} \to \mathbf{0}_K^\top$ as $N \to \infty$, which implies that $(I) \to \mathbf{0}_K^\top$.

$$(II) = \boldsymbol{\lambda}_{\tilde{v}}^\top \boldsymbol{\beta}_{\tilde{v}}^\top \big[\boldsymbol{\Sigma}_{wr}^{-1} - \boldsymbol{\Sigma}_{wr}^{-1}\boldsymbol{\beta}_{\tilde{v}}(\boldsymbol{I}_K + \boldsymbol{\beta}_{\tilde{v}}^\top \boldsymbol{\Sigma}_{wr}^{-1}\boldsymbol{\beta}_{\tilde{v}})^{-1}\boldsymbol{\beta}_{\tilde{v}}^\top \boldsymbol{\Sigma}_{wr}^{-1}\big]\boldsymbol{\beta}_{\tilde{v}} = \boldsymbol{\lambda}_{\tilde{v}}^\top \big[\boldsymbol{I}_K - (\boldsymbol{A} + \boldsymbol{I}_K)^{-1}\big]$$

where $\boldsymbol{A} = \boldsymbol{\beta}_{\tilde{v}}^\top \boldsymbol{\Sigma}_{wr}^{-1}\boldsymbol{\beta}_{\tilde{v}}$. Since the eigenvalues of $\boldsymbol{\beta}_{\tilde{v}}^\top \boldsymbol{\beta}_{\tilde{v}}$ will explode as $N \to \infty$ wheres $\boldsymbol{\Sigma}_{wr}$ has bounded eigenvalues, we have $\lim_{N\to\infty}(\boldsymbol{A} + \boldsymbol{I}_K)^{-1} = \mathbf{0}_{K\times K}$, hence $(II) \to \boldsymbol{\lambda}_{\tilde{v}}^\top$. □

We next use the Lemma to establish asymptotic equivalence between the risk-premium definition in equation (5) and per-period risk premium of the horizon-specific mimicking portfolio.

Proposition OA.1 (Asymptotic equivalence with the mimicking portfolio)**.** *Under the assumptions of Lemma OA.1, as* $N \to \infty$,

$$\lambda_g^{MP} \;\to\; \frac{\boldsymbol{\lambda}_{\tilde{v}}^\top \mathrm{cov}(\tilde{\boldsymbol{v}}_{t-1\to t+S},\, g_{t-1\to t+S})}{1+S} \;=\; -\frac{\mathrm{cov}(m_{t-1\to t+S},\, g_{t-1\to t+S})}{1+S} \;=\; \lambda_g^S,$$

where λ_g^{MP} *is the per-period risk premium of the horizon-specific mimicking portfolio with portfolio weight given by the projection* $\boldsymbol{w}^{MP} = \mathrm{cov}(\boldsymbol{r}_{t-1\to t+S})^{-1}\mathrm{cov}(\boldsymbol{r}_{t-1\to t+S}, g_{t-1\to t+S})$ *of* $g_{t-1\to t+S}$ *onto cumulative excess returns.*

Proof. By construction, the per-period risk premium of the mimicking portfolio is

$$\lambda_g^{MP} = \frac{\big(\mathbb{E}[\boldsymbol{r}_{t-1\to t+S}] + \frac{1}{2}\boldsymbol{\Upsilon}(\boldsymbol{r}_{t-1\to t+S})\big)^\top \boldsymbol{w}^{MP}}{1+S} = \big(\mathbb{E}[\boldsymbol{r}_t] + \tfrac{1}{2}\boldsymbol{\Upsilon}_r\big)^\top \mathrm{cov}(\boldsymbol{r}_t)^{-1}\boldsymbol{\beta}_{\tilde{v}} \frac{\mathrm{cov}(\tilde{\boldsymbol{v}}_{t-1\to t+S},\, g_{t-1\to t+S})}{1+S},$$

[2] Ingersoll (1984) defines the pricing errors $\boldsymbol{\alpha}$ such that $\boldsymbol{\alpha}^\top \boldsymbol{\Sigma}_{wr}^{-1}\boldsymbol{\beta}_{\tilde{v}} = 0$. Our assumption in Lemma OA.1 is weaker than that in Ingersoll (1984). This assumption in (iii) is satisfied, e.g., when $\alpha_n \sim O_p(\frac{1}{\sqrt{N}})$, where the latter is a sufficient condition for the absence of asymptotic arbitrage opportunities defined in Ingersoll (1984).

where the second equality uses the serial uncorrelation of $\boldsymbol{v}_t$ (relaxed in Section 1.1) and the orthogonality of $\boldsymbol{w}_{r,\,t-1\to t+S}$ to g. By Lemma OA.1, the prefactor $\tilde{\boldsymbol{\mu}}_r^\top \mathrm{cov}(\boldsymbol{r}_t)^{-1}\boldsymbol{\beta}_{\tilde{v}} \to \boldsymbol{\lambda}_{\tilde{v}}^\top$ as $N \to \infty$. Substituting and using $m_{t-1\to t+S} = (1+S)\kappa_m - \boldsymbol{\lambda}_{\tilde{v}}^\top \tilde{\boldsymbol{v}}_{t-1\to t+S}$ yields the result. □

OA.2.2 SDF Decomposition with Respect to the Priced Shock f_t

This section derives the SDF decomposition stated in Section 1 of the main text. Let $\boldsymbol{v}_t = \boldsymbol{H}\tilde{\boldsymbol{v}}_t$, where $\boldsymbol{H}^\top = (\tilde{\boldsymbol{\eta}}_g, \boldsymbol{H}_1)$ is $K \times K$ nonsingular and $\boldsymbol{H}_1^\top \tilde{\boldsymbol{\eta}}_g = \boldsymbol{0}$. Then $\boldsymbol{v}_t = (f_t, \boldsymbol{u}_t^\top)^\top$ with $\boldsymbol{u}_t = \boldsymbol{H}_1^\top \tilde{\boldsymbol{v}}_t$ and $f_t \perp \boldsymbol{u}_t$. The log SDF in (3) becomes $m_t = \kappa_m - \boldsymbol{\lambda}_v^\top \boldsymbol{\Sigma}_v^{-1}\boldsymbol{v}_t = \kappa_m - \lambda_f f_t - \boldsymbol{\lambda}_u^\top (\boldsymbol{H}_1^\top \boldsymbol{H}_1)^{-1}\boldsymbol{u}_t$, with $\lambda_f = \tilde{\boldsymbol{\eta}}_g^\top \boldsymbol{\lambda}_{\tilde{v}}$ and $\boldsymbol{\lambda}_u = \boldsymbol{H}_1^\top \boldsymbol{\lambda}_{\tilde{v}}$. The SDF variance, equivalent to the squared maximal Sharpe ratio in the economy, decomposes as $\mathrm{var}(m_t) = \lambda_f^2 + \mathrm{var}\big(\boldsymbol{\lambda}_u^\top (\boldsymbol{H}_1^\top \boldsymbol{H}_1)^{-1}\boldsymbol{u}_t\big)$. Hence λ_f is the per-period model-implied Sharpe ratio of f_t; $\lambda_f^2/\mathrm{var}(m_t)$ quantifies the relative importance of f_t in the SDF, where f_t has the largest power in the log SDF to explain the cross-section of average returns.

OA.2.3 Rotation Invariance of Risk Premia and Shock Propagation

The latent factors $\tilde{\boldsymbol{v}}_t$ are identifiable only up to a linear rotation: any $\boldsymbol{v}_t = \boldsymbol{H}\tilde{\boldsymbol{v}}_t$ with $\boldsymbol{H}$ a $K \times K$ nonsingular matrix yields observably equivalent return and pricing dynamics. Rewriting the model of Section 1 in terms of the observable rotation $\boldsymbol{v}_t$ rather than the latent factors $\tilde{\boldsymbol{v}}_t$:

$$\boldsymbol{r}_t = \boldsymbol{\alpha} + \underbrace{\boldsymbol{\beta}_{\tilde{v}}\boldsymbol{H}^{-1}}_{\boldsymbol{\beta}_v}\underbrace{\boldsymbol{H}\boldsymbol{\lambda}_{\tilde{v}}}_{\boldsymbol{\lambda}_v} - \frac{1}{2}\boldsymbol{\Upsilon}_r + \underbrace{\boldsymbol{\beta}_{\tilde{v}}\boldsymbol{H}^{-1}}_{\boldsymbol{\beta}_v}\underbrace{\boldsymbol{H}\tilde{\boldsymbol{v}}_t}_{\boldsymbol{v}_t} + \boldsymbol{w}_{rt}, \quad g_t = \mu_g + \sum_{s=0}^{\bar{S}} \tilde{\rho}_s \underbrace{\tilde{\boldsymbol{\eta}}_g^\top \boldsymbol{H}^{-1}}_{\boldsymbol{\eta}_g^\top}\underbrace{\boldsymbol{H}\tilde{\boldsymbol{v}}_{t-s}}_{\boldsymbol{v}_{t-s}} + w_{gt}, \text{ and}$$

$$m_t = \kappa_m - \boldsymbol{\lambda}_v^\top (\boldsymbol{H}^{-1})^\top \boldsymbol{H}^{-1}\boldsymbol{v}_t = \kappa_m - \boldsymbol{\lambda}_v^\top \boldsymbol{\Sigma}_v^{-1}\boldsymbol{v}_t, \quad \lambda_g^S = \frac{\sum_{\tau=0}^{S}\sum_{s=0}^{\tau}\tilde{\rho}_s}{1+S} \cdot \underbrace{\tilde{\boldsymbol{\eta}}_g^\top \boldsymbol{H}^{-1}}_{\boldsymbol{\eta}_g}\underbrace{\boldsymbol{H}\boldsymbol{\lambda}_{\tilde{v}}}_{\boldsymbol{\lambda}_v}. \tag{OA.2}$$

The impulse-response coefficients $\{\tilde{\rho}_s\}$ and the risk premia λ_g^S are functions only of products that cancel the rotation $\boldsymbol{H}$ and are therefore point-identified; the rotation-dependent quantities $\boldsymbol{\beta}_v$, $\boldsymbol{\lambda}_v$, $\boldsymbol{\eta}_g$, and $\boldsymbol{\Sigma}_v$ are jointly determined up to $\boldsymbol{H}$.

OA.2.4 Derivations of the Posterior Distributions in Proposition A1

We present a detailed version of Proposition A1 in the main text.

Proposition OA.2 (Gibbs sampler of the baseline model)**.** *Under the assumptions in equations (A2)–(A6), the posterior of model parameters follows the conditional distributions below, where $\mathcal{IG}$, $\mathcal{N}$, $\mathcal{MVN}$, and $\mathcal{W}^{-1}$ denote the inverse-gamma, normal, multivariate normal, and inverse-Wishart distributions, and $\boldsymbol{G}$, $\bar{\boldsymbol{G}}$, $\boldsymbol{V}_\rho$, $\boldsymbol{V}_\eta$, $\hat{\boldsymbol{\Sigma}}_\rho$, $\hat{\boldsymbol{\Sigma}}_\eta$, $\boldsymbol{V}_r$, $\boldsymbol{R}$ are defined in the proof:*

(1) Conditional on the data $\{g_t\}_{t=1+\bar{S}}^{T}$ *and latent factors* $\{\boldsymbol{v}_t\}_{t=1}^{T}$*, parameters in* g_t*'s equation follow a normal-inverse-gamma distribution,*

$$\sigma_{wg}^2 \mid \{g_t\}_{t=1+\bar{S}}^{T}, \boldsymbol{\rho}_g, \boldsymbol{\eta}_g, \{\boldsymbol{v}_t\}_{t=1}^{T} \sim \mathcal{IG}\bigg(\frac{T-\bar{S}}{2}, \frac{(\boldsymbol{G}-\boldsymbol{V}_\rho\boldsymbol{\rho}_g)^\top(\boldsymbol{G}-\boldsymbol{V}_\rho\boldsymbol{\rho}_g)}{2}\bigg), \tag{OA.3}$$

$$\boldsymbol{\rho}_g \mid \boldsymbol{G}, \sigma_{wg}^2, \boldsymbol{\eta}_g, \{\boldsymbol{v}_t\}_{t=1}^{T} \sim \mathcal{N}\bigg(\big(\boldsymbol{V}_{\boldsymbol{\rho}}^\top\boldsymbol{V}_{\boldsymbol{\rho}}\big)^{-1}\boldsymbol{V}_{\boldsymbol{\rho}}^\top\boldsymbol{G},\ \hat{\boldsymbol{\Sigma}}_\rho\bigg),\ \textit{and} \tag{OA.4}$$

$$\boldsymbol{\eta}_g \mid \boldsymbol{G}, \sigma_{wg}^2, \boldsymbol{\rho}_g, \{\boldsymbol{v}_t\}_{t=1}^{T} \sim \mathcal{N}\bigg(\big(\boldsymbol{V}_{\boldsymbol{\eta}}^\top\boldsymbol{V}_{\boldsymbol{\eta}}\big)^{-1}\boldsymbol{V}_{\boldsymbol{\eta}}^\top\bar{\boldsymbol{G}},\ \hat{\boldsymbol{\Sigma}}_\eta\bigg). \tag{OA.5}$$

To identify $\boldsymbol{\rho}_g$ *and* $\boldsymbol{\eta}_g$*, we normalize* $\boldsymbol{\eta}_g$ *after each posterior draw such that* $\boldsymbol{\eta}_g^\top\boldsymbol{\eta}_g = 1$*.*

(2) Conditional on asset returns and latent factors, defining $\boldsymbol{B}_r^\top = (\boldsymbol{\mu}_r, \boldsymbol{\beta}_v)$*, we update model parameters in* $\boldsymbol{r}_t$*'s equation using a normal-inverse-Wishart distribution, as follows:*

$$\boldsymbol{\Sigma}_{wr} \mid \boldsymbol{R}, \{\boldsymbol{v}_t\}_{t=1}^{T}, \boldsymbol{\mu}_r, \boldsymbol{\beta}_v \sim \mathcal{W}^{-1}\bigg(T,\ \big(\boldsymbol{R}-\boldsymbol{V}_r\boldsymbol{B}_r\big)^\top\big(\boldsymbol{R}-\boldsymbol{V}_r\boldsymbol{B}_r\big)\bigg)\ \textit{and} \tag{OA.6}$$

$$\boldsymbol{B}_r \mid \boldsymbol{R}, \{\boldsymbol{v}_t\}_{t=1}^{T}, \boldsymbol{\Sigma}_{wr} \sim \mathcal{MVN}\bigg((\boldsymbol{V}_r^\top\boldsymbol{V}_r)^{-1}\boldsymbol{V}_r^\top\boldsymbol{R},\ \boldsymbol{\Sigma}_{wr}\otimes(\boldsymbol{V}_r^\top\boldsymbol{V}_r)^{-1}\bigg). \tag{OA.7}$$

(3) Conditional on asset returns and $(\boldsymbol{\mu}_r, \boldsymbol{\beta}_v, \boldsymbol{\Sigma}_{wr})$*, we update both latent factors* $\boldsymbol{v}_t$ *and their mean and covariance parameters, as follows:*

$$\boldsymbol{v}_t \mid \boldsymbol{r}_t, \boldsymbol{\mu}_r, \boldsymbol{\beta}_v, \boldsymbol{\Sigma}_{wr}, \boldsymbol{\mu}_v, \boldsymbol{\Sigma}_v \sim \mathcal{N}\bigg(\big(\boldsymbol{\beta}_{\boldsymbol{v}}^\top\boldsymbol{\Sigma}_{\boldsymbol{wr}}^{-\mathbf{1}}\boldsymbol{\beta}_{\boldsymbol{v}}\big)^{-1}\big[\boldsymbol{\beta}_{\boldsymbol{v}}^\top\boldsymbol{\Sigma}_{\boldsymbol{wr}}^{-\mathbf{1}}(\boldsymbol{r}_t-\boldsymbol{\mu}_r+\boldsymbol{\beta}_{\boldsymbol{v}}\boldsymbol{\mu}_v)\big],\ \big(\boldsymbol{\beta}_{\boldsymbol{v}}^\top\boldsymbol{\Sigma}_{\boldsymbol{wr}}^{-\mathbf{1}}\boldsymbol{\beta}_{\boldsymbol{v}}\big)^{-1}\bigg), \tag{OA.8}$$

$$\boldsymbol{\Sigma}_v \mid \{\boldsymbol{v}_t\}_{t=1}^{T} \sim \mathcal{W}^{-1}\bigg(T-1,\ \sum_{t=1}^{T}(\boldsymbol{v}_t-\bar{\boldsymbol{v}})(\boldsymbol{v}_t-\bar{\boldsymbol{v}})^\top\bigg),\ \textit{and} \tag{OA.9}$$

$$\boldsymbol{\mu}_v \mid \boldsymbol{\Sigma}_v, \{\boldsymbol{v}_t\}_{t=1}^{T} \sim \mathcal{N}\bigg(\bar{\boldsymbol{v}},\ \boldsymbol{\Sigma}_v/T\bigg),\ \textit{where}\ \bar{\boldsymbol{v}} = \sum_{t=1}^{T}\boldsymbol{v}_t/T \tag{OA.10}$$

(4) Based on the posterior draws from the time series steps (1)–(3), the posterior distribution of $\boldsymbol{\lambda}_v$ *is a Dirac distribution at* $(\boldsymbol{\beta}_v^\top\boldsymbol{\beta}_v)^{-1}\boldsymbol{\beta}_v^\top\tilde{\boldsymbol{\mu}}_r$*. In addition, the posterior distribution of the term structure of* g_t*'s risk premia is also a Dirac distribution at* $\lambda_g^S = \frac{\sum_{\tau=0}^{S}\sum_{s=0}^{\tau}\rho_s}{1+S}\cdot\boldsymbol{\eta}_g^\top\boldsymbol{\lambda}_{\boldsymbol{v}}$*, where* $0 \le S \le \bar{S}$*.*

We next derive the posterior distribution in g_t's equation. We introduce some matrix nota-

tions, as follows:

$$\boldsymbol{V}_\rho = \begin{pmatrix} 1 & (\boldsymbol{v}_{\bar{S}+1} - \boldsymbol{\mu}_v)^\top \boldsymbol{\eta}_g & \cdots & (\boldsymbol{v}_1 - \boldsymbol{\mu}_v)^\top \boldsymbol{\eta}_g \\ \vdots & \vdots & & \vdots \\ 1 & (\boldsymbol{v}_T - \boldsymbol{\mu}_v)^\top \boldsymbol{\eta}_g & \cdots & (\boldsymbol{v}_{T-\bar{S}} - \boldsymbol{\mu}_v)^\top \boldsymbol{\eta}_g \end{pmatrix},$$

$$\boldsymbol{V}_\eta = \begin{pmatrix} \sum_{s=0}^{\bar{S}} \rho_s(\boldsymbol{v}_{1,1+\bar{S}-s} - \boldsymbol{\mu}_v) & \cdots & \sum_{s=0}^{\bar{S}} \rho_s(\boldsymbol{v}_{K,1+\bar{S}-s} - \boldsymbol{\mu}_v) \\ \vdots & & \vdots \\ \sum_{s=0}^{\bar{S}} \rho_s(\boldsymbol{v}_{1,T-s} - \boldsymbol{\mu}_v) & \cdots & \sum_{s=0}^{\bar{S}} \rho_s(\boldsymbol{v}_{K,T-s} - \boldsymbol{\mu}_v) \end{pmatrix},$$

$$\boldsymbol{G} = (g_{1+\bar{S}}, \ldots, g_T)^\top, \quad \text{and } \bar{\boldsymbol{G}} = (g_{1+\bar{S}} - \mu_g, \ldots, g_T - \mu_g)^\top.$$

Using the notations above, the data likelihood for $\boldsymbol{G}$ can be written as

$$p(\boldsymbol{G} \mid \boldsymbol{\rho}_g, \boldsymbol{\eta}_g, \{\boldsymbol{v}_t\}_{t=1}^T, \sigma_{wg}^2) = (2\pi\sigma_{wg}^2)^{-\frac{T-\bar{S}}{2}} \exp\left\{-\frac{1}{2\sigma_{wg}^2}(\boldsymbol{G} - \boldsymbol{V}_\rho\boldsymbol{\rho}_g)^\top(\boldsymbol{G} - \boldsymbol{V}_\rho\boldsymbol{\rho}_g)\right\},$$

where $(\boldsymbol{G} - \boldsymbol{V}_\rho\boldsymbol{\rho}_g)^\top(\boldsymbol{G} - \boldsymbol{V}_\rho\boldsymbol{\rho}_g) = (\bar{\boldsymbol{G}} - \boldsymbol{V}_\eta\boldsymbol{\eta}_g)^\top(\bar{\boldsymbol{G}} - \boldsymbol{V}_\eta\boldsymbol{\eta}_g)$. Since we assign a flat prior to $(\boldsymbol{\rho}_g, \boldsymbol{\eta}_g, \sigma_{wg}^2)$, the posterior distribution of σ_{wg}^2 is

$$p(\sigma_{wg}^2 \mid \boldsymbol{G}, \boldsymbol{\rho}_g, \boldsymbol{\eta}_g, \{\boldsymbol{v}_t\}_{t=1}^T) \propto \left(\frac{1}{\sigma_{wg}^2}\right)^{\frac{T-\bar{S}}{2}+1} \exp\left\{-\frac{(\boldsymbol{G} - \boldsymbol{V}_\rho\boldsymbol{\rho}_g)^\top(\boldsymbol{G} - \boldsymbol{V}_\rho\boldsymbol{\rho}_g)}{2\sigma_{wg}^2}\right\};$$

hence, the posterior distribution of σ_{wg}^2 is an inverse-gamma in equation (OA.3).

We next consider the posterior distribution of $\boldsymbol{\rho}_g$ and $\boldsymbol{\eta}_g$. From the data likelihood, we can derive the kernel of $\boldsymbol{\rho}_g$'s posterior,

$$p(\boldsymbol{\rho}_g \mid \boldsymbol{G}, \sigma_{wg}^2, \boldsymbol{\eta}_g, \{\boldsymbol{v}_t\}_{t=1}^T) \propto \exp\left\{-\frac{1}{2}(\boldsymbol{\rho}_g - \hat{\boldsymbol{\rho}}_g)^\top \left[\sigma_{wg}^2(\boldsymbol{V}_{\boldsymbol{\rho}}^\top \boldsymbol{V}_{\boldsymbol{\rho}})^{-1}\right]^{-1}(\boldsymbol{\rho}_g - \hat{\boldsymbol{\rho}}_g)\right\},$$

where $\hat{\boldsymbol{\rho}}_g = \left(\boldsymbol{V}_{\boldsymbol{\rho}}^\top \boldsymbol{V}_{\boldsymbol{\rho}}\right)^{-1} \boldsymbol{V}_{\boldsymbol{\rho}}^\top \boldsymbol{G}$. The next step is to make adjustments for the posterior covariance matrix of $\boldsymbol{\rho}_g$ due to the potentially autocorrelated $w_{gt}\boldsymbol{V}_{\rho t}$. A simple solution is given by Müller (2013), which proposes that we can replace $\sigma_{wg}^2\left(\boldsymbol{V}_{\boldsymbol{\rho}}^\top \boldsymbol{V}_{\boldsymbol{\rho}}\right)^{-1}$ with the Newey and West (1987) type of sandwich covariance matrix, denoted as $\hat{\boldsymbol{\Sigma}}_\rho$, as follows:

$$\boldsymbol{\rho}_g \mid \boldsymbol{G}, \sigma_{wg}^2, \boldsymbol{\eta}_g, \{\boldsymbol{v}_t\}_{t=1}^T \sim \mathcal{N}\left(\hat{\boldsymbol{\rho}}_g, \hat{\boldsymbol{\Sigma}}_\rho\right), \quad \hat{\boldsymbol{\Sigma}}_\rho = \left(\boldsymbol{V}_{\boldsymbol{\rho}}^\top \boldsymbol{V}_{\boldsymbol{\rho}}\right)^{-1}\left[(T - \bar{S})\hat{\boldsymbol{S}}_\rho\right]\left(\boldsymbol{V}_{\boldsymbol{\rho}}^\top \boldsymbol{V}_{\boldsymbol{\rho}}\right)^{-1},$$

$$\hat{\boldsymbol{S}}_\rho = \frac{1}{T - \bar{S}} \sum_{t=1+\bar{S}}^{T} \hat{w}_{g,t}^2 (\boldsymbol{V}_{\rho,t}\boldsymbol{V}_{\rho,t}^\top) + \sum_{l=1}^{L} (1 - \frac{l}{1+L})\hat{\boldsymbol{\Gamma}}_{\rho l}, \text{ and}$$

$$\hat{\boldsymbol{\Gamma}}_{\rho l} = \frac{1}{T - \bar{S} - l} \sum_{t=1+\bar{S}+l}^{T} \hat{w}_{g,t}\hat{w}_{g,t-l}(\boldsymbol{V}_{\rho,t}\boldsymbol{V}_{\rho,t-l}^\top + \boldsymbol{V}_{\rho,t-l}\boldsymbol{V}_{\rho,t}^\top) \text{ for } l > 0, \quad \hat{w}_{g,t} = g_t - \boldsymbol{V}_{\rho t}^\top \hat{\boldsymbol{\rho}}_g,$$

where L, the number of lags in the Newey-West estimator, is chosen to be $\bar{S}$ since $w_{gt}\boldsymbol{V}_{\rho t}$ and $w_{g,t-l}\boldsymbol{V}_{\rho t-l}$ are uncorrelated for $l > \bar{S}$.

We finish deriving the multivariate normal in equation (OA.4). A similar derivation can be applied to the posterior distribution of $\boldsymbol{\eta}_g$ in equation (OA.5).

We now proceed to derive the posterior distribution of model parameters in $\boldsymbol{r}_t$'s equation. We stack time series observations into the following matrices:

$$\boldsymbol{R} = \begin{pmatrix} \boldsymbol{r}_1^\top \\ \vdots \\ \boldsymbol{r}_T^\top \end{pmatrix}, \quad \boldsymbol{V}_r = \begin{pmatrix} 1 & (\boldsymbol{v}_1 - \boldsymbol{\mu}_v)^\top \\ \vdots & \vdots \\ 1 & (\boldsymbol{v}_T - \boldsymbol{\mu}_v)^\top \end{pmatrix}, \quad \text{and } \boldsymbol{B}_r = \begin{pmatrix} \boldsymbol{\mu}_r^\top \\ \boldsymbol{\beta}_v^\top \end{pmatrix},$$

and the data likelihood of asset returns is

$$p(\boldsymbol{R} \mid \{\boldsymbol{v}_t\}_{t=1}^T, \boldsymbol{\mu}_r, \boldsymbol{\beta}_v, \boldsymbol{\Sigma}_{wr}) \propto |\boldsymbol{\Sigma}_{wr}|^{-\frac{T}{2}} \exp\{-\frac{1}{2} tr\big[\boldsymbol{\Sigma}_{wr}^{-1}(\boldsymbol{R} - \boldsymbol{V}_r\boldsymbol{B}_r)^\top(\boldsymbol{R} - \boldsymbol{V}_r\boldsymbol{B}_r)\big]\}.$$

Under the prior distribution in equation (A5), we first derive the posterior of $\boldsymbol{\Sigma}_{wr}$,

$$p(\boldsymbol{\Sigma}_{wr} \mid \boldsymbol{R}, \{\boldsymbol{v}_t\}_{t=1}^T, \boldsymbol{\mu}_r, \boldsymbol{\beta}_v) \propto |\boldsymbol{\Sigma}_{wr}|^{-\frac{T+N+1}{2}} \exp\{-\frac{1}{2} tr\big[\boldsymbol{\Sigma}_{wr}^{-1}(\boldsymbol{R} - \boldsymbol{V}_r\boldsymbol{B}_r)^\top(\boldsymbol{R} - \boldsymbol{V}_r\boldsymbol{B}_r)\big]\},$$

which implies the inverse-Wishart distribution of $\boldsymbol{\Sigma}_{wr}$ in equation (OA.6). When $\boldsymbol{\Sigma}_{wr}$ is diagonal, which is assumed in the high-dimensional setting, the inverse-Wishart distribution reduces to independent inverse-gamma distributions of $\{\sigma_{wr,n}^2\}_{n=1}^N$.

We next derive the posterior of $(\boldsymbol{\mu}_r, \boldsymbol{\beta}_v)$:

$$p(\boldsymbol{B}_r \mid \boldsymbol{R}, \{\boldsymbol{v}_t\}_{t=1}^T, \boldsymbol{\Sigma}_{wr}) \propto \exp\{-\frac{1}{2} tr\big[\boldsymbol{\Sigma}_{wr}^{-1}(\boldsymbol{B}_r - \hat{\boldsymbol{B}}_r)^\top \boldsymbol{V}_r^\top \boldsymbol{V}_r(\boldsymbol{B}_r - \hat{\boldsymbol{B}}_r)\big]\},$$

where $\hat{\boldsymbol{B}}_r = (\boldsymbol{V}_r^\top\boldsymbol{V}_r)^{-1}\boldsymbol{V}_r^\top\boldsymbol{R}$, and the formula above is the kernel of the multivariate normal distribution in equation (OA.7). However, when we implement equation (OA.7), we replace $(\boldsymbol{V}_r^\top\boldsymbol{V}_r)^{-1}$ with $(\boldsymbol{V}_r^\top\boldsymbol{V}_r + \boldsymbol{D}_r)^{-1}$, where $\boldsymbol{D}_r = \text{diag}\{0, 1, \ldots, 1\}$. The additional term $\boldsymbol{D}_r$ is a small penalty that preempts numerical difficulties in high-dimensional applications.

Finally, we derive the posterior distribution of latent factors and their means and covariance matrix. The posterior distribution of $\boldsymbol{v}_t$ is

$$\begin{aligned} p(\boldsymbol{v}_t \mid \boldsymbol{r}_t, \boldsymbol{\mu}_r, \boldsymbol{\beta}_v, \boldsymbol{\Sigma}_{wr}, \boldsymbol{\mu}_v, \boldsymbol{\Sigma}_v) &\propto\ p(\boldsymbol{r}_t \mid \boldsymbol{v}_t, \boldsymbol{\mu}_r, \boldsymbol{\beta}_v, \boldsymbol{\Sigma}_{wr})\pi(\boldsymbol{v}_t \mid \boldsymbol{\mu}_v, \boldsymbol{\Sigma}_v) \\ &\propto \exp\{-\frac{1}{2}\big[\boldsymbol{v}_t^\top(\boldsymbol{\beta}_v^\top\boldsymbol{\Sigma}_{wr}^{-1}\boldsymbol{\beta}_v)\boldsymbol{v}_t - 2\boldsymbol{v}_t^\top\boldsymbol{\beta}_v^\top\boldsymbol{\Sigma}_{wr}^{-1}(\boldsymbol{r}_t - \boldsymbol{\mu}_r + \boldsymbol{\beta}_v\boldsymbol{\mu}_v)\big]\}, \end{aligned}$$

which implies equation (OA.8). To avoid potential numerical difficulty in the Gibbs sampler, we replace $\left(\boldsymbol{\beta}_{\boldsymbol{v}}^\top\boldsymbol{\Sigma}_{\boldsymbol{wr}}^{-\boldsymbol{1}}\boldsymbol{\beta}_{\boldsymbol{v}}\right)^{-1}$ with $\left(\boldsymbol{\beta}_{\boldsymbol{v}}^\top\boldsymbol{\Sigma}_{\boldsymbol{wr}}^{-\boldsymbol{1}}\boldsymbol{\beta}_{\boldsymbol{v}} + \boldsymbol{I}_K\right)^{-1}$ when sampling $\boldsymbol{v}_t$ in equation (OA.8). The

posterior distribution of $(\boldsymbol{\mu}_v, \boldsymbol{\Sigma}_v)$ is

$$p(\boldsymbol{\mu}_v, \boldsymbol{\Sigma}_v \mid \{\boldsymbol{v}_t\}_{t=1}^T) \propto |\boldsymbol{\Sigma}_v|^{-\frac{T+K+1}{2}} \exp\{-\frac{1}{2} tr[\boldsymbol{\Sigma}_v^{-1} \sum_{t=1}^{T} (\boldsymbol{v}_t - \boldsymbol{\mu}_v)(\boldsymbol{v}_t - \boldsymbol{\mu}_v)^\top]\},$$

which is the kernel of the normal-inverse-Wishart distribution in equations (OA.9) and (OA.10).

OA.2.5 Estimating Time-Varying Risk Premia

We now extend our Bayesian framework to estimate time-varying term structures presented in Section 2.2.1. The return process again follows an approximate factor structure,

$$\boldsymbol{r}_t = \boldsymbol{\mu}_r + \boldsymbol{\beta}_{\tilde{v}} \tilde{\boldsymbol{v}}_t + \boldsymbol{w}_{rt}, \quad \tilde{\boldsymbol{v}}_t \perp \boldsymbol{w}_{rt}, \quad \mathbb{E}_{t-1}[\boldsymbol{w}_{rt}] = \boldsymbol{0}_N, \quad \mathbb{E}[\tilde{\boldsymbol{v}}_t] = \boldsymbol{0}_K, \tag{OA.11}$$

where, importantly, the priced systematic factors $\tilde{\boldsymbol{v}}_t$ are potentially predictable: $\tilde{\boldsymbol{v}}_t = \boldsymbol{\mu}_{\tilde{v},t-1} + \boldsymbol{\epsilon}_{\tilde{v}t}$, with $\boldsymbol{\mu}_{\tilde{v},t-1} \equiv \mathbb{E}_{t-1}[\tilde{\boldsymbol{v}}_t]$, $\boldsymbol{\mu}_{\tilde{v},t-1} \perp \boldsymbol{\epsilon}_{\tilde{v}t}$, and innovations normalized so that $\text{cov}(\boldsymbol{\epsilon}_{\tilde{v}t}) = \boldsymbol{I}_K$. We let $\tilde{\boldsymbol{v}}_t$ depend on its own lags and on p external predictors $\boldsymbol{z}_t$. Defining $\boldsymbol{x}_t = (\tilde{\boldsymbol{v}}_t^\top, \boldsymbol{z}_t^\top)^\top$, we assume that $\boldsymbol{x}_t$ follows a (partially latent) vector autoregressive (VAR) model of order q:

$$\boldsymbol{x}_t = \boldsymbol{\phi}_0 + \boldsymbol{\phi}_1 \boldsymbol{x}_{t-1} + \cdots + \boldsymbol{\phi}_q \boldsymbol{x}_{t-q} + \boldsymbol{\epsilon}_{xt}, \quad \boldsymbol{\epsilon}_{xt} \overset{\text{iid}}{\sim} \mathcal{N}(\boldsymbol{0}_{K+p}, \boldsymbol{\Sigma}_{\epsilon x}). \tag{OA.12}$$

In estimation, we identify a linear rotation of $\tilde{\boldsymbol{v}}_t$: $\boldsymbol{v}_t = \boldsymbol{H}\tilde{\boldsymbol{v}}_t = \boldsymbol{H}\boldsymbol{\mu}_{\tilde{v},t-1} + \boldsymbol{H}\boldsymbol{\epsilon}_{\tilde{\boldsymbol{v}}\boldsymbol{t}} = \boldsymbol{\mu}_{v,t-1} + \boldsymbol{\epsilon}_{vt}$, which implies that $\boldsymbol{\Sigma}_{\epsilon v} = \text{cov}(\boldsymbol{\epsilon}_{vt}) = \boldsymbol{H}\boldsymbol{H}^\top$. We generalize the rotation invariance as follows:

$$\boldsymbol{r}_t = \boldsymbol{\alpha} - \frac{\boldsymbol{\Upsilon}_r}{2} + \underbrace{\boldsymbol{\beta}_{\tilde{v}}\boldsymbol{H}^{-1}}_{\boldsymbol{\beta}_v}\underbrace{\boldsymbol{H}\boldsymbol{\lambda}_{\tilde{v}}}_{\boldsymbol{\lambda}_v} + \underbrace{\boldsymbol{\beta}_{\tilde{v}}\boldsymbol{H}^{-1}}_{\boldsymbol{\beta}_v}\underbrace{\boldsymbol{H}\tilde{\boldsymbol{v}}_t}_{\boldsymbol{v}_t} + \boldsymbol{w}_{rt}, \quad g_t = \mu_g + \sum_{s=0}^{\bar{S}} \tilde{\rho}_s \underbrace{\tilde{\boldsymbol{\eta}}_g^\top \boldsymbol{H}^{-1}}_{\boldsymbol{\eta}_g^\top}\underbrace{\boldsymbol{H}\boldsymbol{\epsilon}_{\tilde{v},t-s}}_{\boldsymbol{\epsilon}_{v,t-s}} + w_{gt},$$

$$m_t = \kappa_m - \boldsymbol{\lambda}_v^\top (\boldsymbol{H}^{-1})^\top \boldsymbol{H}^{-1}\boldsymbol{\epsilon}_{vt} - \boldsymbol{\mu}_{v,t-1}^\top (\boldsymbol{H}^{-1})^\top \boldsymbol{H}^{-1}\boldsymbol{\epsilon}_{vt} = \kappa_m - \boldsymbol{\lambda}_v^\top \boldsymbol{\Sigma}_{\epsilon v}^{-1}\boldsymbol{\epsilon}_{vt} - \boldsymbol{\mu}_{v,t-1}^\top \boldsymbol{\Sigma}_{\epsilon v}^{-1}\boldsymbol{\epsilon}_{vt}, \text{ and}$$

$$\lambda_{g,t-1}^S = \frac{\sum_{\tau=0}^{S}\sum_{s=0}^{\tau}\tilde{\rho}_s}{1+S} \cdot \underbrace{\tilde{\boldsymbol{\eta}}_g^\top \boldsymbol{H}^{-1}}_{\boldsymbol{\eta}_g^\top}\underbrace{\boldsymbol{H}(\boldsymbol{\lambda}_{\tilde{v}} + \mathbb{E}_{t-1}\left[\boldsymbol{\mu}_{\tilde{v},t+\tau-s-1}\right])}_{\boldsymbol{\lambda}_v + \mathbb{E}_{t-1}\left[\boldsymbol{\mu}_{v,t+\tau-s-1}\right]}. \tag{OA.13}$$

Thus, impulse response coefficients $\{\tilde{\rho}_s\}$ and risk premia $\lambda_{g,t}^S$ are point identified.

Proposition OA.3 (Gibbs sampler of the time-varying model)**.** *Under the assumptions in equations (OA.11)–(OA.12), the posterior distribution of the model parameters can be sampled from the following conditional distributions:*

(1) *Conditional on the data,* $\{g_t\}_{t=1+\bar{S}}^{T}$*, and shocks to latent factors,* $\{\boldsymbol{\epsilon}_{vt}\}_{t=1}^{T}$*, the parameters of the* g_t *process* (σ_{wg}^2, $\boldsymbol{\rho}_g$*, and* $\boldsymbol{\eta}_g$) *follow the normal-inverse-gamma distribution in equations (OA.3)–(OA.5) of Online Appendix OA.2.4. The only difference is that we replace* $\boldsymbol{v}_t$ *with* $\boldsymbol{\epsilon}_{vt}$ *in equations (OA.3)–(OA.5). For point identification purposes, draws of* $\boldsymbol{\rho}_g$ *and* $\boldsymbol{\eta}_g$ *are normalized such that* $\boldsymbol{\eta}_g^\top \boldsymbol{\eta}_g = 1$.

(2) *Conditional on asset returns,* $\{\boldsymbol{r}_t\}_{t=1}^{T}$*, and latent factors,* $\{\boldsymbol{v}_t\}_{t=1}^{T}$*, the parameters of the* $\boldsymbol{r}_t$ *process* ($\boldsymbol{\Sigma}_{wr}$ *and* $\boldsymbol{B}_r^\top = (\boldsymbol{\mu}_r, \boldsymbol{\beta}_v)$) *follow the normal-inverse-Wishart distribution in equations (OA.6)–(OA.7) of Online Appendix OA.2.4.*

(3) *Conditional on asset returns and* $(\boldsymbol{\mu}_r, \boldsymbol{\mu}_v, \boldsymbol{\beta}_v, \boldsymbol{\Sigma}_{wr})$*, the latent factors,* $\boldsymbol{v}_t$*, can be sampled from the normal-inverse-Wishart distribution in equation (OA.8).*

(4) *Conditional on latent factors,* $\{\boldsymbol{v}_t\}_{t=1}^{T}$*, the model parameters in the VAR(q) system of* $\boldsymbol{v}_t$ *can be obtained from equations (OA.14)–(OA.15). The conditional mean of* $\boldsymbol{v}_t$ *equals the first* K *elements of* $\boldsymbol{\phi}_0 + \boldsymbol{\phi}_1 \boldsymbol{x}_{t-1} + \cdots + \boldsymbol{\phi}_q \boldsymbol{x}_{t-q}$*, and the first* K *variables in* $\boldsymbol{\epsilon}_{xt}$ *are shocks to priced systematic factors,* $\boldsymbol{\epsilon}_{vt}$*. We can also obtain the unconditional mean of* $\boldsymbol{v}_t$ *as the first* K *elements in* $(\boldsymbol{I} - \boldsymbol{\phi}_1 - \cdots - \boldsymbol{\phi}_q)^{-1}\boldsymbol{\phi}_0$.

(5) *Conditional on the draws from the time series steps (1)–(4), the posterior distribution of* $\boldsymbol{\lambda}_v$ *is a Dirac distribution at* $(\boldsymbol{\beta}_v^\top \boldsymbol{\beta}_v)^{-1}\boldsymbol{\beta}_v^\top \tilde{\boldsymbol{\mu}}_r$*, where* $\tilde{\boldsymbol{\mu}}_r = \boldsymbol{\mu}_r + \frac{1}{2}\boldsymbol{\Upsilon}_r$*, and* $\boldsymbol{\Upsilon}_{ir} = (\boldsymbol{\beta}_v \boldsymbol{\Sigma}_{\epsilon v} \boldsymbol{\beta}_v^\top + \boldsymbol{\Sigma}_{\boldsymbol{wr}})_{ii}$*,* $i = 1, \ldots, N$*. It further yields a Dirac conditional posterior for the term structure of* g_t*'s risk premia at* $\lambda_{g,t-1}^{S} = \sum_{\tau=0}^{S}\sum_{s=0}^{\tau} \frac{\rho_s \boldsymbol{\eta}_g^\top (\boldsymbol{\lambda}_v + \mathbb{E}_{t-1}\left[\boldsymbol{\mu}_{\tilde{v},t+\tau-s-1}\right])}{1+S}$*, where* $0 \leq S \leq \bar{S}$.

Proof. The only new ingredient in Proposition OA.3 relative to Proposition A1 is step 4, which estimates the VAR(q) parameters governing $\boldsymbol{x}_t$. First, we introduce the following notations:

$$\boldsymbol{X}^{(1)} = \begin{pmatrix} \boldsymbol{x}_{q+1}^\top \\ \vdots \\ \boldsymbol{x}_T^\top \end{pmatrix}, \quad \boldsymbol{X}^{(0)} = \begin{pmatrix} 1 & \boldsymbol{x}_q^\top & \ldots & \boldsymbol{x}_1^\top \\ \vdots & \vdots & & \vdots \\ 1 & \boldsymbol{x}_{T-1}^\top & \ldots & \boldsymbol{x}_{T-q}^\top \end{pmatrix}, \quad \text{and } \boldsymbol{\Phi} = \begin{pmatrix} \boldsymbol{\phi}_0^\top \\ \vdots \\ \boldsymbol{\phi}_q^\top \end{pmatrix},$$

and equation (OA.12) implies that the data likelihood is

$$p(\boldsymbol{X}^{(1)} \mid \boldsymbol{X}^{(0)}, \boldsymbol{\Phi}, \boldsymbol{\Sigma}_{\epsilon x}) \propto |\boldsymbol{\Sigma}_{\epsilon x}|^{-\frac{T-q}{2}} \exp\{-\frac{1}{2} tr[\boldsymbol{\Sigma}_{\epsilon x}^{-1}(\boldsymbol{X}^{(1)} - \boldsymbol{X}^{(0)}\boldsymbol{\Phi})^\top (\boldsymbol{X}^{(1)} - \boldsymbol{X}^{(0)}\boldsymbol{\Phi})]\}.$$

Under the prior distribution $\pi(\boldsymbol{\Phi}, \boldsymbol{\Sigma}_{\epsilon x}) \propto |\boldsymbol{\Sigma}_{\epsilon x}|^{-\frac{K+p+1}{2}}$, we can easily show that $(\boldsymbol{\Phi}, \boldsymbol{\Sigma}_{\epsilon x})$ follow the normal-inverse-Wishart distribution,

$$\boldsymbol{\Sigma}_{\epsilon x} \mid \boldsymbol{\Phi}, \boldsymbol{X}^{(1)}, \boldsymbol{X}^{(0)}, \mathcal{W}^{-1}\Big(T - q,\ (\boldsymbol{X}^{(1)} - \boldsymbol{X}^{(0)}\boldsymbol{\Phi})^\top (\boldsymbol{X}^{(1)} - \boldsymbol{X}^{(0)}\boldsymbol{\Phi})\Big) \text{ and} \tag{OA.14}$$

$$\boldsymbol{\Phi} \mid \boldsymbol{\Sigma}_{\epsilon x}, \boldsymbol{X}^{(1)}, \boldsymbol{X}^{(0)} \sim \mathcal{MVN}\Big(\big((\boldsymbol{X}^{(0)})^\top \boldsymbol{X}^{(0)}\big)^{-1}(\boldsymbol{X}^{(0)})^\top \boldsymbol{X}^{(1)},\ \boldsymbol{\Sigma}_{\epsilon x} \otimes \big((\boldsymbol{X}^{(0)})^\top \boldsymbol{X}^{(0)}\big)^{-1}\Big), \quad \text{(OA.15)}$$

following similar derivations as in equations (OA.6)–(OA.7). □

OA.3 Simulations

We consider two sample sizes, $T \in \{200, 600\}$, matching the quarterly and monthly frequencies, respectively. Asset returns are simulated from a five-factor model as in equations (1) and (2): $\boldsymbol{r}_t = \hat{\boldsymbol{\alpha}} + \hat{\boldsymbol{\beta}}_{\tilde{v}}\hat{\boldsymbol{\lambda}}_{\tilde{v}} - \frac{1}{2}\hat{\boldsymbol{\Upsilon}}_r + \hat{\boldsymbol{\beta}}_{\tilde{v}}\tilde{\boldsymbol{v}}_t + \boldsymbol{w}_{rt}$, $\tilde{\boldsymbol{v}}_t \overset{\text{iid}}{\sim} \mathcal{N}(\boldsymbol{0}_K, \boldsymbol{I}_K)$. Specifically, $\boldsymbol{r}_t$ contain Fama-French 275 portfolio returns (FF275; see Online Appendix OA.4), and factor loadings $\hat{\boldsymbol{\beta}}_{\tilde{v}}$ are calibrated as the eigenvectors corresponding to the five largest eigenvalues of the sample covariance matrix of $\boldsymbol{r}_t$. Risk premia $\hat{\boldsymbol{\lambda}}_{\tilde{v}}$ are estimated using the observed data. To ensure that $\boldsymbol{\alpha}$ and $\boldsymbol{\beta}_{\tilde{v}}$ are orthogonal in simulations, we regress the estimated $\boldsymbol{\alpha}$ on $\boldsymbol{\beta}_{\tilde{v}}$ and extract the residual term, denoted by $\hat{\boldsymbol{\alpha}}$. We allow for a non-diagonal covariance matrix of $\boldsymbol{w}_{rt}$. Following Bai and Ng (2002), we simulate w_{irt} as follows:

$$w_{irt} = \hat{\sigma}_{irt} \cdot \Big[e_{it} + \sum_{j\neq 0, j=-J}^{J} \beta e_{i-j,t}\Big], \quad e_{it} \overset{\text{iid}}{\sim} \mathcal{N}(0, \frac{1}{1+2J\beta^2}), \quad \text{(OA.16)}$$

where $J = \max\{10, \text{int}\big(N/20\big)\}$, $\beta = 0.1$,[3] and $\{\hat{\sigma}_{ir}^2\}_{i=1}^N$ are the estimated variance of idiosyncratic shocks for each asset.

We then simulate strong factors. For $T = 200$, we use nondurable consumption growth to estimate impulse responses, denoted by $\{\hat{\rho}_s\}_{s=0}^{\bar{S}}$, assuming the true $\bar{S} = 8$ (quarters). For $T = 600$, we use monthly industrial production growth to obtain $\{\hat{\rho}_s\}_{s=0}^{\bar{S}}$, with the true $\bar{S}$ equal to 16 (months). With these parameters, the strong g_t is simulated as

$$g_t = c \cdot \sum_{s=0}^{\bar{S}} \hat{\rho}_s f_{t-s} + w_{gt}, \quad f_t = \frac{1}{\sqrt{3}}(\tilde{v}_{1t} + \tilde{v}_{3t} + \tilde{v}_{5t}), \quad w_{gt} \overset{\text{iid}}{\sim} \mathcal{N}(0, \sigma_{wg}^2), \quad \text{(OA.17)}$$

where f_t relates to both large and small principal components (PCs) of asset returns. We consider three signal-to-noise ratios, summarized by the time-series fit $R_g^2 \in \{30\%, 20\%, 10\%\}$.

For the weak factor, we simulate f_t independently from the standard normal distribution. The simulated weak factor g_t is autocorrelated, allowing us to assess whether the Newey and

[3] β cannot be too large since we need to ensure that the largest eigenvalue of $\hat{\boldsymbol{\Sigma}}_{wr}$ is less than the smallest eigenvalue of $\hat{\boldsymbol{\beta}}_{\tilde{v}}^\top \hat{\boldsymbol{\beta}}_{\tilde{v}}$. Otherwise, some common factors cannot be identified.

West (1987) type of sandwich covariance matrix delivers proper Bayesian credible intervals when the measurement error is autocorrelated. The pseudo-true number of latent factors is five. To explore the performance of our approach when we erroneously omit some priced factors or include redundant ones, we estimate models with $K \in \{4, 5, 7\}$. We estimate the term structure of g_t's risk premia using $\bar{S} = 12$ for $T = 200$ and $\bar{S} = 24$ for $T = 600$.

Tables OA.IV and OA.V report the empirical size of our test for strong factors in 1,000 simulations. Our method delivers appropriate credible intervals for g_t's risk premia as long as we include all priced latent factors in the estimation ($K \geq 5$), even in environments with low signal-to-noise ratios and small sample sizes. If we omit some priced factors (i.e., $K = 4$), estimates are biased because g_t loads on the fifth PC of asset returns. Including more factors than in the pseudo-true model has no sizable detrimental effect, confirming that the approach is conservative in this dimension.

Can we recover the priced information embedded in g_t if we consider only the contemporaneous correlation between g_t and asset returns? The left panel of Figure OA.3 plots the average correlation between the true f_t and its estimate, $\hat{f}_t = \hat{\boldsymbol{\eta}}_g^\top \hat{\boldsymbol{v}}_t$, for different choices of $\bar{S}$. When we project g_t only on contemporaneous asset return shocks ($\bar{S} = 0$ in equation (A2)), $\text{corr}(f_t, \hat{f}_t)$ is small, ranging from 0.4 to 0.65. As we include more lagged asset pricing information in g_t, this correlation rises substantially, so the lagged information is essential for identifying the priced shock driving the nontradable factor. The detrimental effect of including more lags than in the pseudo-true specification is generally very small.

The right panel of Figure OA.3 reports the corresponding power of rejecting zero risk premia for strong factors. The model with $\bar{S} = 0$ generally has low test power. As we include more lagged latent factors in g_t's estimation, test power rises substantially. Hence the MA representation of g_t is the key ingredient for detecting significant risk premia in persistent factors. Including more factors than in the pseudo-true specification tends to be a conservative strategy, since it delivers proper but wider credible intervals for risk premia estimates.

In Tables OA.VI and OA.VII, we investigate useless yet persistent factors that do not correlate with asset returns. In these tables, a larger R_g^2 corresponds to a more persistent process. Fama-MacBeth and GMM estimates of useless factor risk premia tend to appear spuriously significant (e.g., Kan and Zhang, 1999). Our Bayesian estimates do not suffer from this issue: credible intervals for the risk premia of useless factors are conservative.

A potential concern is that including many lags of multiple latent factors might lead to

severe overfitting of the data. The posterior means of R_g^2 across simulations, reported in Table OA.VIII, show that this is not the case.

We further examine the performance of our Bayesian estimator for factors that correlate with only the contemporaneous asset return shocks, the setting studied in Giglio and Xiu (2021). We simulate priced factors using equation (OA.17) by setting $\bar{S} = 0$ and tuning c such that $R_g^2 \in \{10\%, 20\%, 30\%\}$. Table OA.IX displays both the size and power of (i) our Bayesian test based on Proposition A1 with $\bar{S} = 0$ and (ii) the frequentist test of Theorem 1 of Giglio and Xiu (2021). Our Bayesian test has almost identical size and power to the frequentist test in this special case.

OA.3.1 Time-Varying Risk Premia

In this section, we explore the finite-sample performance of our Bayesian estimator in Proposition OA.3 when latent factors command time-varying risk premia. Different from the unconditional risk premia model, we simulate latent factors, $\tilde{\boldsymbol{v}}_t$, from the VAR(1) process, $\tilde{\boldsymbol{v}}_t = \hat{\boldsymbol{\phi}}_1 \tilde{\boldsymbol{v}}_{t-1} + \boldsymbol{\epsilon}_{\tilde{v}t}$, $\boldsymbol{\epsilon}_{\tilde{v}t} \overset{\text{iid}}{\sim} \mathcal{N}(\mathbf{0}_K, \boldsymbol{I}_K)$, where $\hat{\boldsymbol{\phi}}_1$ is calibrated by running the VAR(1) regression using the top five PCs of asset returns.[4] Next, we simulate the asset returns as before, assuming a five-factor model. Finally, we generate g_t such that it is driven by $\boldsymbol{\epsilon}_{\tilde{v}t}$ instead of $\tilde{\boldsymbol{v}}_t$: $g_t = c \cdot \sum_{s=0}^{\bar{S}} \hat{\rho}_s f_{t-s} + w_{gt}$, $f_t = \frac{1}{\sqrt{3}}(1, 0, 1, 0, 1)\boldsymbol{\epsilon}_{\tilde{v}t}$.

Similar to the simulations in the main text, we report the size, power, and time series fit in g_t's equation (R_g^2) and the correlation between estimated and pseudo-true latent process f_t in Tables OA.X–OA.XI. Overall, our Bayesian estimator in Proposition OA.3 has satisfactory finite-sample performance, delivering consistent estimates of unconditional risk premia.

OA.4 Data Description

We consider a cross-section of 275 equity portfolios collected from Ken French's website (FF275): 25 (5×5) portfolios sorted by (1) size and book-to-market ratio, (2) size and accrual, (3) size and beta, (4) size and investment, (5) size and long-term reversals, (6) size and momentum, (7) size and net issuance, (8) size and profitability, (9) size and residual variance, (10) size and variance, and (11) size and short-term reversals. The sample ranges from Q3 1963 to Q4 2019. Table OA.III presents the factors studied in Section 2. We show each variable's name, description, sample, and data source. When the sample of factors differs from that of asset returns, we use

[4] If a parameter in $\boldsymbol{\phi}_1$ is not significant at the 10% level, we set it to be zero in $\hat{\boldsymbol{\phi}}_1$.

the overlapping sample. Hence, different factors use different samples in estimation.

OA.5 Alternative Formulation for g_t

The priced Wold decomposition in Theorem A1 implies that the factor g_t can be driven by both $\boldsymbol{\epsilon}_{\tilde{\boldsymbol{v}}\boldsymbol{t}}$ and $\boldsymbol{\mu}_{\tilde{v},t-1}^{\top}\boldsymbol{\epsilon}_{\tilde{v},t}$, where the latter captures time-varying risk premia of latent factors. In this appendix, we rewrite the dynamics of g_t as follows:

$$g_t = \mu_g + \sum_{s=0}^{\bar{S}} \tilde{\rho}_s\big(\tilde{\boldsymbol{\eta}}_{g1}^{\top}\boldsymbol{\epsilon}_{\tilde{v},t-s} + \tilde{\eta}_{g2}\boldsymbol{\mu}_{\tilde{v},t-s-1}^{\top}\boldsymbol{\epsilon}_{\tilde{v},t-s}\big) + w_{gt} = \mu_g + \sum_{s=0}^{\bar{S}} \tilde{\rho}_s \underbrace{\tilde{\boldsymbol{\eta}}_g^{\top}\boldsymbol{\epsilon}_{g,t-s}}_{f_{t-s}} + w_{gt}, \tag{OA.18}$$

where $\tilde{\boldsymbol{\eta}}_g^{\top}\tilde{\boldsymbol{\eta}}_g = 1$, $\tilde{\boldsymbol{\eta}}_g^{\top} = (\tilde{\boldsymbol{\eta}}_{g1}^{\top}, \tilde{\eta}_{g2})^{\top}$ and $\boldsymbol{\epsilon}_{g,t-s}^{\top} = (\boldsymbol{\epsilon}_{\tilde{v},t-s}^{\top}, \boldsymbol{\mu}_{\tilde{v},t-s-1}^{\top}\boldsymbol{\epsilon}_{\tilde{v},t-s})^{\top}$. Under this assumption, we show that the term structure of g's risk premia is

$$\lambda_{g,t-1}^{S} = \sum_{\tau=0}^{S}\sum_{s=0}^{\tau} \tilde{\rho}_s \frac{\tilde{\boldsymbol{\eta}}_{g1}^{\top}\boldsymbol{\lambda}_{\tilde{v}} + (\tilde{\boldsymbol{\eta}}_{g1} + \tilde{\eta}_{g2}\boldsymbol{\lambda}_{\tilde{v}})^{\top}\mathbb{E}_{t-1}\big[\boldsymbol{\mu}_{\tilde{v},t+\tau-s-1}\big] + \tilde{\eta}_{g2}\mathbb{E}_{t-1}\big[\boldsymbol{\mu}_{\tilde{v},t+\tau-s-1}^{\top}\boldsymbol{\mu}_{\tilde{v},t+\tau-s-1}\big]}{1+S}. \tag{OA.19}$$

If $\tilde{\eta}_{g2} = 0$, the above definition is exactly identical to that in equation (9).

In estimation, we identify a linear rotation of $\tilde{\boldsymbol{v}}_t$: $\boldsymbol{v}_t = \boldsymbol{H}\tilde{\boldsymbol{v}}_t = \boldsymbol{H}\boldsymbol{\mu}_{\tilde{v},t-1} + \boldsymbol{H}\boldsymbol{\epsilon}_{\tilde{\boldsymbol{v}}\boldsymbol{t}} = \boldsymbol{\mu}_{v,t-1} + \boldsymbol{\epsilon}_{vt}$, which implies that $\boldsymbol{\Sigma}_{\epsilon v} = \mathrm{cov}(\boldsymbol{\epsilon}_{vt}) = \boldsymbol{H}\boldsymbol{H}^{\top}$. We generalize the rotation invariance to identify the time-varying risk premia as follows:

$$\begin{aligned}
\boldsymbol{r}_t &= \boldsymbol{\alpha} - \frac{\boldsymbol{\Upsilon}_r}{2} + \underbrace{\boldsymbol{\beta}_{\tilde{v}}\boldsymbol{H}^{-1}}_{\boldsymbol{\beta}_v}\underbrace{\boldsymbol{H}\boldsymbol{\lambda}_{\tilde{v}}}_{\boldsymbol{\lambda}_v} + \underbrace{\boldsymbol{\beta}_{\tilde{v}}\boldsymbol{H}^{-1}}_{\boldsymbol{\beta}_v}\underbrace{\boldsymbol{H}\tilde{\boldsymbol{v}}_t}_{\boldsymbol{v}_t} + \boldsymbol{w}_{rt},\\
m_t &= \kappa_m - \boldsymbol{\lambda}_v^{\top}(\boldsymbol{H}^{-1})^{\top}\boldsymbol{H}^{-1}\boldsymbol{\epsilon}_{vt} - \boldsymbol{\mu}_{v,t-1}^{\top}(\boldsymbol{H}^{-1})^{\top}\boldsymbol{H}^{-1}\boldsymbol{\epsilon}_{vt} = \kappa_m - \boldsymbol{\lambda}_v^{\top}\boldsymbol{\Sigma}_{\epsilon v}^{-1}\boldsymbol{\epsilon}_{vt} - \boldsymbol{\mu}_{v,t-1}^{\top}\boldsymbol{\Sigma}_{\epsilon v}^{-1}\boldsymbol{\epsilon}_{vt},\\
g_t &= \mu_g + \sum_{s=0}^{\bar{S}} \tilde{\rho}_s\Bigg(\underbrace{\tilde{\boldsymbol{\eta}}_{g1}^{\top}\boldsymbol{H}^{-1}}_{\boldsymbol{\eta}_{g1}^{\top}}\underbrace{\boldsymbol{H}\boldsymbol{\epsilon}_{\tilde{v},t-s}}_{\boldsymbol{\epsilon}_{v,t-s}} + \eta_{g2}\underbrace{\boldsymbol{\mu}_{v,t-s-1}^{\top}(\boldsymbol{H}^{-1})^{\top}}_{\boldsymbol{\mu}_{\tilde{v},t-s-1}^{\top}}\underbrace{\boldsymbol{H}^{-1}\boldsymbol{\epsilon}_{v,t-s}}_{\boldsymbol{\epsilon}_{\tilde{v},t-s}}\Bigg) + w_{gt}, \text{ and}\\
\lambda_{g,t-1}^{S} &= \sum_{\tau=0}^{S}\sum_{s=0}^{\tau} \tilde{\rho}_s \frac{\boldsymbol{\eta}_{g1}^{\top}\boldsymbol{\lambda}_v + (\boldsymbol{\eta}_{g1} + \tilde{\eta}_{g2}\boldsymbol{\Sigma}_{\boldsymbol{\epsilon}\boldsymbol{v}}^{-1}\boldsymbol{\lambda}_v)^{\top}\mathbb{E}_{t-1}\big[\boldsymbol{\mu}_{v,t+\tau-s-1}\big] + \tilde{\eta}_{g2}\mathbb{E}_{t-1}\big[\boldsymbol{\mu}_{v,t+\tau-s-1}^{\top}\boldsymbol{\Sigma}_{\boldsymbol{\epsilon}\boldsymbol{v}}^{-1}\boldsymbol{\mu}_{v,t+\tau-s-1}\big]}{1+S}.
\end{aligned} \tag{OA.20}$$

We perform a formal test to determine whether the additional component, $\boldsymbol{\mu}_{v,t-1}^{\top}\boldsymbol{\Sigma}_{\epsilon v}^{-1}\boldsymbol{\epsilon}_{vt}$, is essential in driving the dynamics of g_t. First, including $\boldsymbol{\mu}_{v,t-1}^{\top}\boldsymbol{\Sigma}_{\epsilon v}^{-1}\boldsymbol{\epsilon}_{vt}$ in the dynamics of g_t only marginally improves the time-series fit, with the incremental R_g^2 below 1% across fac-

tors. Furthermore, we investigate the cumulative impulse response functions (CIRFs) of g_t to one-standard-deviation innovations in $\boldsymbol{\mu}_{v,t-1}^{\top}\boldsymbol{\Sigma}_{\boldsymbol{\epsilon v}}\boldsymbol{\epsilon}_{v,t}$, that is, $\left(\sum_{s=0}^{\bar{S}}\rho_s\right)\cdot\eta_{g2}/\sigma\left(\boldsymbol{\mu}_{v,t-1}^{\top}\boldsymbol{\Sigma}_{\boldsymbol{\epsilon v}}\boldsymbol{\epsilon}_{v,t}\right)$. Except for HKM and VIX factors, the CIRFs of other factors are not significantly different from zero, and estimates of CIRFs tend to be rather volatile for quarterly macro factors, leading to noisy risk-premia estimates. Therefore, omitting $\boldsymbol{\mu}_{v,t-1}^{\top}\boldsymbol{\Sigma}_{\boldsymbol{\epsilon v}}\boldsymbol{\epsilon}_{v,t}$ in the g_t dynamics, from the empirical perspective, results in at most a slight bias in risk premia estimates.

OA.6 Contemporaneous Innovations in Macro Factors

The main text documented that the risk premia of many core macro factors are small and insignificant at $S = 0$, but large and highly significant at business-cycle horizons. This appendix shows that the insignificance at $S = 0$ is robust to alternative specifications and estimators: identification of priced macro risk hinges on the inclusion of *lagged* asset return shocks through the MA representation of g_t, not on any specific feature of our Bayesian implementation.

Table OA.XII reports the evidence. Panel A re-estimates the risk premia of the macro factors in Table 1 setting $\bar{S} = 0$; quarterly factors related to production, consumption, investment, and labour market conditions all display tiny and largely insignificant risk premia. Panel B repeats the exercise on the AR(1) innovations of these factors and reaches the same conclusion. Hence, although the AR(1) model is commonly adopted in empirical and theoretical work, extracting AR(1) innovations is insufficient to recover the risk premia of most macro variables – either because the AR(1) shocks are inconsequential or because the AR(1) assumption itself is questionable. By contrast, our MA representation takes no stance on the exact data-generating process and yields a flexible function of current and lagged asset return innovations. The same conclusion obtains with the frequentist estimator of Giglio and Xiu (2021).

The intuition lies in the time-series fit R_g^2, which is considerably larger in Table 1 than in Table OA.XII. For instance, contemporaneous asset return shocks explain only 2% of investment growth, but R_g^2 rises to about 36% at $\bar{S} = 12$ quarters, sharply raising the signal-to-noise ratio. What looks unpriced in standard contemporaneous specifications is in fact strongly priced once the propagation of priced shocks into macro variables is properly accounted for.

OA.7 PPI Inflation Decomposition

PPI	Description	Matched IP	Description
PPIACO	All Commodities	INDPRO	Total Industrial Production
PPIIDC	Industrial Commodities	IPMAN	Manufacturing
WPU02	Processed Foods and Feeds	IPG311A2N	Food, Beverage, and Tobacco Mfg.
WPU05	Fuels and Related Products	IPG211S	Mining: Oil and Gas Extraction
WPU06	Chemicals and Allied Prods.	IPG325S	Chemical Manufacturing
WPU07	Rubber and Plastic Products	IPG326S	Plastics and Rubber Products
WPU08	Lumber and Wood Products	IPG321S	Wood Products
WPU09	Pulp, Paper, and Allied	IPG322S	Paper Manufacturing
WPU10	Metals and Metal Products	IPG331S	Primary Metal Manufacturing
WPU11	Machinery and Equipment	IPG333S	Machinery Manufacturing
WPU12	Furniture and Household	IPG337S	Furniture and Related Prods.
WPU13	Nonmetallic Mineral Prods.	IPG327S	Nonmetallic Mineral Products
WPU14	Transportation Equipment	IPG336S	Transportation Equipment
WPU15	Miscellaneous Products	IPG339S	Miscellaneous Manufacturing

Table OA.II: PPI commodity groups and matched NAICS-3 industrial-production indices. All series from FRED except WPU05 (BLS public API).

OA.7.1 Data

We construct producer-side counterparts to the demand- and supply-driven inflation series of Shapiro (2022), using two data inputs: monthly BLS Producer Price Indices for twelve disaggregated commodity groups (plus the BLS PPIACO and PPIIDC aggregates) and matched NAICS-3 industrial-production indices from the Federal Reserve's G.17 release. Table OA.II lists the series; all are obtained from FRED except WPU05 (Fuels, not redistributed by FRED), which is pulled from the BLS public API. WPU01 (Farm Products) and WPU03 (Textile Products and Apparel) are dropped for lack of a clean matched NAICS-3 IP series; WPU04 (Hides, Skins, Leather) was discontinued by the BLS and is also excluded. Sample is January 1947 through March 2026, with NAICS-3 disaggregated IP series starting January 1972 in the modern vintage. For external validation we use the West Texas Intermediate spot oil price (FRED series WTISPLC) as a cost-push benchmark, the NBER recession indicator (USREC) for the demand-side validation, and the published demand- and supply-driven PCE inflation series of Shapiro (2022), available monthly from January 1970 at the San Francisco Fed.[5]

OA.7.2 Construction of Demand- and Supply-Driven PPI Inflation

We adapt the methodology of Shapiro (2022) to the producer-price data. His identification operates on ∼130 disaggregated PCE categories where idiosyncratic price–quantity variation at the category level supports a sign-based classification. The PPI sample contains many fewer

[5]Source: frbsf.org/research-and-insights/data-and-indicators/supply-and-demand-driven-pce-inflation.

matched pairs listed in Table OA.II. As Shapiro's, our rolling-window length is one hundred and twenty. The effective sample of NAICS-3 data starts in January 1972. For each matched commodity-group / industrial-production pair $i = 1, \ldots, 14$ and each month t at which a 60-month training window is available, we estimate a bivariate reduced-form VAR in monthly log differences $p_{i,t} = \Delta \log \mathrm{PPI}_{i,t}$ and $q_{i,t} = \Delta \log \mathrm{IP}_{i,t}$:

$$p_{i,t} = \alpha^p_{i,0} + \alpha^p_{i,1}\, p_{i,t-1} + \alpha^p_{i,12}\, p_{i,t-12} + \beta^p_{i,1}\, q_{i,t-1} + \beta^p_{i,12}\, q_{i,t-12} + \varepsilon^p_{i,t}, \tag{OA.21}$$

$$q_{i,t} = \alpha^q_{i,0} + \alpha^q_{i,1}\, q_{i,t-1} + \alpha^q_{i,12}\, q_{i,t-12} + \beta^q_{i,1}\, p_{i,t-1} + \beta^q_{i,12}\, p_{i,t-12} + \varepsilon^q_{i,t}. \tag{OA.22}$$

We Cholesky-orthogonalize the one-step-ahead residuals $(\hat{\varepsilon}^q_{i,t}, \hat{\varepsilon}^p_{i,t})$ with quantity ordered first, identifying the demand- and supply-driven contributions to producer-price inflation as $\pi^{D,i}_t \equiv \gamma_i\, \hat{\varepsilon}^q_{i,t}$, $\pi^{S,i}_t \equiv \hat{\varepsilon}^p_{i,t} - \gamma_i\, \hat{\varepsilon}^q_{i,t}$, $\gamma_i \equiv \frac{\mathrm{Cov}(\hat{\varepsilon}^p_{i,t}, \hat{\varepsilon}^q_{i,t})}{\mathrm{Var}(\hat{\varepsilon}^q_{i,t})}$. The identifying restriction is that supply shocks affect quantities only with a lag, while prices respond contemporaneously to both shocks. By construction $\pi^{D,i}_t + \pi^{S,i}_t = \hat{\varepsilon}^p_{i,t}$ and $\mathrm{Cov}(\pi^{S,i}_t, \hat{\varepsilon}^q_{i,t}) = 0$. Braun et al. (2024) apply a sign-restricted bivariate SVAR to manufacturing PPI, identifying the rotation with the Census Bureau's Quarterly Survey of Plant Capacity, available from 2008.[6]

The aggregate demand- and supply-driven PPI inflation series are equal-weighted averages across the twelve disaggregated commodity groups (excluding PPIACO and PPIIDC, which are themselves BLS aggregates and would double-count):

$$\pi^D_t = \frac{1}{12}\sum_{i=1}^{12} \pi^{D,i}_t, \qquad \pi^S_t = \frac{1}{12}\sum_{i=1}^{12} \pi^{S,i}_t, \tag{OA.23}$$

with a minimum of eight commodity groups required at each t. The resulting series run monthly from February 1978 (sixty months plus twelve lags after the January 1972 NAICS-3 start) through March 2026. Variance-share and empirical-Laspeyres weighting schemes give qualitatively identical results.

Figure OA.2 plots the resulting equal-weighted aggregate π^D_t and π^S_t series. The supply-driven series spikes upward at each major cost-push episode — Iran, the Gulf War, the Iraq War, Hurricane Katrina, the 2008 oil-price peak, and the Russian invasion of Ukraine — and turns

[6] As outlined by the authors, without this external identification of the rotation, the simple sign-based identification at the commodity-group level fails. With PPI data, this yields a high degree of misclassification: aggregating Shapiro's discrete sign-based classification across the twelve disaggregated commodity groups gives a supply-driven series whose correlation with oil-price growth is lower than that of the implied demand-driven series (0.38 versus 0.50).

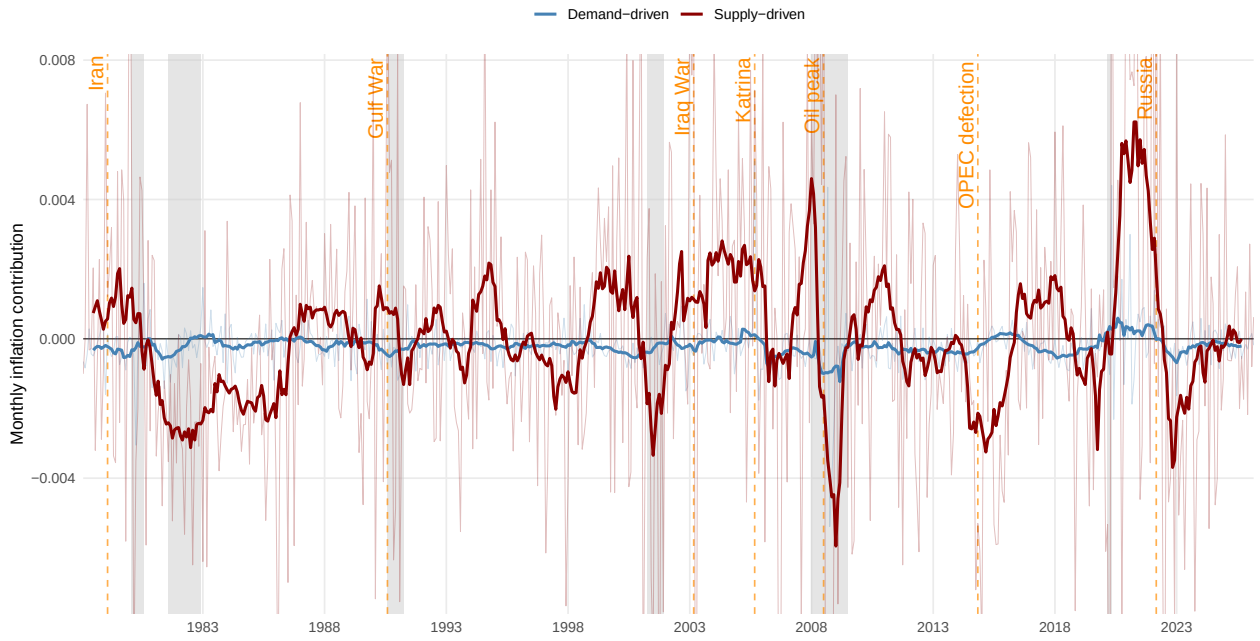

Figure OA.2: Aggregate demand- and supply-driven PPI inflation. The figure plots the monthly equal-weighted aggregate demand-driven contribution π_t^D (blue) and supply-driven contribution π_t^S (red) to unexpected PPI inflation, constructed by Cholesky-orthogonalizing the bivariate VAR residuals with quantity ordered first and averaging across the twelve disaggregated PPI/NAICS-3 IP pairs of Table OA.II. Faint lines show the raw monthly series; bold lines show centered 12-month moving averages. Grey shaded regions denote NBER recessions. Orange dashed vertical lines mark major cost-push episodes. Sample is February 1978 through March 2026 (578 monthly observations).

sharply negative around the November 2014 OPEC defection that triggered the 2014–2016 oil-price collapse. The demand-driven series collapses in NBER recessions and rises sharply during the 2021–2022 post-pandemic demand boom. Both patterns are consistent with the economic content of the decomposition.

OA.8 Connection to Dividend Strips

Let D_t denote the dividend payment at time t, and $P_{s,t}$ denotes the time-t price of the dividend strip delivering D_{t+s} at time $t+s$. We define: holding period return $= R_{t,t+S} = \frac{D_{t+s}}{P_{s,t}}$; spot equity yield $= e_{s,t} = \frac{1}{s}\log\left(\frac{D_t}{P_{s,t}}\right)$; forward equity yield $= e^f_{s,t} = \frac{1}{s}\log\left(\frac{D_t}{P_{s,t}}\right) - \frac{1}{s}r_{f,t,t+s}$, where $\frac{1}{s}r_{f,t,t+s}$ is log risk-free rate with time-to-maturity s.

The fundamental asset pricing equation implies that $P_{s,t} = \mathbb{E}_t[M_{t,t+s} \cdot D_{t+s}]$, where $M_{t,t+s}$ is the multi-period SDF between time t and $t+s$. Accordingly, the gross risk-free rate with

time-to-maturity s is $R_{f,t,t+s} = 1/\mathbb{E}_t[M_{t,t+s}]$.

The s-period return on the dividend strip with time-to-maturity s can be expressed as $R_{t,t+s} = \frac{D_{t+s}}{P_{s,t}} = \frac{D_t}{P_{s,t}}\frac{D_{t+s}}{D_t}$, which implies the following per-period log strip return:

$$r_{t+s} = \frac{1}{s}\log(R_{t,t+s}) = \frac{1}{s}\log\left(\frac{D_t}{P_{s,t}}\right) + \frac{1}{s}\log\left(\frac{D_{t+s}}{D_t}\right) = e_{s,t} + g_{d,t,t+s}, \tag{OA.24}$$

where $e_{s,t} = \frac{1}{s}\log\left(\frac{D_t}{P_{s,t}}\right)$ is the spot equity yield for maturity s, and $g_{d,t,t+s} = \frac{1}{s}\log\left(\frac{D_{t+s}}{D_t}\right)$ is the per-period log growth rate of dividend payments. Equation (OA.24) also implies that the conditional variance of r_{t+s} is identical to that of $g_{d,t,t+s}$, that is, $\text{var}_t(r_{t+s}) = \text{var}_t(g_{d,t,t+s})$.

Assuming the joint log normality of SDF and dividend growth and the SDF, we can rewrite:

$$\frac{P_{s,t}}{D_t} = \mathbb{E}_t\left[e^{m_{t,t+s}+\Delta d_{t,t+s}}\right] = \exp\left\{\mathbb{E}_t[m_{t,t+s}]+\frac{1}{2}\text{var}_t(m_{t,t+s})+\mathbb{E}_t[\Delta d_{t,t+s}]+\frac{1}{2}\text{var}_t(\Delta d_{t,t+s})+\text{cov}_t(m_{t,t+s},\Delta d_{t,t+s})\right\},$$

which implies that the spot equity yield, $e_{s,t}$, can be expressed as

$$e_{s,t} = -\frac{1}{s}\left[\mathbb{E}_t[m_{t,t+s}] + \frac{1}{2}\text{var}_t(m_{t,t+s})\right] - \frac{1}{s}\mathbb{E}_t[\Delta d_{t,t+s}] - \frac{1}{2s}\text{var}_t(\Delta d_{t,t+s}) - \frac{1}{s}\text{cov}_t(m_{t,t+s},\Delta d_{t,t+s}).$$

This further implies that the expected per-period strip return is

$$\mathbb{E}_t[r_{t+s}] = e_{s,t} + \mathbb{E}_t[g_{d,t,t+s}] = \frac{1}{s}r_{f,t,t+s} - \frac{1}{2s}\text{var}_t(\Delta d_{t,t+s}) - \frac{1}{s}\text{cov}_t(m_{t,t+s},\Delta d_{t,t+s}). \tag{OA.25}$$

Note that $\text{var}_t(\Delta d_{t,t+s}) = s^2\text{var}_t(r_{t+s})$ and $-\frac{1}{s}\text{cov}_t(m_{t,t+s},\Delta d_{t,t+s})$ is the risk premium of the dividend growth defined in equation (9); hence, we can express the expected per-period strip return, after accounting for the Jensen's correction term, as: $\mathbb{E}_t[r_{t+s}] + \frac{s}{2}\text{var}_t(r_{t+s}) = \frac{1}{s}r_{f,t,t+s} + \lambda^s_{dt}$. Note that under the joint log normality assumption, $\mathbb{E}_t[r_{t+s}]+\frac{s}{2}\text{var}_t(r_{t+s}) = \frac{1}{s}\log\mathbb{E}_t[R_{t,t+s}]$. Therefore, λ^s_{dt}, which equals $\frac{1}{s}\log\mathbb{E}_t[R_{t,t+s}] - \frac{1}{s}r_{f,t,t+s}$, can be interpreted as the per-period risk premium on the hold-to-maturity dividend strips.

Using equation (OA.25), we can derive the forward equity yield, as: $e^f_{s,t} = e_{s,t} - \frac{1}{s}r_{f,t,t+s} = \lambda^s_{dt} - \mathbb{E}_t[g_{d,t,t+s}] - \frac{1}{2s}\text{var}_t(\Delta d_{t,t+s})$, where the last term, $\frac{1}{2s}\text{var}_t(\Delta d_{t,t+s})$ is negligible in the data.

OA.9 Additional Tables and Figures

Table OA.III: List of Factors

Number and description of factors:	Sample	Source
AEM intermediary factor (Adrian et al. (2014))	Q1 1968 – Q3 2017	Tyler Muir's Website
Consumer price index (CPI), log growth	Q3 1963 – Q4 2019	Federal Reserve Bank of St. Louis
Industrial production growth (log change in real per capita)	Q3 1963 – Q4 2019	Federal Reserve Bank of St. Louis
GDP growth (log change in real per capita)	Q3 1963 – Q4 2019	BEA Table 7.1
Durable consumption growth (log change in real per capita)	Q3 1963 – Q4 2019	BEA Table 7.1
Nondurable consumption growth (log change in real per capita)	Q3 1963 – Q4 2019	BEA Table 7.1
Service consumption growth (log change in real per capita)	Q3 1963 – Q4 2019	BEA Table 7.1
Labor income growth (defined in Lettau and Ludvigson (2001))	Q3 1963 – Q3 2019	Martin Lettau's website
Total factor productivity (TFP) growth	Q3 1963 – Q4 2019	John Fernald's website
Utilization-adjusted TFP growth in Fernald (2014)	Q3 1963 – Q4 2019	John Fernald's website
Civilian unemployment rate (UNRATE) change	Q3 1963 – Q4 2019	Federal Reserve Bank of St. Louis
Hours worked, log growth	Q3 1963 – Q4 2019	Federal Reserve Bank of St. Louis
Real Investment per capita, log growth	Q3 1963 – Q4 2019	Federal Reserve Bank of St. Louis
(Non)traded HKM intermediary factors (He et al. (2017))	Jan 1970 – Dec 2019	Zhiguo He's website
PS liquidity factors (Pástor and Stambaugh (2003))	Jul 1963 – Dec 2019	Lubos Pastor's website
$\Delta \log(\text{VIX}_t) = \log(\text{VIX}_t) - \log(\text{VIX}_{t-1})$	Jan 1986 – Dec 2019	Federal Reserve Bank of St. Louis
Real dividend (log) growth of the S&P500 index	Q3 1963 – Q4 2019	Robert Shiller's website
Price-earning ratio of the S&P500 index (PE_{t-1})	Q3 1963 – Q4 2019	Robert Shiller's website
Term spread (TS_{t-1}) from FRED-QD/MD	Q3 1963 – Q4 2019	Michael W. McCracken's website
Default spread (DS_{t-1}) from FRED-QD/MD	Q3 1963 – Q4 2019	Michael W. McCracken's website
Value spread (VS_{t-1})	Q3 1963 – Q4 2019	Ken French's website
MKT (market), SMB (size), HML (value)	Jul 1963 – Dec 2019	Ken French's website
Tobin's Q (Corporate Equities as a Percentage of Net Worth)	Q3 1963 – Q4 2019	Federal Reserve Bank of St. Louis
Capacity utilization (FRED: TCU)	Q2 1967 – Q4 2019	Federal Reserve Bank of St. Louis
Composite Consumer Confidence for US	Q3 1963 – Q4 2019	Federal Reserve Bank of St. Louis
Michigan Consumer Sentiment	Q3 1963 – Q4 2019	Federal Reserve Bank of St. Louis
SPF forecast error of GDP growth	Q1 1969 – Q4 2019	Philadelphia Fed SPF
SPF cross-forecaster dispersion of GDP growth	Q4 1968 – Q4 2019	Philadelphia Fed SPF
SPF cross-forecaster dispersion of GDP deflator	Q4 1968 – Q4 2019	Philadelphia Fed SPF
GDP revision magnitudes	Q3 1965 – Q4 2019	Philadelphia Fed real-time data
Real and Macro uncertainty	Q3 1963 – Q4 2019	Ludvigson website
Economic Policy Uncertainty	Q3 1963 – Q4 2019	policyuncertainty.com
Personal savings rate	Q3 1963 – Q4 2019	Federal Reserve Bank of St. Louis
Consumption-to-income ratio (PCE / disposable personal income)	Q3 1963 – Q4 2019	BEA Table 7.1
Gilchrist-Zakrajšek Excess bond premium	Q1 1973 – Q4 2019	Federal Reserve Board
Bank credit growth (Commercial and Industrial Loans)	Q3 1963 – Q4 2019	Federal Reserve Bank of St. Louis
Senior Loan Officer net tightening	Q2 1990 – Q4 2019	Federal Reserve Bank of St. Louis
Relative price of equipment (FRED: PERIC)	Q3 1963 – Q4 2019	Federal Reserve Bank of St. Louis
Equipment investment (FRED: Y033RC1Q027SBEA)	Q3 1963 – Q4 2019	Federal Reserve Bank of St. Louis
Structures investment (FRED: B009RC1Q027SBEA)	Q3 1963 – Q4 2019	Federal Reserve Bank of St. Louis
Job-finding rate (Probability of transitioning from U to E)	Q3 1967 – Q2 2007	Shimer's website
Separation rate (Probability of transitioning from E to U)	Q3 1967 – Q2 2007	Shimer's website
Consumer price index	Q3 1963 – Q4 2019	Federal Reserve Bank of St. Louis
Nonfarm Business Sector: Unit Labor Costs for All Workers	Q3 1963 – Q4 2019	Federal Reserve Bank of St. Louis
Labor share (FRED: PRS85006173)	Q3 1963 – Q4 2019	Federal Reserve Bank of St. Louis

List of factors used in Section 2 with descriptions, samples, and data sources. Dividends: monthly real S&P500 dividend payments from Robert Shiller's website; to avoid mechanical seasonality, we use smoothed dividends D_t (sum of previous 12 months) with growth rate $\log(D_t/D_{t-1})$. Following Angeletos, Collard, and Dellas (2020), hours worked = log(Nonfarm business sector: average weekly hours × Employment Level / Civilian non-institutional population); real investment per capita = log[(Share of GDP: personal durable consumption expenditures + Share of GDP: gross private domestic investment) × Real GDP per capita]. Term spread: difference between 10-year and 3-month Treasury yields. Default spread: difference between BAA and AAA corporate bond yields. Value spread: constructed following Campbell and Vuolteenaho (2004) and Campbell et al. (2013). Michigan consumer sentiment: for the pre-1978 data, only one observation is available per quarter (in February, May, August, and November); therefore, we construct the quarterly series using the observed value for each quarter.

Table OA.IV: Testing risk premia of strong factors at quarterly frequencies ($T = 200$)

	$S=0$	1	2	3	4	5	6	7	8	9	10	11	12
Panel A: $R_g^2 = 30\%$													
Number of Factors = 5													
10%	0.134	0.110	0.114	0.111	0.113	0.108	0.109	0.107	0.109	0.112	0.110	0.113	0.113
5%	0.075	0.068	0.064	0.068	0.063	0.066	0.064	0.064	0.064	0.066	0.065	0.060	0.063
1%	0.014	0.020	0.019	0.019	0.019	0.016	0.015	0.014	0.012	0.014	0.014	0.014	0.016
Number of Factors = 4													
10%	0.338	0.331	0.331	0.336	0.327	0.328	0.328	0.328	0.325	0.327	0.331	0.326	0.328
5%	0.233	0.225	0.228	0.229	0.233	0.235	0.233	0.232	0.233	0.233	0.219	0.235	0.224
1%	0.089	0.095	0.096	0.094	0.094	0.091	0.090	0.092	0.091	0.091	0.088	0.087	0.089
Number of Factors = 7													
10%	0.141	0.108	0.115	0.124	0.120	0.119	0.111	0.111	0.112	0.117	0.115	0.118	0.119
5%	0.080	0.075	0.074	0.072	0.073	0.069	0.069	0.066	0.071	0.076	0.070	0.071	0.075
1%	0.014	0.018	0.014	0.016	0.017	0.017	0.016	0.017	0.014	0.014	0.015	0.013	0.011
Panel B: $R_g^2 = 20\%$													
Number of Factors = 5													
10%	0.134	0.126	0.122	0.120	0.116	0.115	0.114	0.115	0.115	0.118	0.118	0.123	0.120
5%	0.069	0.064	0.069	0.060	0.059	0.057	0.058	0.058	0.059	0.059	0.057	0.050	0.052
1%	0.008	0.015	0.015	0.013	0.010	0.010	0.011	0.009	0.009	0.011	0.009	0.011	0.012
Number of Factors = 4													
10%	0.307	0.339	0.327	0.320	0.328	0.322	0.327	0.328	0.331	0.336	0.330	0.339	0.337
5%	0.198	0.217	0.219	0.221	0.225	0.220	0.221	0.221	0.218	0.219	0.212	0.214	0.218
1%	0.047	0.085	0.077	0.073	0.078	0.077	0.073	0.077	0.077	0.072	0.067	0.072	0.071
Number of Factors = 7													
10%	0.141	0.131	0.138	0.125	0.128	0.121	0.120	0.125	0.132	0.140	0.142	0.134	0.138
5%	0.074	0.065	0.069	0.066	0.064	0.063	0.067	0.063	0.062	0.057	0.060	0.064	0.062
1%	0.009	0.017	0.013	0.014	0.010	0.010	0.010	0.008	0.011	0.009	0.009	0.012	0.011
Panel C: $R_g^2 = 10\%$													
Number of Factors = 5													
10%	0.117	0.166	0.169	0.159	0.172	0.175	0.174	0.175	0.174	0.173	0.166	0.169	0.172
5%	0.049	0.082	0.085	0.090	0.102	0.099	0.098	0.096	0.095	0.099	0.092	0.091	0.089
1%	0.007	0.018	0.021	0.017	0.024	0.022	0.025	0.029	0.028	0.027	0.019	0.024	0.020
Number of Factors = 4													
10%	0.194	0.287	0.296	0.306	0.313	0.308	0.316	0.318	0.308	0.302	0.284	0.290	0.297
5%	0.093	0.176	0.174	0.173	0.193	0.202	0.188	0.193	0.182	0.187	0.182	0.188	0.184
1%	0.012	0.058	0.055	0.052	0.062	0.061	0.064	0.062	0.066	0.064	0.063	0.063	0.057
Number of Factors = 7													
10%	0.117	0.178	0.168	0.178	0.193	0.197	0.193	0.189	0.191	0.187	0.192	0.186	0.185
5%	0.041	0.100	0.103	0.097	0.112	0.116	0.113	0.113	0.115	0.106	0.104	0.111	0.098
1%	0.004	0.022	0.019	0.017	0.026	0.026	0.025	0.026	0.030	0.031	0.025	0.028	0.023

The table reports the frequency of rejecting the null hypothesis $H_0 : \lambda_g^S = \lambda_g^{S,\star}$ based on the 90%, 95%, and 99% credible intervals of our Bayesian estimates in Proposition A1. λ_g^S is defined in equation (5), and $\lambda_g^{S,\star}$ is λ_g^S's pseudo-true value. We consider strong factors, with $R_g^2 \in \{10\%, 20\%, 30\%\}$. We simulate quarterly observations of g_t and $\boldsymbol{r}_t$ by assuming that i) the true number of latent factors is 5, ii) the time series sample size is 200 quarters, and iii) the true $\bar{S} = 8$. We estimate several model configurations with different numbers of factors (4, 5, and 7) and $\bar{S} = 12$. The number of Monte Carlo simulations is 1,000.

Table OA.V: Testing risk premia of strong factors at monthly frequencies ($T = 600$)

	$S=0$	2	4	6	8	10	12	14	16	18	20	22	24
Panel A: $R_g^2 = 30\%$													
					Number of Factors = 5								
10%	0.075	0.112	0.102	0.104	0.103	0.099	0.103	0.103	0.101	0.102	0.099	0.102	0.095
5%	0.024	0.062	0.047	0.046	0.050	0.045	0.045	0.046	0.044	0.043	0.044	0.051	0.049
1%	0.002	0.016	0.019	0.015	0.015	0.014	0.015	0.013	0.013	0.014	0.013	0.013	0.013
					Number of Factors = 4								
10%	0.030	0.395	0.442	0.442	0.451	0.448	0.449	0.447	0.442	0.443	0.448	0.445	0.446
5%	0.007	0.293	0.331	0.333	0.338	0.327	0.327	0.332	0.332	0.330	0.331	0.330	0.333
1%	0.001	0.134	0.158	0.156	0.153	0.146	0.146	0.149	0.152	0.150	0.147	0.150	0.147
					Number of Factors = 7								
10%	0.070	0.110	0.100	0.102	0.106	0.102	0.105	0.101	0.099	0.098	0.093	0.097	0.094
5%	0.020	0.063	0.051	0.047	0.046	0.044	0.044	0.044	0.046	0.045	0.043	0.050	0.052
1%	0.001	0.016	0.017	0.015	0.015	0.017	0.016	0.014	0.016	0.016	0.016	0.015	0.016
Panel B: $R_g^2 = 20\%$													
					Number of Factors = 5								
10%	0.059	0.111	0.107	0.094	0.096	0.094	0.091	0.090	0.094	0.089	0.093	0.092	0.090
5%	0.028	0.061	0.051	0.054	0.049	0.049	0.044	0.047	0.052	0.053	0.056	0.053	0.051
1%	0.004	0.008	0.011	0.009	0.011	0.009	0.008	0.008	0.010	0.009	0.012	0.011	0.011
					Number of Factors = 4								
10%	0.026	0.390	0.432	0.421	0.420	0.424	0.417	0.429	0.422	0.427	0.428	0.438	0.435
5%	0.008	0.275	0.312	0.311	0.310	0.308	0.312	0.316	0.312	0.303	0.310	0.309	0.305
1%	0.000	0.111	0.133	0.131	0.130	0.134	0.136	0.138	0.142	0.134	0.136	0.134	0.139
					Number of Factors = 7								
10%	0.051	0.126	0.102	0.101	0.097	0.096	0.092	0.092	0.091	0.090	0.091	0.089	0.092
5%	0.026	0.062	0.052	0.053	0.053	0.052	0.051	0.051	0.048	0.052	0.056	0.056	0.056
1%	0.003	0.009	0.011	0.010	0.011	0.012	0.010	0.011	0.010	0.011	0.013	0.011	0.010
Panel C: $R_g^2 = 10\%$													
					Number of Factors = 5								
10%	0.042	0.149	0.149	0.136	0.133	0.140	0.133	0.142	0.137	0.136	0.134	0.134	0.139
5%	0.017	0.070	0.076	0.086	0.082	0.083	0.085	0.082	0.082	0.083	0.077	0.079	0.090
1%	0.003	0.007	0.024	0.021	0.025	0.019	0.021	0.021	0.017	0.017	0.019	0.020	0.022
					Number of Factors = 4								
10%	0.018	0.313	0.373	0.376	0.382	0.384	0.378	0.386	0.384	0.379	0.375	0.369	0.366
5%	0.004	0.191	0.258	0.255	0.269	0.269	0.264	0.261	0.267	0.269	0.268	0.261	0.261
1%	0.002	0.037	0.110	0.111	0.117	0.119	0.121	0.121	0.117	0.108	0.107	0.108	0.112
					Number of Factors = 7								
10%	0.039	0.144	0.155	0.150	0.142	0.136	0.140	0.138	0.143	0.138	0.146	0.136	0.140
5%	0.013	0.075	0.089	0.086	0.088	0.093	0.093	0.089	0.090	0.093	0.087	0.087	0.087
1%	0.002	0.006	0.029	0.026	0.026	0.025	0.025	0.025	0.020	0.022	0.026	0.026	0.027

Frequency of rejecting $H_0 : \lambda_g^S = \lambda_g^{S,\star}$ using 90%, 95%, and 99% credible intervals from Proposition A1, where λ_g^S is defined in equation (5) and $\lambda_g^{S,\star}$ is the pseudo-true value. Strong factors with $R_g^2 \in \{10\%, 20\%, 30\%\}$. Simulations: monthly data, true model has 5 factors with $\bar{S} = 16$ and $T = 600$; estimated models use 4, 5, or 7 factors with $\bar{S} = 24$. 1,000 Monte Carlo simulations.

Table OA.VI: Testing risk premia of useless factors at quarterly frequencies ($T = 200$)

	$S=0$	1	2	3	4	5	6	7	8	9	10	11	12
Panel A: $R_g^2 = 30\%$													
					Number of Factors = 5								
10%	0.032	0.036	0.043	0.047	0.052	0.051	0.057	0.056	0.060	0.067	0.072	0.073	0.073
5%	0.016	0.015	0.014	0.019	0.022	0.027	0.027	0.029	0.036	0.034	0.039	0.038	0.039
1%	0.003	0.001	0.002	0.005	0.007	0.008	0.008	0.007	0.010	0.012	0.012	0.012	0.012
					Number of Factors = 4								
10%	0.027	0.038	0.048	0.049	0.051	0.048	0.047	0.053	0.052	0.052	0.059	0.063	0.065
5%	0.011	0.016	0.021	0.027	0.027	0.026	0.027	0.027	0.031	0.028	0.030	0.030	0.031
1%	0.001	0.000	0.003	0.006	0.005	0.004	0.008	0.004	0.006	0.006	0.008	0.009	0.009
					Number of Factors = 7								
10%	0.023	0.029	0.040	0.040	0.046	0.053	0.049	0.054	0.054	0.056	0.060	0.062	0.063
5%	0.008	0.009	0.017	0.022	0.024	0.028	0.027	0.028	0.029	0.031	0.033	0.038	0.034
1%	0.002	0.001	0.002	0.004	0.005	0.006	0.006	0.012	0.009	0.008	0.009	0.009	0.010
Panel B: $R_g^2 = 20\%$													
					Number of Factors = 5								
10%	0.015	0.025	0.029	0.036	0.038	0.043	0.047	0.049	0.050	0.054	0.050	0.053	0.053
5%	0.006	0.011	0.013	0.014	0.019	0.021	0.021	0.025	0.023	0.025	0.028	0.028	0.030
1%	0.002	0.003	0.003	0.007	0.006	0.004	0.006	0.005	0.005	0.007	0.005	0.004	0.004
					Number of Factors = 4								
10%	0.027	0.028	0.034	0.040	0.043	0.043	0.045	0.047	0.050	0.053	0.053	0.051	0.051
5%	0.012	0.011	0.010	0.018	0.017	0.018	0.017	0.019	0.021	0.025	0.026	0.027	0.027
1%	0.001	0.002	0.002	0.002	0.001	0.003	0.003	0.004	0.004	0.005	0.005	0.006	0.004
					Number of Factors = 7								
10%	0.011	0.022	0.023	0.028	0.036	0.039	0.039	0.045	0.050	0.051	0.055	0.052	0.050
5%	0.006	0.008	0.013	0.018	0.018	0.022	0.023	0.023	0.024	0.026	0.023	0.022	0.019
1%	0.002	0.001	0.003	0.004	0.004	0.003	0.004	0.004	0.004	0.005	0.005	0.005	0.006
Panel C: $R_g^2 = 10\%$													
					Number of Factors = 5								
10%	0.026	0.022	0.027	0.030	0.033	0.034	0.033	0.033	0.032	0.031	0.033	0.036	0.035
5%	0.010	0.007	0.014	0.014	0.015	0.014	0.016	0.018	0.017	0.017	0.018	0.018	0.016
1%	0.001	0.000	0.000	0.002	0.002	0.001	0.002	0.002	0.003	0.000	0.002	0.003	0.003
					Number of Factors = 4								
10%	0.023	0.024	0.027	0.029	0.036	0.033	0.027	0.031	0.026	0.032	0.031	0.031	0.033
5%	0.010	0.010	0.019	0.016	0.019	0.013	0.013	0.014	0.013	0.013	0.015	0.015	0.014
1%	0.002	0.003	0.001	0.003	0.003	0.004	0.004	0.005	0.004	0.003	0.004	0.003	0.003
					Number of Factors = 7								
10%	0.025	0.017	0.021	0.022	0.025	0.019	0.022	0.021	0.021	0.019	0.021	0.025	0.022
5%	0.005	0.006	0.009	0.008	0.010	0.008	0.013	0.013	0.011	0.010	0.014	0.014	0.016
1%	0.000	0.000	0.000	0.001	0.001	0.001	0.001	0.001	0.000	0.001	0.000	0.000	0.002

Frequency of rejecting $H_0 : \lambda_g^S = 0$ using 90%, 95%, and 99% credible intervals from Proposition A1, where λ_g^S is defined in equation (5). Useless factors with varying persistence: the persistent component in g_t accounts for 10%, 20%, or 30% of time series variation. Simulations: quarterly data, true model has 5 factors with $T = 200$ and $g_t \perp \boldsymbol{r}_t$; estimated models use 4, 5, or 7 factors with $\bar{S} = 12$. 1,000 Monte Carlo simulations.

Table OA.VII: Testing risk premia of useless factors at monthly frequencies ($T = 600$)

	$S=0$	2	4	6	8	10	12	14	16	18	20	22	24
Panel A: $R_g^2 = 30\%$													
					Number of Factors = 5								
10%	0.019	0.038	0.046	0.051	0.055	0.061	0.066	0.078	0.083	0.085	0.086	0.090	0.089
5%	0.006	0.013	0.017	0.024	0.029	0.033	0.035	0.035	0.046	0.048	0.049	0.053	0.049
1%	0.001	0.001	0.002	0.003	0.006	0.006	0.007	0.007	0.009	0.013	0.013	0.014	0.013
					Number of Factors = 4								
10%	0.015	0.032	0.044	0.054	0.059	0.065	0.076	0.082	0.086	0.088	0.093	0.094	0.089
5%	0.009	0.013	0.019	0.024	0.032	0.033	0.039	0.043	0.045	0.051	0.051	0.049	0.050
1%	0.000	0.002	0.003	0.006	0.009	0.011	0.013	0.011	0.010	0.011	0.015	0.013	0.013
					Number of Factors = 7								
10%	0.013	0.024	0.029	0.041	0.050	0.053	0.063	0.065	0.075	0.077	0.089	0.088	0.082
5%	0.005	0.014	0.016	0.022	0.025	0.026	0.029	0.034	0.038	0.043	0.043	0.043	0.044
1%	0.000	0.000	0.002	0.004	0.005	0.006	0.007	0.007	0.008	0.011	0.014	0.016	0.017
Panel B: $R_g^2 = 20\%$													
					Number of Factors = 5								
10%	0.017	0.035	0.040	0.056	0.060	0.060	0.073	0.072	0.070	0.076	0.073	0.076	0.073
5%	0.003	0.016	0.026	0.027	0.040	0.040	0.035	0.042	0.045	0.045	0.042	0.044	0.042
1%	0.001	0.005	0.007	0.006	0.012	0.010	0.009	0.008	0.011	0.013	0.015	0.014	0.014
					Number of Factors = 4								
10%	0.020	0.037	0.052	0.052	0.062	0.068	0.072	0.075	0.076	0.079	0.074	0.081	0.079
5%	0.007	0.013	0.026	0.030	0.034	0.039	0.035	0.039	0.037	0.042	0.040	0.044	0.042
1%	0.001	0.004	0.004	0.005	0.008	0.009	0.008	0.007	0.012	0.010	0.009	0.010	0.010
					Number of Factors = 7								
10%	0.009	0.026	0.034	0.036	0.046	0.045	0.053	0.057	0.053	0.054	0.058	0.058	0.063
5%	0.003	0.012	0.018	0.018	0.020	0.023	0.027	0.030	0.036	0.035	0.036	0.041	0.040
1%	0.000	0.003	0.003	0.004	0.006	0.007	0.007	0.008	0.006	0.009	0.010	0.007	0.008
Panel C: $R_g^2 = 10\%$													
					Number of Factors = 5								
10%	0.011	0.021	0.024	0.032	0.038	0.040	0.044	0.042	0.043	0.043	0.045	0.046	0.046
5%	0.003	0.005	0.008	0.010	0.013	0.011	0.014	0.021	0.017	0.018	0.018	0.022	0.021
1%	0.000	0.000	0.001	0.001	0.001	0.001	0.003	0.002	0.003	0.002	0.003	0.008	0.006
					Number of Factors = 4								
10%	0.018	0.029	0.028	0.035	0.037	0.037	0.041	0.047	0.049	0.045	0.054	0.044	0.040
5%	0.005	0.010	0.006	0.015	0.015	0.013	0.015	0.019	0.022	0.021	0.018	0.019	0.020
1%	0.000	0.001	0.002	0.001	0.002	0.002	0.001	0.001	0.001	0.002	0.004	0.004	0.003
					Number of Factors = 7								
10%	0.007	0.010	0.015	0.018	0.023	0.028	0.032	0.032	0.035	0.031	0.034	0.037	0.039
5%	0.001	0.005	0.003	0.007	0.009	0.007	0.010	0.010	0.012	0.009	0.010	0.013	0.013
1%	0.000	0.000	0.001	0.001	0.001	0.002	0.001	0.000	0.002	0.002	0.002	0.002	0.002

Frequency of rejecting $H_0 : \lambda_g^S = 0$ using 90%, 95%, and 99% credible intervals from Proposition A1, where λ_g^S is defined in equation (5). Useless factors with varying persistence: the persistent component in g_t accounts for 10%, 20%, or 30% of time series variation. Simulations: monthly data, true model has 5 factors with $T = 600$ and $g_t \perp \boldsymbol{r}_t$; estimated models use 4, 5, or 7 factors with $\bar{S} = 24$. 1,000 Monte Carlo simulations.

Table OA.VIII: Bayesian estimates of R_g^2 and $\text{corr}(\hat{f}_t, f_t)$ for strong and useless factors

Number of factors:	$K=4$			$K=5$			$K=7$		
True R_g^2 =	10%	20%	30%	10%	20%	30%	10%	20%	30%
Panel A. Posterior distributions of R_g^2									
			T = 200, strong factors						
median	0.122	0.187	0.259	0.142	0.224	0.311	0.156	0.235	0.320
5th	0.065	0.109	0.155	0.081	0.142	0.206	0.094	0.152	0.217
95th	0.199	0.288	0.370	0.228	0.325	0.421	0.240	0.337	0.428
			T = 600, strong factors						
median	0.104	0.185	0.272	0.112	0.204	0.297	0.116	0.207	0.300
5th	0.064	0.130	0.201	0.073	0.148	0.227	0.074	0.151	0.231
95th	0.149	0.249	0.344	0.158	0.264	0.370	0.163	0.267	0.373
			T = 200, useless factors						
median	0.081	0.083	0.084	0.091	0.094	0.097	0.109	0.113	0.117
5th	0.045	0.046	0.045	0.054	0.055	0.054	0.069	0.072	0.073
95th	0.133	0.140	0.145	0.145	0.154	0.167	0.165	0.178	0.195
			T = 600, useless factors						
median	0.041	0.042	0.044	0.046	0.047	0.049	0.052	0.055	0.059
5th	0.027	0.026	0.026	0.030	0.031	0.030	0.035	0.037	0.037
95th	0.063	0.071	0.080	0.067	0.077	0.087	0.075	0.086	0.102
Panel B. Posterior distributions of $\text{corr}(\hat{f}_t, f_t)$									
			T = 200, strong factors						
median	0.702	0.810	0.842	0.773	0.902	0.937	0.677	0.855	0.910
5th	0.324	0.605	0.736	0.386	0.745	0.860	0.294	0.665	0.809
95th	0.849	0.883	0.895	0.910	0.951	0.967	0.864	0.926	0.951
			T = 600, strong factors						
median	0.885	0.916	0.927	0.919	0.960	0.972	0.882	0.944	0.963
5th	0.760	0.873	0.893	0.812	0.925	0.953	0.747	0.901	0.940
95th	0.928	0.944	0.950	0.955	0.974	0.980	0.934	0.964	0.974

Bayesian estimates of R_g^2 and $\text{corr}(\hat{f}_t, f_t)$ for strong and useless factors, where R_g^2 measures the percentage of g_t's time series variation explained by latent factors and $\text{corr}(\hat{f}_t, f_t)$ is the correlation between true f_t and its estimate $\hat{f}_t = \hat{\boldsymbol{\eta}}_g^\top \hat{\mathbf{v}}_t$. For useless factors, only R_g^2 is reported. Each cell shows median, 5th, and 95th percentiles from 1,000 simulations. Strong and useless factors with varying persistence: the persistent component in g_t accounts for 10%, 20%, or 30% of time series variation. Simulations: true model has 5 factors; estimated models use $K \in \{4, 5, 7\}$ factors with $\bar{S} = 12$ for $T = 200$ or $\bar{S} = 24$ for $T = 600$.

Table OA.IX: Size and power of the Bayesian estimates and Giglio and Xiu (2021)

	Bayesian Estimation						Giglio and Xiu (2021)					
	Five factors			Seven factors			Five factors			Seven factors		
	10%	5%	1%	10%	5%	1%	10%	5%	1%	10%	5%	1%
Panel A. Size												
						$T = 200$						
10%	0.066	0.030	0.012	0.068	0.026	0.009	0.072	0.033	0.012	0.075	0.029	0.012
20%	0.087	0.042	0.008	0.085	0.045	0.005	0.091	0.048	0.008	0.082	0.046	0.005
30%	0.095	0.058	0.008	0.089	0.053	0.008	0.096	0.059	0.009	0.093	0.055	0.008
						$T = 600$						
10%	0.101	0.047	0.009	0.098	0.043	0.010	0.103	0.053	0.007	0.111	0.041	0.007
20%	0.100	0.050	0.011	0.097	0.048	0.008	0.099	0.051	0.009	0.100	0.056	0.008
30%	0.104	0.050	0.016	0.106	0.048	0.016	0.110	0.048	0.013	0.099	0.050	0.012
Panel B. Power												
						$T = 200$						
10%	0.278	0.190	0.051	0.267	0.160	0.046	0.286	0.188	0.045	0.288	0.189	0.040
20%	0.403	0.279	0.119	0.387	0.265	0.101	0.397	0.282	0.101	0.396	0.273	0.099
30%	0.484	0.371	0.169	0.466	0.358	0.154	0.478	0.359	0.151	0.480	0.370	0.155
						$T = 600$						
10%	0.520	0.410	0.186	0.499	0.391	0.189	0.523	0.414	0.174	0.507	0.391	0.176
20%	0.658	0.545	0.307	0.659	0.530	0.298	0.652	0.540	0.295	0.649	0.530	0.287
30%	0.715	0.598	0.365	0.708	0.583	0.364	0.711	0.590	0.343	0.699	0.581	0.334

Panel A: frequency of rejecting $H_0 : \lambda_g = \lambda_g^\star$ using 90%, 95%, and 99% credible intervals from our Bayesian estimates (Proposition A1) and frequentist test statistics (Giglio and Xiu (2021), Theorem 1), where $\lambda_g^\star$ is the pseudo-true value. Panel B: frequency of rejecting $H_0 : \lambda_g = 0$. Strong factors with $R_g^2 \in \{10\%, 20\%, 30\%\}$. We simulate quarterly ($T = 200$) and monthly ($T = 600$) observations of g_t and $\boldsymbol{r}_t$ by assuming that i) the true number of latent factors is five and ii) g_t correlates with only the contemporaneous $\tilde{\boldsymbol{v}}_t$ ($\bar{S} = 0$). We estimate several model configurations with different numbers of factors (5, 7). 1,000 Monte Carlo simulations.

Table OA.X: Bayesian estimates of R_g^2 and $\text{corr}(\hat{f}_t, f_t)$ of strong factors when factors command time-varying risk premia in simulations

	Panel A. R_g^2						**Panel B.** $\text{corr}(\hat{f}_t, f_t)$					
Number of factors:	$K = 5$			$K = 7$			$K = 5$			$K = 7$		
True $R_g^2 =$	10%	20%	30%	10%	20%	30%	10%	20%	30%	10%	20%	30%
						Quarterly frequency ($T = 200$)						
median	0.146	0.223	0.310	0.157	0.232	0.318	0.762	0.883	0.921	0.677	0.831	0.888
5th	0.081	0.139	0.208	0.097	0.144	0.219	0.343	0.724	0.846	0.283	0.635	0.795
95th	0.219	0.328	0.424	0.229	0.333	0.428	0.893	0.936	0.953	0.842	0.905	0.931
						Monthly frequency ($T = 600$)						
median	0.115	0.208	0.299	0.118	0.210	0.301	0.913	0.953	0.965	0.874	0.935	0.953
5th	0.069	0.148	0.227	0.074	0.151	0.229	0.794	0.916	0.942	0.717	0.888	0.928
95th	0.165	0.270	0.376	0.168	0.272	0.377	0.951	0.969	0.976	0.926	0.957	0.968

Bayesian estimates of R_g^2 and $\text{corr}(\hat{f}_t, f_t)$ for strong factors, where R_g^2 measures the percentage of g_t's time series variation explained by $\boldsymbol{\epsilon}_{vt}$ and $\text{corr}(\hat{f}_t, f_t)$ is the correlation between true f_t and its estimate $\hat{f}_t = \hat{\boldsymbol{\eta}}_g^\top \hat{\boldsymbol{\epsilon}}_{vt}$. Each cell shows median, 5th, and 95th percentiles from 1,000 simulations. Varying persistence: the persistent component in g_t accounts for 10%, 20%, or 30% of time series variation. We simulate monthly or quarterly observations of g_t and $\boldsymbol{r}_t$ assuming: true model has 5 factors; estimated models use $K \in \{5, 7\}$ factors with $\bar{S} = 12$ for $T = 200$ or $\bar{S} = 24$ for $T = 600$.

Table OA.XI: Testing unconditional risk premia of strong factors when factors command time-varying risk premia in simulations

		$S=0$	1	2	3	4	5	6	7	8	9	10	11	12
Quarterly frequency ($T=200$)	**Panel A:** $R_g^2=30\%$													
	Number of Factors = 5													
	10%	0.088	0.099	0.102	0.111	0.115	0.115	0.111	0.114	0.113	0.115	0.111	0.113	0.112
	5%	0.041	0.054	0.058	0.059	0.060	0.060	0.061	0.059	0.059	0.059	0.058	0.058	0.056
	1%	0.010	0.013	0.017	0.015	0.015	0.016	0.016	0.017	0.019	0.017	0.017	0.018	0.019
	Number of Factors = 7													
	10%	0.092	0.103	0.108	0.112	0.114	0.111	0.111	0.107	0.106	0.107	0.105	0.102	0.095
	5%	0.048	0.050	0.056	0.056	0.053	0.055	0.057	0.055	0.057	0.053	0.054	0.054	0.055
	1%	0.010	0.011	0.012	0.015	0.015	0.014	0.014	0.015	0.015	0.013	0.014	0.012	0.014
	Panel B: $R_g^2=20\%$													
	Number of Factors = 5													
	10%	0.103	0.104	0.103	0.097	0.096	0.100	0.103	0.099	0.103	0.108	0.110	0.114	0.103
	5%	0.054	0.048	0.052	0.047	0.048	0.049	0.045	0.049	0.050	0.053	0.050	0.055	0.052
	1%	0.008	0.013	0.014	0.011	0.008	0.008	0.011	0.013	0.013	0.012	0.013	0.012	0.013
	Number of Factors = 7													
	10%	0.091	0.086	0.086	0.087	0.083	0.082	0.088	0.092	0.091	0.093	0.096	0.097	0.095
	5%	0.048	0.045	0.046	0.048	0.045	0.044	0.044	0.043	0.047	0.050	0.054	0.051	0.051
	1%	0.005	0.009	0.011	0.010	0.009	0.009	0.012	0.013	0.011	0.012	0.012	0.013	0.012
	Panel C: $R_g^2=10\%$													
	Number of Factors = 5													
	10%	0.084	0.118	0.121	0.127	0.127	0.132	0.124	0.133	0.132	0.127	0.122	0.124	0.125
	5%	0.034	0.064	0.067	0.063	0.070	0.071	0.065	0.067	0.069	0.064	0.068	0.065	0.067
	1%	0.007	0.015	0.016	0.015	0.018	0.015	0.012	0.014	0.014	0.014	0.012	0.012	0.012
	Number of Factors = 7													
	10%	0.072	0.121	0.113	0.123	0.129	0.127	0.136	0.134	0.137	0.129	0.127	0.126	0.122
	5%	0.027	0.066	0.069	0.069	0.072	0.072	0.071	0.064	0.069	0.071	0.069	0.066	0.065
	1%	0.004	0.015	0.015	0.012	0.015	0.017	0.016	0.012	0.011	0.011	0.012	0.010	0.011

		$S=0$	2	4	6	8	10	12	14	16	18	20	22	24
Monthly frequency ($T=600$)	**Panel D:** $R_g^2=30\%$													
	Number of Factors = 5													
	10%	0.080	0.107	0.127	0.117	0.121	0.121	0.121	0.117	0.119	0.118	0.119	0.115	0.116
	5%	0.038	0.054	0.068	0.062	0.063	0.062	0.062	0.065	0.056	0.058	0.056	0.056	0.059
	1%	0.005	0.012	0.012	0.016	0.016	0.017	0.017	0.017	0.015	0.016	0.016	0.017	0.017
	Number of Factors = 7													
	10%	0.077	0.110	0.123	0.115	0.117	0.115	0.120	0.113	0.118	0.115	0.121	0.120	0.114
	5%	0.038	0.054	0.062	0.065	0.062	0.058	0.056	0.058	0.053	0.053	0.054	0.052	0.049
	1%	0.006	0.006	0.011	0.012	0.013	0.013	0.014	0.012	0.014	0.015	0.013	0.014	0.016
	Panel E: $R_g^2=20\%$													
	Number of Factors = 5													
	10%	0.075	0.092	0.107	0.107	0.106	0.109	0.112	0.110	0.111	0.109	0.117	0.112	0.110
	5%	0.035	0.050	0.059	0.060	0.062	0.063	0.059	0.065	0.063	0.059	0.058	0.059	0.055
	1%	0.004	0.011	0.013	0.011	0.011	0.011	0.012	0.012	0.013	0.013	0.012	0.013	0.013
	Number of Factors = 7													
	10%	0.069	0.099	0.100	0.105	0.105	0.103	0.103	0.107	0.104	0.102	0.105	0.105	0.109
	5%	0.027	0.050	0.054	0.054	0.059	0.057	0.058	0.061	0.060	0.056	0.057	0.057	0.053
	1%	0.003	0.008	0.012	0.009	0.013	0.011	0.013	0.013	0.014	0.013	0.011	0.013	0.015
	Panel F: $R_g^2=10\%$													
	Number of Factors = 5													
	10%	0.045	0.104	0.102	0.111	0.117	0.116	0.117	0.116	0.116	0.119	0.118	0.110	0.114
	5%	0.020	0.049	0.051	0.056	0.052	0.069	0.072	0.068	0.066	0.064	0.068	0.065	0.062
	1%	0.004	0.003	0.018	0.014	0.012	0.012	0.017	0.017	0.016	0.017	0.014	0.013	0.011
	Number of Factors = 7													
	10%	0.044	0.100	0.104	0.106	0.116	0.114	0.120	0.116	0.115	0.123	0.115	0.117	0.113
	5%	0.022	0.057	0.052	0.061	0.057	0.060	0.063	0.061	0.060	0.060	0.059	0.064	0.061
	1%	0.004	0.004	0.016	0.012	0.011	0.011	0.010	0.011	0.012	0.013	0.013	0.012	0.013

Frequency of rejecting $H_0 : \lambda_g^S = \lambda_g^{S,\star}$ (unconditional risk premia: $\lambda_g^S = \sum_{\tau=0}^{S} \sum_{s=0}^{\tau} \frac{\rho_s \boldsymbol{\eta}_g^\top \boldsymbol{\lambda}_v}{1+S}$) using 90%, 95%, and 99% credible intervals from Proposition OA.3, where $\lambda_g^{S,\star}$ is the pseudo-true value. Strong factors with $R_g^2 \in \{10\%, 20\%, 30\%\}$. Simulations: true model has 5 VAR(1) factors with $\bar{S}=8$ and $T=200$ (quarterly, Panels A–C) or $\bar{S}=16$ and $T=600$ (monthly, Panels D–F); estimated models use 5 or 7 factors with $\bar{S}=12$ (quarterly) or $\bar{S}=24$ (monthly). 1,000 Monte Carlo simulations.

Table OA.XII: Factors' risk premia: $\bar{S} = 0$, Bayesian and Frequentist estimates

	Bayesian estimates						Frequentist estimates (Giglio and Xiu, 2021)					
	$\mathbb{E}[\lambda_g \mid \mathcal{D}]$			$\mathbb{E}[R_g^2 \mid \mathcal{D}]$			$\mathbb{E}[\lambda_g \mid \mathcal{D}]$			$\mathbb{E}[R_g^2 \mid \mathcal{D}]$		
Number of factors:	5	6	7	5	6	7	5	6	7	5	6	7
Panel A. Original factors												
Quarterly variables												
AEM intermediary	0.141***	0.176***	0.175***	10.4%	12.2%	12.4%	0.160***	0.183***	0.184***	11.7%	13.3%	13.5%
CPI growth	-0.080**	-0.044	-0.048	5.8%	6.0%	7.7%	-0.068**	-0.042	-0.043	3.2%	5.7%	6.0%
GDP growth	0.005	0.013	0.013	4.2%	4.3%	4.3%	0.007	0.010	0.009	4.2%	4.2%	4.3%
IP growth	-0.028	0.004	0.003	2.9%	4.3%	4.3%	-0.015	-0.001	-0.003	3.2%	4.0%	4.3%
Durable cons. growth	-0.011	0.000	-0.002	7.7%	7.9%	8.2%	-0.015	-0.002	-0.006	7.1%	7.7%	8.7%
Nondurable cons. growth	0.042	0.058	0.056	3.7%	4.1%	4.1%	0.045	0.058	0.057	3.8%	4.4%	4.5%
Service cons. growth	0.015	0.053	0.052	4.0%	6.4%	6.5%	0.036	0.048	0.047	5.0%	5.5%	5.7%
Nondurable + service	0.032	0.067*	0.066*	4.0%	5.9%	6.0%	0.049	0.063*	0.062*	4.9%	5.6%	5.8%
Labor income growth	-0.006	0.035	0.028	1.5%	3.8%	8.7%	0.016	0.027	0.020	2.8%	3.3%	7.9%
Dividend growth of SP500	0.037	0.037	0.044	5.1%	5.4%	11.7%	0.045	0.035	0.043	4.3%	4.7%	10.8%
TFP growth	0.014	0.002	-0.003	6.9%	7.3%	8.2%	0.003	-0.001	-0.006	7.1%	7.2%	9.8%
TFP growth (util.-adj.)	-0.016	-0.048	-0.054	2.9%	4.9%	6.7%	-0.037	-0.047	-0.052	4.4%	4.7%	7.4%
Unemployment rate chg.	-0.034	-0.040	-0.045	2.5%	2.7%	3.5%	-0.039	-0.033	-0.035	2.3%	2.4%	2.8%
Hours worked growth	0.049	0.070*	0.072*	2.3%	3.4%	4.3%	0.062*	0.064*	0.067*	3.0%	3.0%	3.8%
Investment growth	0.000	0.014	0.015	2.2%	2.5%	3.1%	0.003	0.009	0.011	2.1%	2.2%	2.5%
Monthly variables												
Nontraded HKM interm.	0.100***	0.104***	0.104***	60.3%	61.0%	61.1%	0.099***	0.101***	0.104***	61.3%	61.8%	61.8%
Traded HKM interm.	0.112***	0.116***	0.116***	70.3%	71.0%	71.2%	0.110***	0.112***	0.114***	71.5%	72.1%	72.1%
PS liquidity	0.061***	0.059***	0.062***	11.9%	12.2%	12.9%	0.062***	0.060***	0.053***	11.9%	12.3%	12.4%
$\Delta \log(\text{VIX})$	-0.120***	-0.118***	-0.118***	42.8%	43.0%	43.1%	-0.118***	-0.118***	-0.118***	42.8%	42.9%	42.9%
Panel B. AR(1) shocks of quarterly macro factors												
AEM intermediary	0.144***	0.182***	0.182***	10.8%	12.9%	13.3%	0.166***	0.189***	0.190***	12.3%	14.0%	14.3%
CPI growth	-0.094***	-0.065*	-0.071*	5.9%	5.8%	9.4%	-0.081**	-0.062*	-0.066*	3.8%	5.0%	6.3%
GDP growth	0.005	0.012	0.012	4.2%	4.3%	4.3%	0.007	0.010	0.009	4.2%	4.2%	4.3%
IP growth	-0.021	0.001	-0.002	3.6%	4.3%	4.9%	-0.009	-0.003	-0.008	3.8%	3.9%	6.1%
Durable cons. growth	-0.010	0.002	0.000	7.4%	7.6%	7.8%	-0.013	0.000	-0.003	6.8%	7.4%	8.1%
Nondurable cons. growth	0.042	0.058	0.057	3.7%	4.1%	4.1%	0.045	0.058	0.057	3.8%	4.4%	4.4%
Service cons. growth	0.016	0.055	0.055	3.7%	6.3%	6.4%	0.037	0.051	0.050	4.9%	5.5%	5.6%
Nondurable + service	0.031	0.069*	0.069*	3.7%	6.0%	6.0%	0.049	0.065*	0.065*	4.7%	5.6%	5.6%
Labor income growth	-0.007	0.033	0.027	1.4%	3.6%	8.3%	0.015	0.026	0.019	2.7%	3.1%	7.3%
Dividend growth of SP500	0.067*	0.068*	0.074*	3.3%	3.4%	9.5%	0.068**	0.066*	0.073*	2.9%	2.9%	8.0%
TFP growth	0.019	0.006	0.001	7.2%	7.7%	8.6%	0.007	0.003	-0.002	7.5%	7.6%	10.1%
TFP growth (util.-adj.)	-0.012	-0.044	-0.050	3.1%	5.1%	6.9%	-0.033	-0.043	-0.048	4.6%	5.0%	7.6%
Unemployment rate chg.	-0.038	-0.041	-0.045	2.7%	2.8%	3.3%	-0.042	-0.034	-0.035	2.3%	2.5%	2.7%
Hours worked growth	0.055	0.074**	0.075*	2.6%	3.7%	4.2%	0.067**	0.068*	0.070*	3.3%	3.3%	3.7%
Investment growth	-0.005	0.007	0.006	2.2%	2.5%	2.5%	-0.001	0.003	0.003	2.1%	2.2%	2.2%

Factors' risk premia and time series fit R_g^2 using Bayesian methods (left panel) and Giglio and Xiu (2021) frequentist method (right panel). Panel A: original variables; Panel B: AR(1) shocks of macro factors. Bayesian estimates from Proposition A1 with $\bar{S} = 0$. Base assets: 275 Fama-French characteristic-sorted portfolios. Five-, six-, and seven-factor models for returns. Significance: * (**, ***) indicates 90% (95%, 99%) credible interval excludes zero for Bayesian estimates or 10% (5%, 1%) significance for frequentist estimates. Data sources in Online Appendix OA.4.

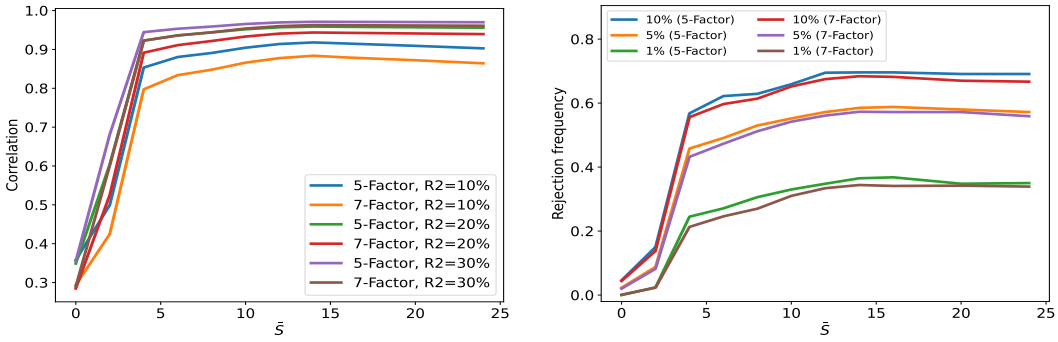

(a) $\text{corr}(\hat{f}_t, f_t)$, $T = 600$ **(b)** Power, $R_g^2 = 30\%$, $T = 600$

Figure OA.3: Identification and power gains from the MA representation, $T = 600$

Left panel: average correlation between true and estimated priced shock, $\text{corr}(\hat{f}_t, f_t)$ with $\hat{f}_t = \hat{\boldsymbol{\eta}}_g^\top \hat{\boldsymbol{v}}_t$, across 1,000 simulations, for strong factors with $R_g^2 \in \{10\%, 20\%, 30\%\}$. Right panel: frequency, in 1,000 simulations, of rejecting $H_0 : \lambda_g^{\bar{S}} = 0$ based on the 90%, 95%, and 99% Bayesian credible intervals from Proposition A1, for strong factors with $R_g^2 = 30\%$. Both panels use $T = 600$. $\lambda_g^{\bar{S}}$ is defined in equation (5).

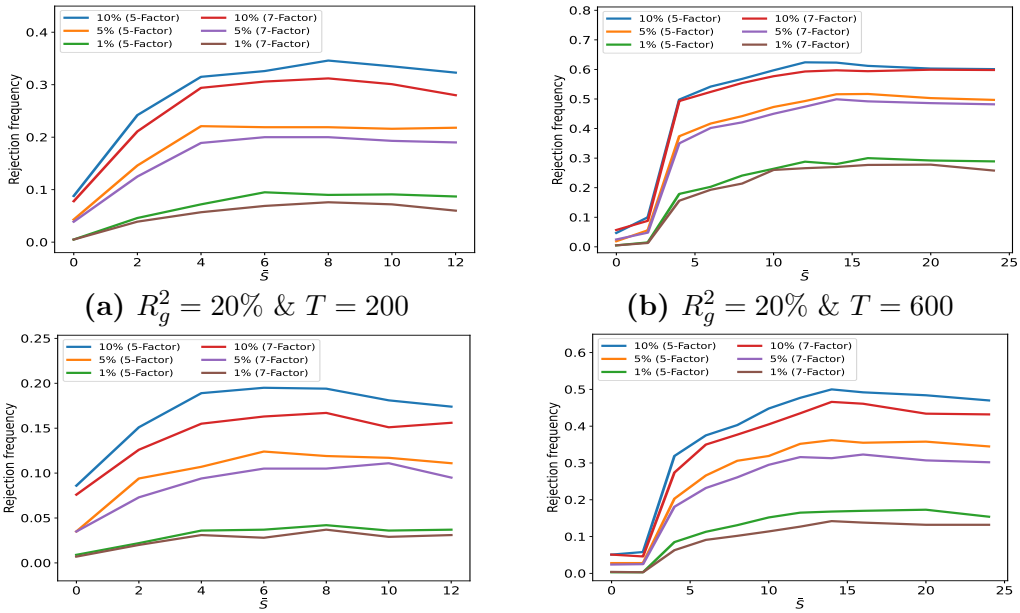

(a) $R_g^2 = 20\%$ & $T = 200$ **(b)** $R_g^2 = 20\%$ & $T = 600$

(c) $R_g^2 = 10\%$ & $T = 200$ **(d)** $R_g^2 = 10\%$ & $T = 600$

Figure OA.4: Power of identifying strong factors

Frequency of rejecting $H_0 : \lambda_g^{\bar{S}} = 0$ using 90%, 95%, and 99% credible intervals from Proposition A1, where $\lambda_g^{\bar{S}}$ is defined in equation (5). Strong factors with $R_g^2 \in \{10\%, 20\%, 30\%\}$ and sample sizes $T \in \{200, 600\}$. Each simulation estimates multiple model configurations varying the number of factors and $\bar{S}$. 1,000 simulations.

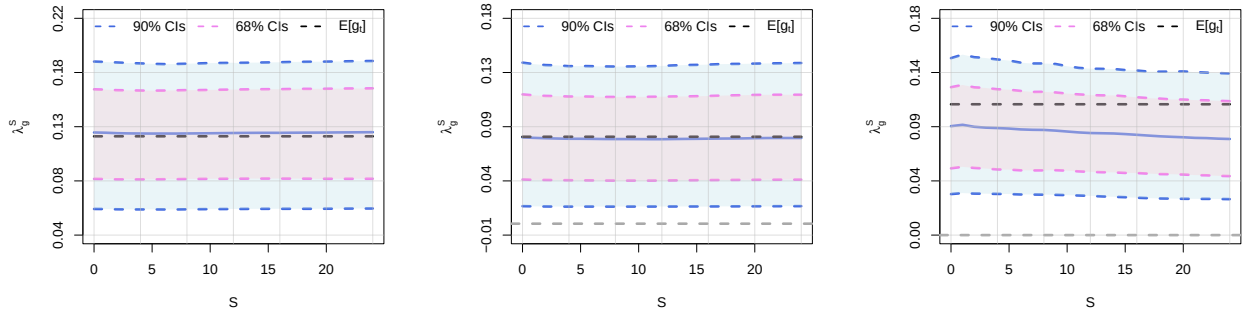

(a) MKT **(b)** SMB **(c)** HML

Figure OA.5: Term structure of risk premia: Fama and French (1993) three factors

Term structure of risk premia (monthly Sharpe ratio units) using Proposition A1, where λ_g^S is defined in equation (5). Base assets: 275 Fama-French characteristic-sorted portfolios. Five-factor model for returns. We estimate risk premia for the Fama and French (1993) three factors using 24-month lags in g_t's equations. Grey dotted lines show in-sample monthly Sharpe ratios. Shaded areas show 68% (pink) and 90% (blue) Bayesian credible intervals. Data sources in Internet Appendix OA.4. Sample: July 1963–December 2019.

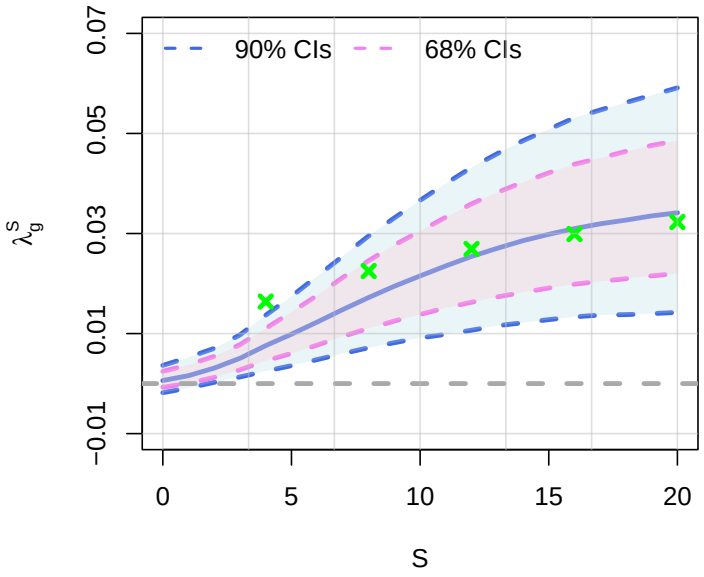

Figure OA.6: Term structure of unconditional dividend risk premia

Term structure of dividend risk premia (not standardized, unlike Table 1). Base assets: 275 Fama-French characteristic-sorted portfolios. Five-factor model for returns using 20-quarter lags in g_t's equations. Pink and blue shaded areas show 68% and 90% Bayesian credible intervals, respectively. Green crosses: risk premia estimates from Bansal et al. (2021), Table 4.